

**SYNTHESIS AND STRUCTURAL CHARACTERIZATION  
OF SOME Fe, Ru, Rh AND Ir COMPLEXES**

**A THESIS  
SUBMITTED FOR THE DEGREE OF  
DOCTOR OF PHILOSOPHY**

**BY  
H. ANEETHA**

**SCHOOL OF CHEMISTRY  
UNIVERSITY OF HYDERABAD  
HYDERABAD 500 046  
INDIA**

**AUGUST 1997**

*to*

*my parents*

## CONTENTS

Statement	i
Certificate	ii
Acknowledgments	iii
Abbreviations	v
Preface	vi

### **Chapter 1: Introduction**

1.1. Abstract	1
1.2. Phenoxy bridged macrocyclic and acyclic complexes	2
1.3. Transition-metal complexes as catalysts for epoxidation reactions	24
1.4. Pentamethylcyclopentadienyl complexes of Rh(III) and Ir(III)	36
1.5. References	45

### **Chapter 2: Synthesis and Molecular Structure of Di- and Mononuclear Schiff base Phenolate Complexes: Facile Formation of Cyclometallated Ruthenium Complexes**

2.1. Abstract	57
2.2. Introduction	59
2.3. Experimental	61
2.4. Physical measurements	66
2.5. Results and discussion	69
2.6. Conclusions	107
2.7. References	108

### **Chapter 3: Synthesis, Characterization and Catalytic Activity of Dinuclear Fe(III) and Ru(III) Complexes**

3.1. Abstract	113
3.2. Introduction	114
3.3. Experimental	115
3.4. Physical measurements	119
3.5. Results and discussion	120
3.6. Conclusions	133
3.7. References	134

### **Chapter 4: Synthesis and Characterization of (Pentamethylcyclopentadienyl) Rh(III) and Ir(III) Polypyridyl Complexes: Molecular Structure of [Cp\*Rh(Ph-terpy)Cl]BF<sub>4</sub> Complex**

4.1. Abstract	137
4.2. Introduction	138
4.3. Experimental	139
4.4. Physical measurements	142
4.5. Results and discussion	143
4.6. Conclusions	169
4.7. References	170

<b>Appendix</b>	<b>173</b>
-----------------	------------



## STATEMENT

I hereby declare that the matter embodied in this thesis is the result of investigations carried out by me in the School of Chemistry, University of Hyderabad, Hyderabad, under the supervision of Prof. P. S. Zacharias.

In keeping with the general practice of reporting scientific observations, due acknowledgment has been made wherever the work described is based on the findings of other investigators. Any omission which might have occurred by oversight or error is regretted.

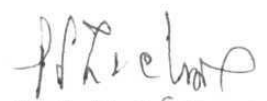


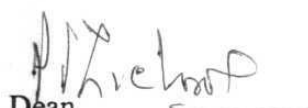
H. Aneetha

## CERTIFICATE

Certified that the work contained in the thesis entitled **“Synthesis and Structural Characterization of some Fe, Ru, Rh and Ir Complexes”** has been carried out by Ms. H. Aneetha under my supervision and the same has not been submitted elsewhere for any degree.

Hyderabad  
August 1997

  
P. S. Zacharias  
(Thesis Supervisor)

  
Dean  
School of Chemistry

## ACKNOWLEDGMENTS

I express my profound gratitude to Prof. P. S. Zacharias, my research supervisor for his guidance, support and encouragement which has made this work a pleasant endeavor. I am also thankful to him for the freedom he has given me in carrying out the research.

I thank Prof. T. C. W. Mak and Mr. Xue Feng from Chinese University of Hongkong, Dr. B. Srinivas and Prof. M. Y. Chiang from National Sun-Yat-Sen University, Taiwan for solving the X-ray crystal structures.

I am grateful to the faculty members of the school for their help on various occasions.

I am thankful to my labmates Dr. K. Mohan Rao, Dr. Ch. Ramakishan Rao, Dr. M. S. Ameerunisha Begum, Mr. K. Srinivasa Rao, Ms. N. Mangayarkarasi and Mr. G. Aditya for helpful discussions and for creating a pleasant work atmosphere.

I thank my friends and colleagues Soujanya, Chandrakala, Anita, Manjula, Sindhu, Vijjulatha, Saroja, Sudha, Ramalakshmi, Madhavi, Padmaja, Prasuna and Prabhavathi for their help and without whom the stay in the school would not have been such a memorable experience.

I also wish to acknowledge all my teachers in my previous courses of study for their guidance.

I thank Dr. K. Mohan Rao and Dr. P. Nachimuthu for their helpful advice and timely help. I also thank Dr. F. A. Khan and Mr. C. Ravikrishna for helping me in recording GC.

I thank Mr. S. Satyanarayana and Mr. V. Bhaskara Rao for patiently recording the various NMR spectra. I also thank Mrs. G. Vijaya Lakshmi, Mr. Ramana and all the non-teaching staff of the school for their cooperation.

Financial support from the DST and CSIR is gratefully acknowledged.

Finally, I am thankful to my parents, my sister Ameetha and my brothers Amarnath and Abhijith for their love, affection, encouragement and understanding without which this work would have been impossible. I also thank my grandparents and my aunts for their encouragement.

H. Aneetha

## ABBREVIATIONS

bpy	2,2'-bipyridine
Cp*	pentamethylcyclopentadienyl
DBT	dibenzothiophene
diterpy	1,4-bis(2,2': 6', 2"-terpyridin-4'-yl)benzene
dmsO	dimethyl sulphoxide
Im	imidazole
phen	1,10 phenanthroline
ph-terpy	4'-phenyl-2,2': 6', 2"terpyridine
pz	pyrazole
py	pyridine
salen	N,N'-ethylenebis(salicylaldimine)
saloph	N,N'- <i>o</i> -Phenylene(salicylaldimine)
TBAP	tetrabutyl ammonium perchlorate
terpy	2,2': 6', 2"terpyridine

## PREFACE

The work presented in this thesis deals with synthesis and structural characterization of some Fe, Ru, Rh and Ir complexes. The first chapter is an introduction in three parts. The first part is a review on phenoxy bridged macrocyclic and acyclic complexes of 2,6-diformyl-4-methylphenol and the various Schiff bases formed from it. In the second part, the role of various transition metal complexes as catalysts for epoxidation reactions is discussed. The third part presents some reactions of  $[\text{Cp}^*\text{M}(\mu\text{-Cl})\text{Cl}]_2$  ( $\text{M} = \text{Rh}$  or  $\text{Ir}$ ) with various ligands.

The second chapter explores the role of ruthenium as a template ion in the condensation reactions of 2,6-diformyl-4-methylphenol with various amines to study the pattern of product formation. Reaction of 2,6-diformyl-4-methylphenol with aliphatic diamines in presence of  $[\text{Ru}(\text{dmsO})_4\text{Cl}_2]$  form acyclic dinuclear complexes  $[\text{Ru}_2\text{L}^n(\text{dmsO})_4\text{Cl}_4]$ , **1-3** ( $n = 1-3$ ). These reactions in the presence of triphenylphosphine give four-membered cyclometallated dinuclear complexes  $[\text{Ru}_2\text{L}^{n'}(\text{PPh}_3)_4(\text{CO})_2\text{Cl}_2]$ , **9-11** ( $n = 1-3$ ). The reactions of ligands  $\text{L}^{4-8}$  with  $[\text{Ru}(\text{dmsO})_4\text{Cl}_2]$  gave complexes, but structure could not be assigned based on spectral data. Attempts to grow single crystals were also unsuccessful. However these reactions in presence of triphenylphosphine give cyclometallated mononuclear complexes  $[\text{RuL}^{n'}(\text{PPh}_3)_2(\text{CO})\text{Cl}]$ , **4-8** ( $n = 4-8$ ). All the complexes are characterized by analytical and various spectral techniques. They were confirmed by the crystal

structures of complexes **2** and **5**. Complex **2** crystallizes in the orthorhombic space group Pbca. The asymmetric unit consists of two octahedral ruthenium ions bridged by a Schiff base ligand which acts as a tetradentate O<sub>4</sub> donor. The complexes **4-11** are formed by decarbonylation of the aldehyde group resulting in cyclometallation of phenyl ring. The structure is confirmed from crystal structure of complex **5**. It crystallizes in the monoclinic space group C2/c and the geometry around Ru(II) is distorted octahedral, coordinated by phenolate oxygen and C(2) carbon to form planar four-membered metallacycle. The facile formation of cyclometallated complexes is rationalized. Attempts to synthesize macrocyclic complexes by transmetallation of Na<sub>2</sub>L<sup>9-11</sup> (synthesized by condensation of sodium salt of 2,6-diformyl-4-methylphenol with diamines, NH<sub>2</sub>-(CH<sub>2</sub>)<sub>n</sub>-NH<sub>2</sub>, n = 2-4) results in hydrolysis of Schiff base macrocycle and only acyclic complexes are formed.

The third chapter deals with synthesis and characterization of dinuclear Fe(III) and Ru(III) complexes. A number of Fe(III) and Ru(III) complexes from triazene-1-oxide and Schiff base ligands are synthesized. Based on analytical, spectral and magnetic data, the complexes from triazene-1-oxide ligands [Fe<sub>2</sub>L<sub>2</sub><sup>n</sup>Cl<sub>2</sub>], **12-14** (n = 12-14) and the Schiff base complexes [Fe<sub>2</sub>L<sub>2</sub><sup>n</sup>Cl<sub>2</sub>]Cl<sub>4</sub>, **17-20** (n = 15-18) are assigned dinuclear structure. The geometry around Fe(III) is square-pyramidal. The analogous dinuclear ruthenium complexes [Ru<sub>2</sub>L<sub>2</sub><sup>n</sup>(PPh<sub>3</sub>)<sub>2</sub>Cl<sub>2</sub>], **15-16** (n = 12, 14) and [Ru<sub>2</sub>L<sub>2</sub><sup>n</sup>(PPh<sub>3</sub>)<sub>2</sub>Cl<sub>2</sub>]Cl<sub>4</sub>, **21-22** (n = 15, 17) have octahedral geometry at

the metal center. Catalytic efficiency of these complexes for epoxidation reactions is investigated.

The fourth chapter describes synthesis and characterization of mono and dinuclear polypyridyl complexes of Rh(III) and Ir(III) ions. Reaction of  $[\text{Cp}^*\text{M}(\mu\text{-Cl})\text{Cl}]_2$  ( $\text{M} = \text{Rh}, \text{Ir}$ ) with 4'-phenyl-2,2': 6', 2'' terpyridine, (Ph-terpy)  $\text{L}^{19}$  and 1,4-bis(2,2': 6', 2''-terpyridin-4'-yl)benzene, (diterpy)  $\text{L}^{20}$  results in formation of cationic complexes by cleavage of halide bridge. The complexes  $[\text{Cp}^*\text{RhL}^{19}\text{Cl}]\text{BF}_4$ , **23**,  $[(\text{Cp}^*\text{RhCl})_2\text{L}^{20}](\text{BF}_4)_2$ , **24**,  $[\text{Cp}^*\text{IrL}^{19}\text{Cl}]\text{BF}_4$ , **25** and  $[(\text{Cp}^*\text{IrCl})_2\text{L}^{20}](\text{BF}_4)_2$ , **26** are characterized by various spectral methods. Ph-terpy ligand coordinates the metal ion in a bidentate fashion to form mononuclear complexes while diterpy bridges two metal ions to form dinuclear complexes where each metal ion is coordinated by two nitrogens. Complex **23** is crystallographically characterized. It crystallizes in triclinic space group  $P\bar{1}$ . The asymmetric unit consists of a rhodium ion displaying the characteristic three legged "piano stool" geometry coordinated by one  $\text{C}_5(\text{CH}_3)_5$  group, one chloride and one Ph-terpy ligand in the bidentate bonding mode. In solution, the complexes  $[\text{Cp}^*\text{RhL}^{19}\text{Cl}]\text{BF}_4$  and  $[(\text{Cp}^*\text{RhCl})_2\text{L}^{20}](\text{BF}_4)_2$  show fluxional behavior. This is supported by variable temperature  $^1\text{H}$  NMR spectral data. The proposed structures of iridium complexes are analogous to the structures of the rhodium complexes.



Parts of the work described in this thesis have been published.

1. Catalytic oxidation of two electron donors by dinuclear Cu(II), Ni(II) and Co(II) complexes and epoxidation of olefins using Fe(III) complexes, Rao, Ch. R. K.; Aneetha, H.; Srinivas, B.; Zacharias, P. S.; Ramachandraiah, A. *Polyhedron*, 1994, **13**, 2659.
2. Dinuclear metal complexes of Schiff base ligands as catalysts for oxidation and epoxidation reactions, Zacharias, P. S.; Srinivas, B.; Aneetha, H. *Proc., Indian Acad. Sci. Chem. Sci.* 1995, **107**, 297.
3. Synthesis, characterization and catalytic activity of dinuclear Fe(III) and Ru(III) complexes, Aneetha, H.; Padmaja, J.; Zacharias, P. S. *Polyhedron*, 1996, **15**, 2445.
4. Synthesis and molecular structure of di and mononuclear Schiff base phenolate complexes: Facile formation of cyclometallated ruthenium complexes, Aneetha, H.; Rao, Ch. R. K.; Mohan Rao, K.; Zacharias, P. S.; Xue Feng; Mak, T. C. W.; Srinivas, B.; Chiang, M. Y. *J. Chem. Soc., Dalton Trans.* 1997, 1697.
5. Synthesis and molecular structure of (pentamethylcyclopentadienyl) (polypyridyl) Rh(III) and Ir(III) complexes: Ph-terpy acting as a fluxional bidentate ligand, Aneetha, H.; Zacharias, P. S.; Srinivas, B.; Lee, G.-H.; Wang, Y. Manuscript under preparation.

## ***CHAPTER 1***

### **Introduction**

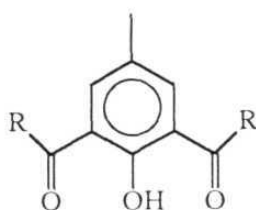
#### **1.1. Abstract**

The introduction is in three parts. The first part is a review on phenoxy bridged macrocyclic and acyclic complexes of 2,6-dicarbonyl-4-methylphenol and the various Schiff bases formed from them. The second part presents a discussion on transition metal complexes as catalysts for the epoxidation reactions. The third part consists of a brief literature survey on some reactions of pentamethylcyclopentadienyl complexes of rhodium(III) and iridium(III).

## 1.2. Phenoxy bridged macrocyclic and acyclic complexes

Design, synthesis and study of polydentate Schiff bases and their multimetallic complexes have been of interest. Of these dinuclear complexes containing metal centers in close proximity have received considerable attention since homo or heterodinuclear metal centers form the active sites in many enzymes (tyrosinase, superoxide dismutase and hemocyanin etc.) and are involved in a variety of biochemical processes.<sup>1-5</sup> Molecular systems with redox active sites in close proximity capable of cooperative interactions are also of interest as potential catalysts for non-biological substrate oxidations.<sup>6</sup>

Polydentate ligands capable of securing two metal ions are termed as dinucleating ligands. Since 1970 there has been a steady increase in the synthesis and investigation of such ligands and their complexes. A number of dinucleating Schiff base ligands are derived from 2,6-dicarbonyl-4-methyl phenols, thiophenols, 1,3,5-triketones,  $\beta$ -keto phenols, keto-acids, diamino alcohol and polyamines. These ligand systems are termed compartmental ligands since the metal ions share atleast one donor atom containing adjacent



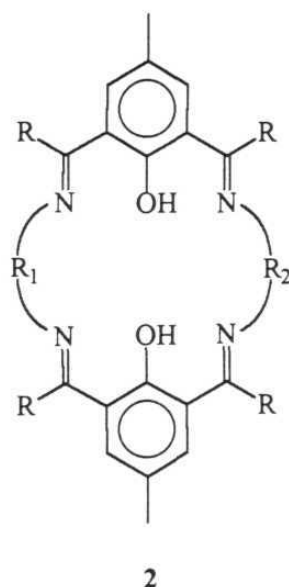
R	H	CH <sub>3</sub>	C <sub>3</sub> H <sub>7</sub>	C <sub>6</sub> H <sub>5</sub>
Ligand	HL <sup>1</sup>	HL <sup>2</sup>	HL <sup>3</sup>	HL <sup>4</sup>

sites in which the central donor atom provides a bridge. Because the subject matter in chapter 2 deals with the Schiff base complexes of 2,6-diformyl-4-methylphenol, this discussion will be limited to 2,6-dicarbonyl-4-methylphenols and their complexes. 2,6-dicarbonyl-4-methylphenol, **1** and the various Schiff bases from it with mono and diamines form dinuclear complexes. The dinucleating ability of these ligands stems from the readiness of the phenolic proton to deprotonate and bridge two metal ions in close proximity. Several review articles covering phenoxy bridged macrocyclic and acyclic complexes have appeared.<sup>7</sup>

### Dinuclear complexes

In 1970 Robson *et al.* synthesized a series of macrocyclic complexes of composition  $[M_2L^6Cl_2]$  ( $M = Zn(II), Cu(II), Ni(II), Co(II), Fe(II)$  and  $Mn(II)$ ) by the condensation of 2,6-diformyl-4-methylphenol and 1,3-diaminopropane in 2:2 ratio using metal ion as a template.<sup>8</sup> The generalized structure of the macrocyclic ligands synthesized by condensation of 2,6-dicarbonyl-4-methylphenol with various diamines is shown in structure **2** and the details are given in Table 1.1.

Based on the analytical, spectral and magnetic data,  $[M_2L^6Cl_2]$  complexes were assigned dinuclear structure **3**. The geometry around the metal ion is square-pyramidal with chlorides occupying the axial positions. Variable-temperature magnetic susceptibility studies on these complexes suggested antiferromagnetic exchange interactions between the metal ions

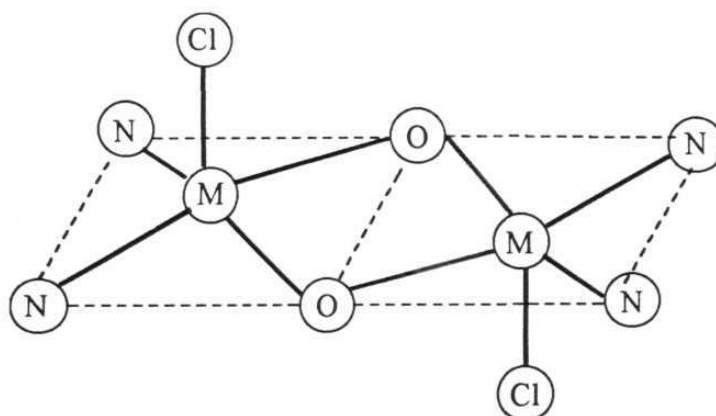


which decreases in the series Cu(II), Ni(II), Co(II) and becomes ferromagnetic interaction with Mn(II) complex. This change in magnetic behavior was attributed to the changing number of unpaired electrons and increased metal-ligand distance from Cu(II) to Mn(II).<sup>9</sup> The structure of these complexes has been confirmed in the case of Cu(II)<sup>10</sup> and Co(II)<sup>11</sup> complexes by single crystal X-ray analysis.

Analogous Cu(II) complexes with Br<sup>-</sup> and I<sup>-</sup> as axial ligands were synthesized to investigate the influence of electron-withdrawing axial ligands on spin exchange interaction.<sup>12</sup> Variable-temperature magnetic susceptibility experiments showed marked difference in exchange interaction between the axially bound Cl<sup>-</sup>, Br<sup>-</sup> and I<sup>-</sup> ions. The variations of  $-2J$  values, Cl < Br < I,

**Table 1.1.** Ligands of structure **2** with various diamines

R	R <sub>1</sub>	R <sub>2</sub>	Ligand
H	(CH <sub>2</sub> ) <sub>2</sub>	(CH <sub>2</sub> ) <sub>2</sub>	H <sub>2</sub> L <sup>5</sup>
H	(CH <sub>2</sub> ) <sub>3</sub>	(CH <sub>2</sub> ) <sub>3</sub>	H <sub>2</sub> L <sup>6</sup>
H	(CH <sub>2</sub> ) <sub>4</sub>	(CH <sub>2</sub> ) <sub>4</sub>	H <sub>2</sub> L <sup>7</sup>
H	CH <sub>2</sub> CH(OH)CH <sub>2</sub>	CH <sub>2</sub> CH(OH)CH <sub>2</sub>	H <sub>2</sub> L <sup>8</sup>
H	(CH <sub>2</sub> ) <sub>2</sub>	(CH <sub>2</sub> ) <sub>3</sub>	H <sub>2</sub> L <sup>9</sup>
H	(CH <sub>2</sub> ) <sub>3</sub>	CH <sub>2</sub> CH(OH)CH <sub>2</sub>	H <sub>2</sub> L <sup>10</sup>
CH <sub>3</sub>	(CH <sub>2</sub> ) <sub>2</sub>	(CH <sub>2</sub> ) <sub>2</sub>	H <sub>2</sub> L <sup>11</sup>
CH <sub>3</sub>	(CH <sub>2</sub> ) <sub>3</sub>	(CH <sub>2</sub> ) <sub>3</sub>	H <sub>2</sub> L <sup>12</sup>
C <sub>3</sub> H <sub>7</sub>	(CH <sub>2</sub> ) <sub>3</sub>	(CH <sub>2</sub> ) <sub>3</sub>	H <sub>2</sub> L <sup>13</sup>
C <sub>6</sub> H <sub>5</sub>	(CH <sub>2</sub> ) <sub>3</sub>	(CH <sub>2</sub> ) <sub>3</sub>	H <sub>2</sub> L <sup>14</sup>



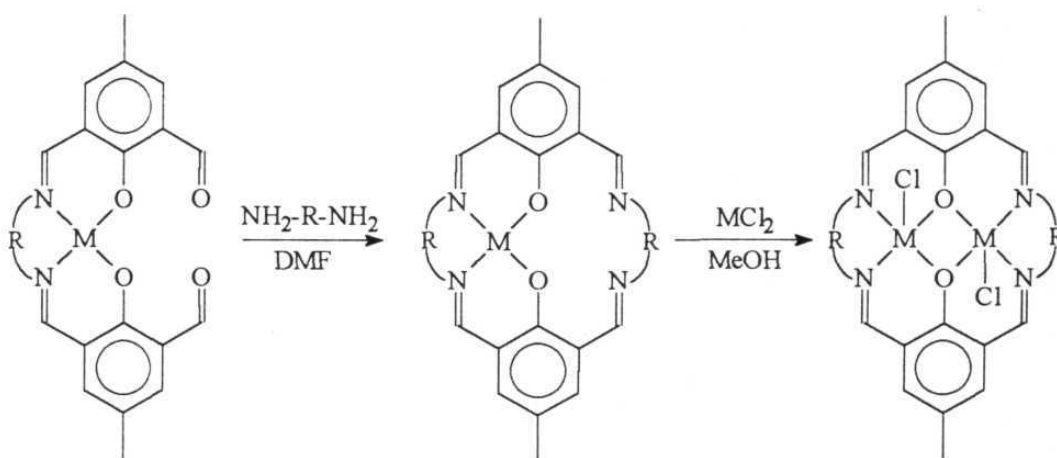
which parallels the trend in the electronegativity of the halogens indicate that the axially bound halogens have a primary influence on exchange even though they are orthogonally bound to the copper magnetic orbital.

The crystal structure of the complex,  $[\text{Cu}_2\text{L}^7(\text{ClO}_4)_2]$  shows two six-coordinate Cu(II) centers with two asymmetrically bound axial bidentate perchlorates.<sup>13</sup> The dinuclear center dimensions of  $[\text{Cu}_2\text{L}^6(\text{H}_2\text{O})_2]$ ,  $[\text{Cu}_2\text{L}^6(\text{H}_2\text{O})_2(\text{ClO}_4)_2](\text{ClO}_4)_2$  and  $[\text{Cu}_2\text{L}^7(\text{ClO}_4)_2]$  are very similar and both the compounds exhibit comparable, strong antiferromagnetic exchange ( $-2J = 850 \text{ cm}^{-1}$  and  $857 \text{ cm}^{-1}$  respectively) whereas  $[\text{Cu}_2\text{L}^{11}(\text{H}_2\text{O})_2](\text{BF}_4)_2$  has a smaller dinuclear center with a reduced Cu-O-Cu bridge angle and is less strongly coupled ( $-2J = 689 \text{ cm}^{-1}$ ). Studies showed that the expected increase in the antiferromagnetic interaction in the six-coordinate complexes compared to the analogous five-coordinate complexes is not observed due to increased ligand field splitting in the former which attenuated the increased antiferromagnetic interaction.<sup>14</sup>

Okawa and Kida synthesized<sup>15</sup>  $[\text{M}_2\text{L}^{5,6}\text{Cl}_2]$  ( $\text{M} = \text{Cu(II)}, \text{Ni(II)}$ ) complexes in a stepwise synthesis as shown in Scheme 1.1. A series of dinuclear Cu(II), Ni(II) and Co(II) complexes of ligands  $\text{H}_2\text{L}^{5-7}$  with chelate rings of various sizes have been synthesized and studied.<sup>16</sup>  $[\text{Fe}_2\text{L}^6(\text{Im})_4](\text{BF}_4)_2$  and  $[\text{Zn}_2\text{L}^6(\text{ClO}_4)_2] \cdot 2\text{H}_2\text{O}$  were structurally characterized.<sup>14,17</sup> Recently metal free compartmental macrocyclic ligands,  $\text{H}_2\text{L}^5$  and  $\text{H}_2\text{L}^6$  have been isolated as  $\text{Br}^-$  and  $\text{PF}_6^-$  salts and are used as starting materials for the synthesis of various transition metal complexes.<sup>18</sup>

Macrocyclic complexes were also synthesized from substituted 2,6-dicarbonyl-4-methylphenols to study the effect of substitution on the

electrochemical properties. Single crystal X-ray structure of complex  $[\text{Cu}_2\text{L}^{11}(\text{H}_2\text{O})_2](\text{BF}_4)_2$  showed the dinuclear cation to be planar apart from apical water molecules.<sup>19</sup> Electrochemical data<sup>20</sup> on complexes,



**Scheme 1.1**

$[\text{Cu}_2\text{L}^6](\text{ClO}_4)_2$  and  $[\text{Cu}_2\text{L}^{12-14}](\text{ClO}_4)_2$  showed that the first reduction step remains invariant throughout the series, and is independent of the extent of magnetic interaction. The potentials of the second reduction step varied with the alkyl and aryl groups present.

Dinuclear Cu(II) complexes with varying ring sizes undergo two successive one-electron reductions at two different potentials producing Cu(II)-Cu(I) and Cu(I)-Cu(I) species.<sup>13</sup> A comparison of  $E_{1/2}$  of the first electron reductions shows that the most thermodynamically favoured process occurs for  $[\text{Cu}_2\text{L}^7(\text{ClO}_4)_2]$  complex and has been rationalized in terms of

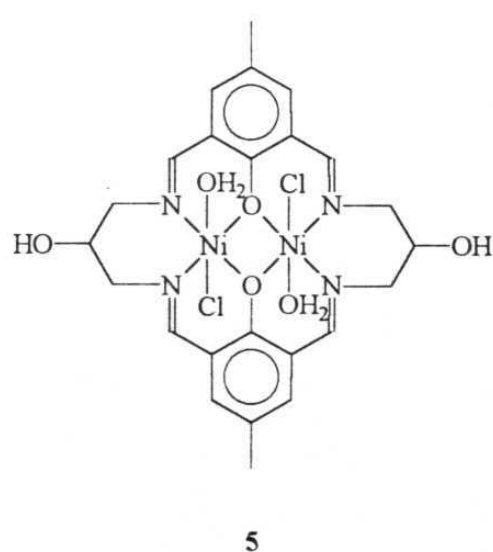
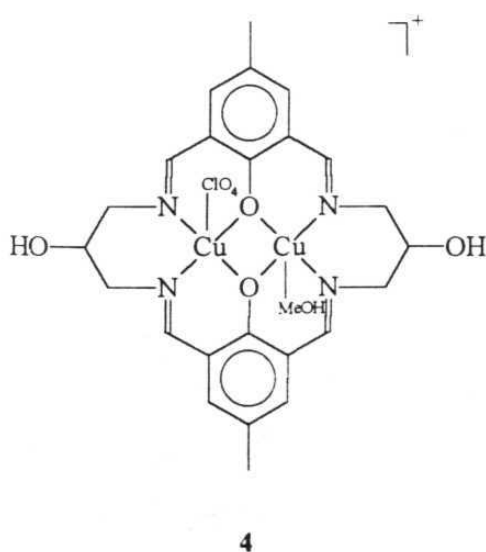


stabilization of Cu(II)-Cu(I) species. The second one-electron reduction also occurs at the most positive potential for this system. The first electron transfer for  $[\text{Cu}_2\text{L}^{11}(\text{H}_2\text{O})_2](\text{BF}_4)_2$  and  $[\text{Cu}_2\text{L}^6(\text{H}_2\text{O})_2][\text{Cu}_2\text{L}^6(\text{H}_2\text{O})_2(\text{ClO}_4)_2](\text{ClO}_4)_2$  complexes occur at the same potential and indicate that the change in ring size from five to six does not influence the reduction potential. Electronic effects associated with methyl and propyl groups on the ring do not appear to influence the first electron reduction process very much, but differences in  $E_{1/2}$  values for the second reduction vs. the  $E_{1/2}$  of  $[\text{Cu}_2\text{L}^6(\text{H}_2\text{O})_2][\text{Cu}_2\text{L}^6(\text{H}_2\text{O})_2(\text{ClO}_4)_2](\text{ClO}_4)_2$  indicate possible electronic influence. Replacement of 4-methyl by  $\text{CF}_3$  in complexes with ethylene and butylene bridges shows increased  $E_{1/2}$  values for one-electron reduction steps in DMF indicating the transmission of electron-withdrawing effect to the Cu(II) centers.<sup>21</sup> The electrochemical properties of dinuclear Ni(II), Co(II), Fe(II) and Mn(II) complexes of  $\text{H}_2\text{L}^6$  ligands are also studied.<sup>22</sup>

Gagne *et al.* synthesized dinuclear Cu(II) complexes of composition  $[\text{Cu}_2\text{L}^6](\text{ClO}_4)_2$  and electrochemically reduced them to the mixed-valent Cu(II)-Cu(I) and Cu(I)-Cu(I) complexes in separate one-electron processes.<sup>23</sup> The electronic and the EPR spectra of complex,  $[\text{Cu}_2\text{L}^6]\text{ClO}_4$  indicate interaction between the copper ions. The room-temperature EPR spectrum of the complex exhibits an isotropic seven line spectrum which is explained in the terms of intramolecular electron transfer between the two copper ions.<sup>24</sup> In frozen media, (77 K) anisotropic pattern was observed with four lines for  $g_{\parallel}$  and unresolved  $g_{\perp}$ . Electronic spectrum of the complex exhibit two bands at 1700 and 1200 nm which are not present in Cu(II)-Cu(II) complex and they have been attributed to the intramolecular electron transfer process. The

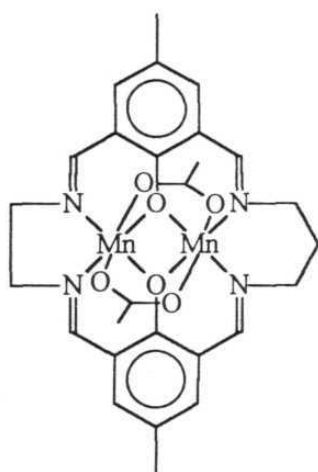
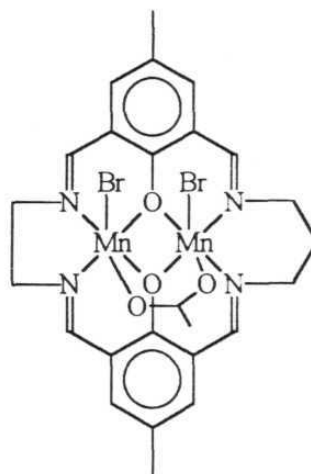
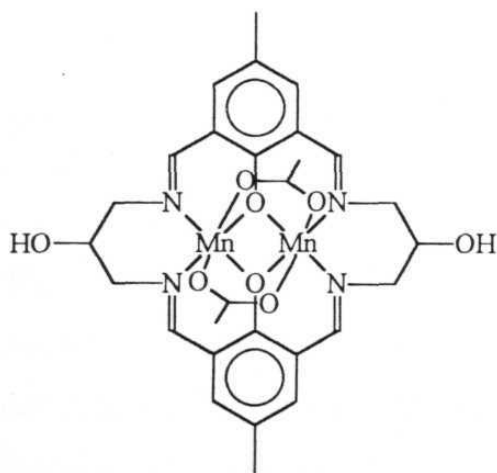
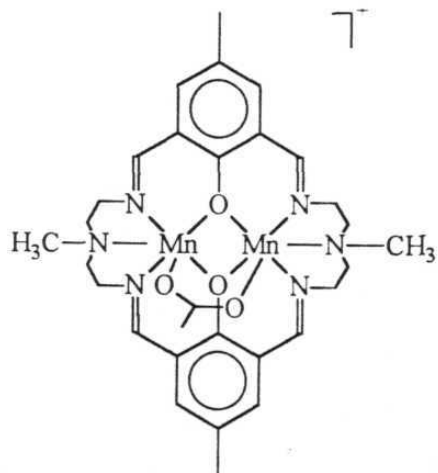
single crystal X-ray structure of  $[\text{Cu}_2\text{L}^6]\text{ClO}_4$  complex was described in terms of localized valence states in solid state with one divalent copper ion and two types of monovalent copper ions.<sup>25</sup> When R is  $\text{CH}_3$ , the room-temperature EPR spectrum of the analogous complex shows four line copper hyperfine pattern indicating localized unpaired electron on one copper ion on the EPR time scale.<sup>26</sup> A series of mixed-valence dinuclear  $\text{Cu(II)-Cu(I)}$  complexes have been prepared to study the factors affecting intramolecular electron transfer.<sup>27</sup>

The dinuclear complexes,  $[\text{Cu}_2\text{L}^8(\text{CH}_3\text{OH})(\text{ClO}_4)]\text{ClO}_4$ , **4** and  $[\text{Ni}_2\text{L}^8\text{Cl}_2(\text{H}_2\text{O})_2]\cdot 2\text{H}_2\text{O}$ , **5** have been crystallographically characterized.<sup>28,29</sup>



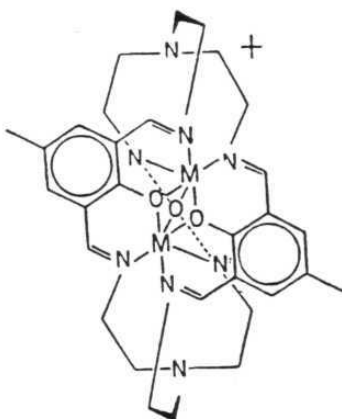
Oxidation of  $[\text{Mn}_2\text{L}^6(\text{CH}_3\text{COO})_2]$  and  $[\text{Mn}_2\text{L}^9(\text{CH}_3\text{COO})_2]$ , **6** complexes with  $\text{Br}_2$  forms mixed-valent  $[\text{Mn(II)Mn(III)}\text{L}^{6,9}(\text{CH}_3\text{COO})\text{-Br}_2]\cdot\text{H}_2\text{O}$ , **7**. Both the complexes show catalytic activity for the

decomposition of  $\text{H}_2\text{O}_2$ .<sup>30</sup>  $[\text{Mn}_2\text{L}^8(\text{CH}_3\text{COO})_2] \cdot 2\text{CH}_3\text{OH}$ , **8** and  $[\text{Mn}_2\text{L}^{15}(\text{CH}_3\text{COO})]\text{ClO}_4$ , **9** complexes are also structurally characterized.<sup>29,31</sup>

**6****7****8****9**

Homodinuclear Cu(II), Co(II), Fe(II) and Mn(II) complexes, **10** with dinucleating ligand  $\text{H}_2\text{L}^{16}$  resulting from the condensation of 3 moles of 2,6-

diformyl-4-methylphenol and 2 moles of 2,2',2''-tri-aminotriethylamine exhibit weak antiferromagnetic interaction because of the metal coordination and bridging geometry.<sup>37</sup>

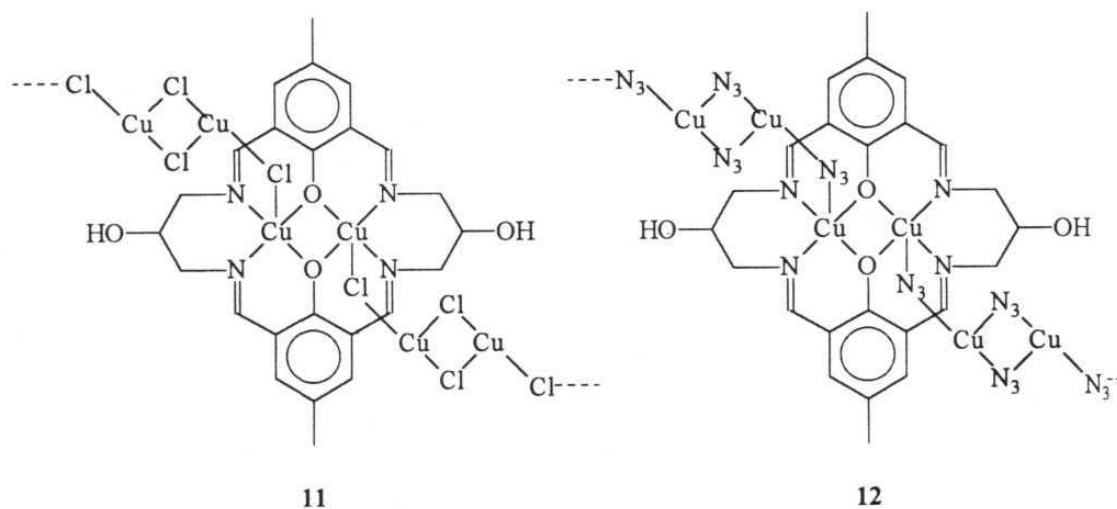


10

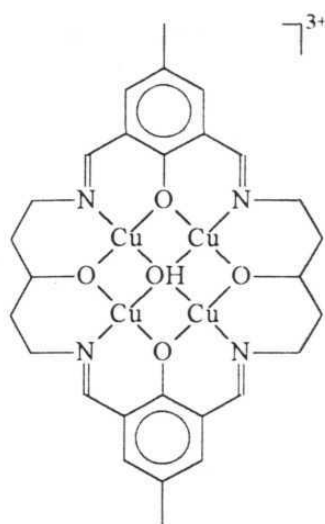
### Multinuclear complexes

Recent efforts have resulted in the synthesis and characterization of several multinuclear complexes. The polymeric mixed-valent  $[\text{Cu}_2\text{L}^8][\text{Cu}_2\text{Cl}_4]$ , **11** complex having a dinuclear chloro bridged  $[\text{Cu}_2\text{Cl}_4]^{2-}$  anion and the polymeric complex,  $[\text{Cu}_2\text{L}^8][\text{Cu}_2(\text{N}_3)_6]$ , **12** synthesized by template condensation in presence of copper acetate and  $\text{NaN}_3$  have been structurally characterized.<sup>28</sup> Comparison of the magnetic data of the complexes **4**, **11** and **12** show a net antiferromagnetic interaction and it is much larger in the azide bridged polymer. This is due to the extended interaction in which intra-ring antiferromagnetic exchange and independent

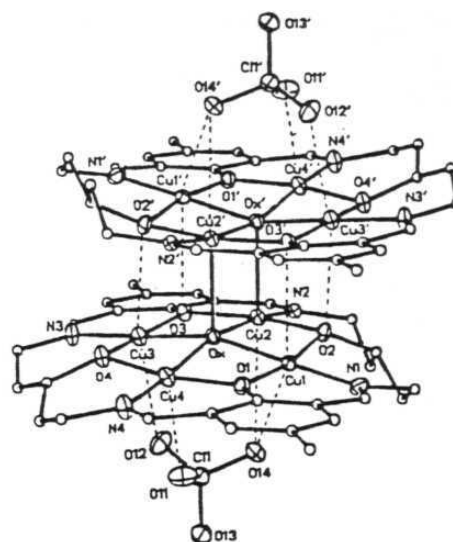
exchange within the anion are accompanied by extended antiferromagnetic interdimer exchange.



A series of tetracopper(II) complexes of the type  $[\text{Cu}_4(\mu_4\text{-OH})\text{L}^{17}](\text{NO}_3)_3 \cdot 2\text{H}_2\text{O}$ , **13** were synthesized and they dimerize with the loss of hydroxo proton to form octacopper(II) complexes which contain two  $\text{Cu}_4(\mu_5\text{-O})$  units. The crystal structure of the complex,  $[\{\text{Cu}_4(\mu_5\text{-O})\text{L}^{17}(\text{ClO}_4)\}_2](\text{ClO}_4)_2 \cdot \text{CH}_3\text{OH}$ , **14** shows that it is a centrosymmetric dimer and within each macrocycle the arrangement is similar to that observed in the tetranuclear complex. However, the central oxygen atom is five-coordinated oxo anion and the coordination sphere is completed by a copper atom from the second macrocyclic unit of the dimer.<sup>33</sup> Magnetic studies on these complexes indicate net antiferromagnetic interaction and the octacopper complexes show stronger coupling than the tetracopper complexes.

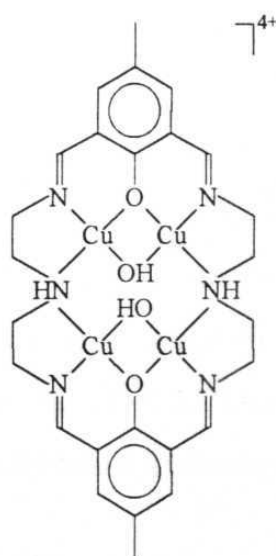


13



14

The tetranuclear  $[\text{Cu}_4\text{L}^{18}(\mu_2\text{-OH})_2](\text{ClO}_4)_4$  complex, **15** has been synthesized by template condensation of 2,6-diformyl-4-methylphenol and



15

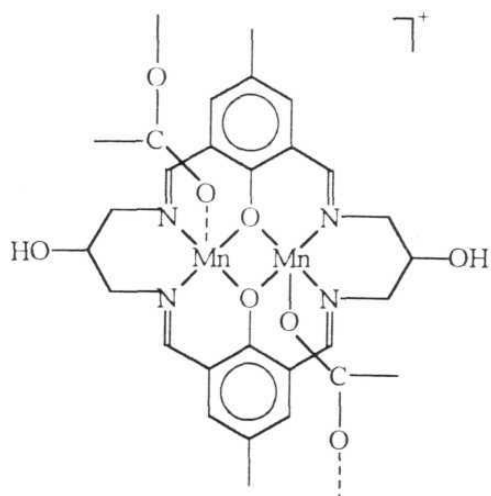
triethylenetetramine.<sup>34</sup> Cyclic voltammetric data of the complex shows four redox couples and were assigned to the step wise reduction of  $\text{Cu}_4(\text{II}, \text{II}, \text{II}, \text{II})$  to  $\text{Cu}_4(\text{I}, \text{I}, \text{I}, \text{I})$  species.

Polynuclear Mn(II) complexes of  $\text{H}_2\text{L}^6$  and  $\text{H}_2\text{L}^{10}$  consists of dinuclear units bridged by acetato groups to form infinite chains, **16** where each Mn(II) ion is in square-pyramidal geometry with one oxygen atom of the bridging acetato group bonded to each manganese ion in an axial position. In the case of  $[\text{Mn}_2\text{L}^{10}(\text{ClO}_4)]_2$  complex, coordination of alcoholate function of  $\text{H}_2\text{L}^{10}$  ligands of the two adjacent dinuclear units to one of the Mn ions of the partner dinuclear unit affords a tetranuclear structure of the type **17**.<sup>35</sup>

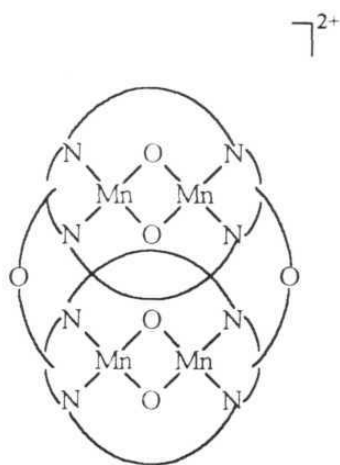
Tetranuclear mixed-valent  $[\text{Mn}_2(\text{II})\text{Mn}_2(\text{III})\text{L}^{17}(\text{O})\text{Cl}(\text{CH}_3\text{COO})_3-(\text{CH}_3\text{OH})].3\text{CH}_3\text{OH}$ , **18** and  $[\text{Mn}_4\text{L}^{19}(\text{C}_6\text{H}_5\text{COO})_6((\text{CH}_3)_2\text{CHOH})_2].2\text{CH}_2\text{Cl}_2$ , **19** complexes have also been crystallographically characterized.<sup>36,37</sup> The complex **19** has two pairs of Mn(II) ions with antiferromagnetic interaction between the Mn(II) ions in a pair ( $J = -4 \text{ cm}^{-1}$ ) and no interaction between the pairs.

$\text{Ni}_4$  and  $\text{Zn}_4$  complexes of a tetranucleating Schiff base macrocycle  $\text{H}_4\text{L}^{20}$  have been characterized.<sup>38</sup> Crystal structure of the complex,  $[\text{Ni}_4\text{L}^{20}(\text{CH}_3\text{COO})_2(\text{OH})(\text{CH}_3\text{O.H.OCH}_3)].4\text{CH}_3\text{OH}$ , **20** shows that the arrangement of the macrocyclic ligand resembles that of a bowl.

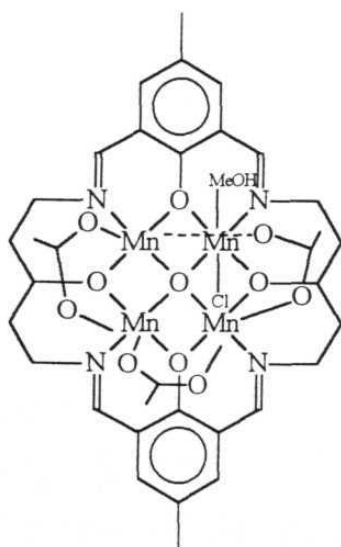
Hexanuclear Cu(II) and Ni(II) complexes and dodecanuclear Cu(II) complexes have also been synthesized and studied.<sup>39,40</sup>



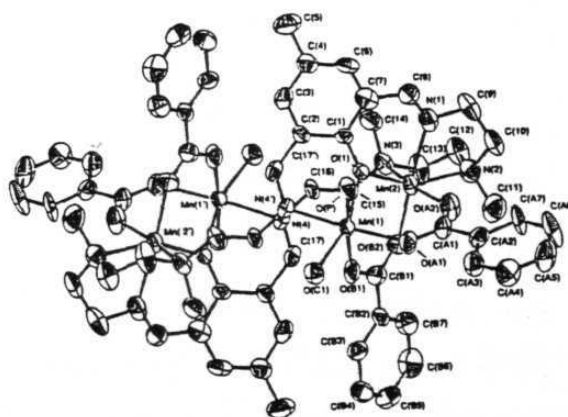
16



17

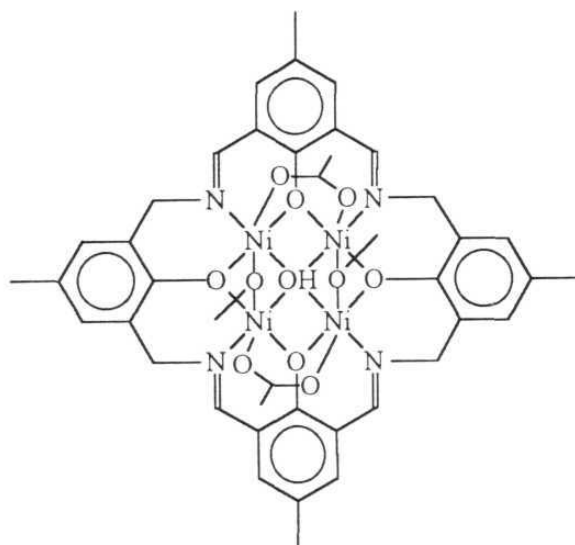


18



19



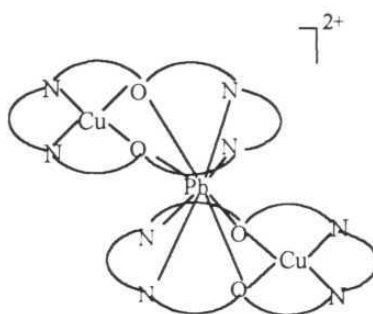


### Heteronuclear complexes

Heterodinuclear complexes of composition  $[\text{CuML}^6\text{Cl}_2] \cdot n\text{H}_2\text{O}$  have been synthesized and characterized. ( $\text{M} = \text{Mn(II)}$ ,  $\text{Fe(II)}$ ,  $\text{Co(II)}$  and  $\text{Ni(II)}$ ). The geometry around both the metal ions is square-pyramidal. Magnetic susceptibility experiments showed the presence of antiferromagnetic exchange interactions between the metal ions.<sup>22,41</sup> Heterodinuclear  $\text{Co(II)-Fe(II)}$  and  $\text{Mn(II)-Fe(II)}$  complexes of ligand  $\text{H}_2\text{L}^{16}$  are also known.<sup>32</sup>

Tricationic macrocyclic complexes,  $[\text{Pb}(\text{ML}^6)_2](\text{ClO}_4)_2$  where  $\text{M} = \text{Cu(II)}$  and  $\text{Ni(II)}$  have been characterized.<sup>42</sup> The crystal structure of  $[\text{Pb}(\text{CuL}^6)_2](\text{ClO}_4)_2 \cdot \text{DMF}$ , **21** has two  $\text{CuL}^6$  entities, the  $\text{Cu(II)}$  ion being

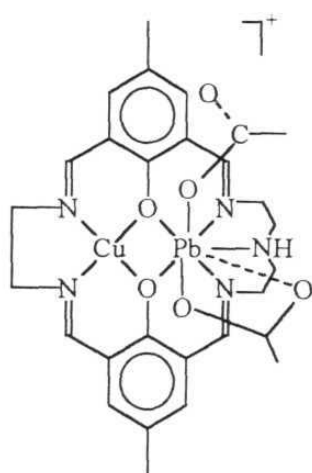
bound at one of the  $\text{N}_2\text{O}_2$  sites. The  $\text{Pb(II)}$  ion is sandwiched between the two  $\text{CuL}^6$  units forming eight-coordinate square antiprism.



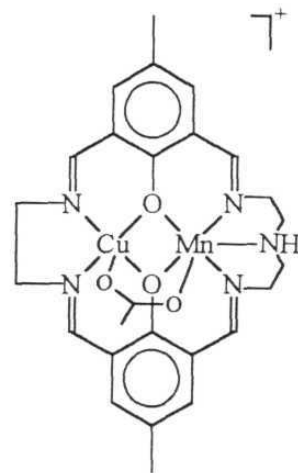
21

The heterodinuclear complex  $[\text{CuPbL}^{21}(\text{CH}_3\text{COO})]\text{BPh}_4\cdot\text{DMF}$ , **22** reacts with metal sulphates and forms a series of  $\text{Cu(II)M(II)}$  complexes where  $\text{M} = \text{Mn(II)}, \text{Fe(II)}, \text{Co(II)}, \text{Ni(II)}$  and  $\text{Zn(II)}$ .<sup>43</sup> In  $[\text{CuMnL}^{21}(\text{CH}_3\text{COO})]\text{BPh}_4$  complex, **23** the geometry at  $\text{Cu(II)}$  is square-pyramidal and  $\text{Mn(II)}$  is highly distorted octahedral with acetate groups bridging the two metal ions.

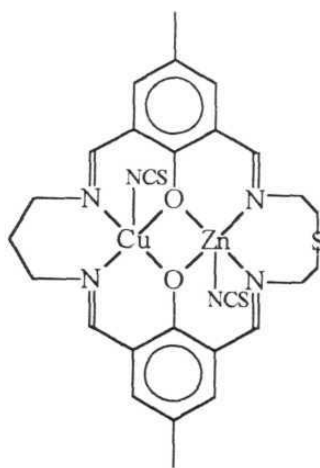
Mononuclear  $[\text{CuH}_2\text{L}^{22}](\text{ClO}_4)_2$  complex in basic media reacts with a second metal ion to form heterodinuclear complexes of the type  $[\text{CuML}^{22}(\text{NCS})_2]\cdot\text{H}_2\text{O}$  where  $\text{M} = \text{Co(II)}, \text{Ni(II)}$  and  $\text{Zn(II)}$ . In  $[\text{Cu(II)Zn(II)L}^{22}(\text{NCS})_2]\cdot\text{DMF}$ , **24** complex the  $\text{Cu(II)}$  ion occupies  $\text{N}_2\text{O}_2$  site and  $\text{Zn(II)}$  ion lies in  $\text{N}_2\text{O}_2\text{S}$  cavity with no coordination to sulphur.<sup>44</sup>



22



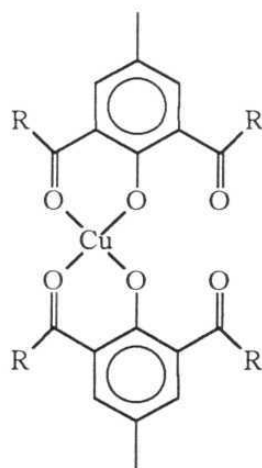
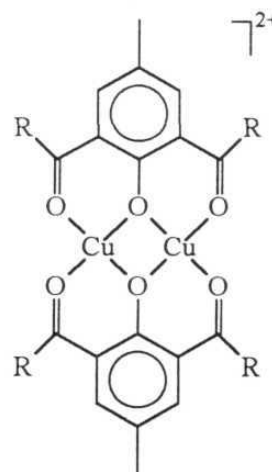
23



24

### Acyclic complexes

Acyclic mono and dinuclear copper(II) complexes, **25** and **26** of the ligands HL<sup>1-4</sup> were synthesized and characterized.<sup>45</sup> The dinuclear complexes

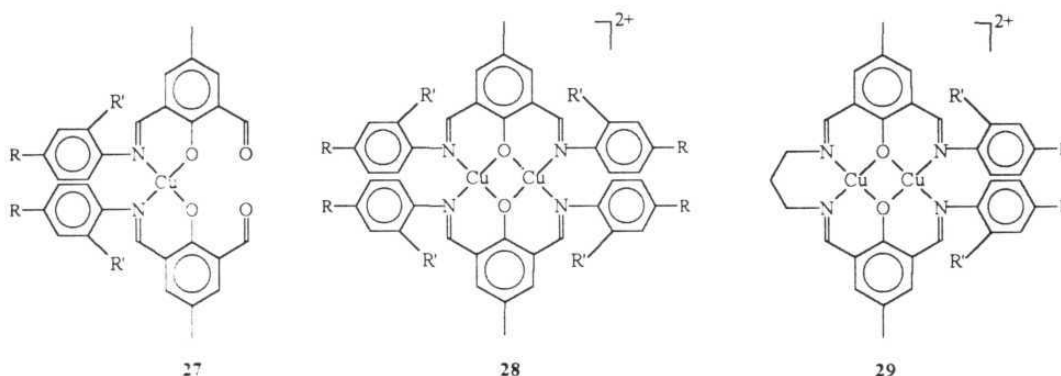
**25****26**

are characterized by a single reversible reduction couple at  $\sim -0.035$  V to  $-0.045$  V corresponding to the reduction of Cu(II)-Cu(II) to Cu(I)-Cu(I) species. The substituents show very little effect on the  $E_{1/2}$  values. The mononuclear  $[\text{CuL}_2^3]$  and  $[\text{CuL}_2^4]$  complexes undergo quasi-reversible reduction at a relatively more negative potential at  $\sim -0.43$  V.

Studies on homo and heterodinuclear complexes of composition  $[\text{M}_2\text{L}_2^1](\text{ClO}_4)_2$ ,  $[\text{CuML}_2^{1,2}](\text{ClO}_4)_2$  ( $\text{M} = \text{Ni(II)}, \text{Co(II)}, \text{Mn(II)}$ ) and  $[\text{CuML}_2^2\text{Cl}_2] \cdot 2\text{H}_2\text{O}$  ( $\text{M} = \text{Ni(II)}, \text{Co(II)}$ ) indicated the presence of

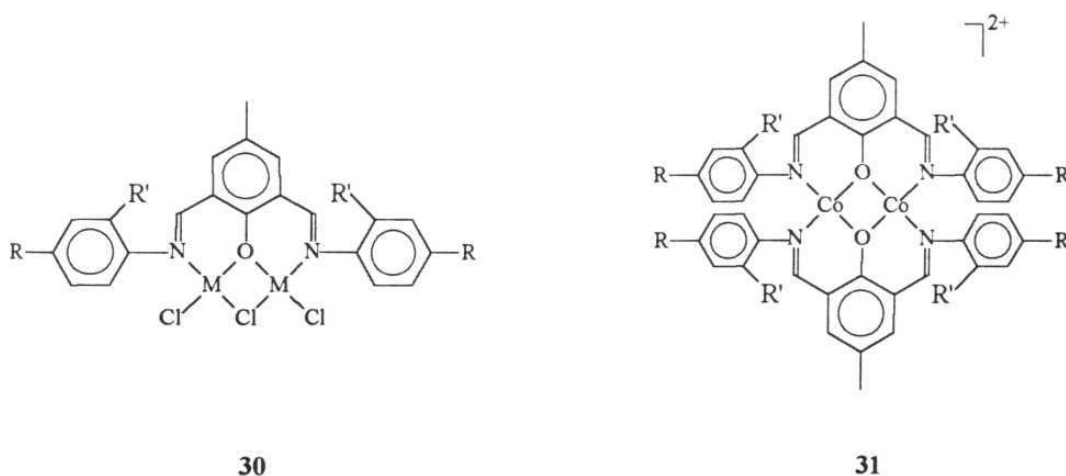
antiferromagnetic interaction. Electrochemical experiments on the homodinuclear complexes showed that in  $[\text{Co}_2\text{L}_2]^{2+}$  complex both the  $\text{Co(II)}$  centers undergo reduction at the same potential like  $\text{Cu(II)}$  whereas in the case of  $\text{Ni(II)}$  and  $\text{Mn(II)}$  complexes irreversible reduction occurs at two different potentials.<sup>46</sup>

Mono and dinuclear copper complexes, **27** and **28** of the ligands  $\text{HL}^{23-24}$  and dinuclear complexes, **29** of  $\text{H}_2\text{L}^{25}$  are characterized.<sup>47</sup> Based on



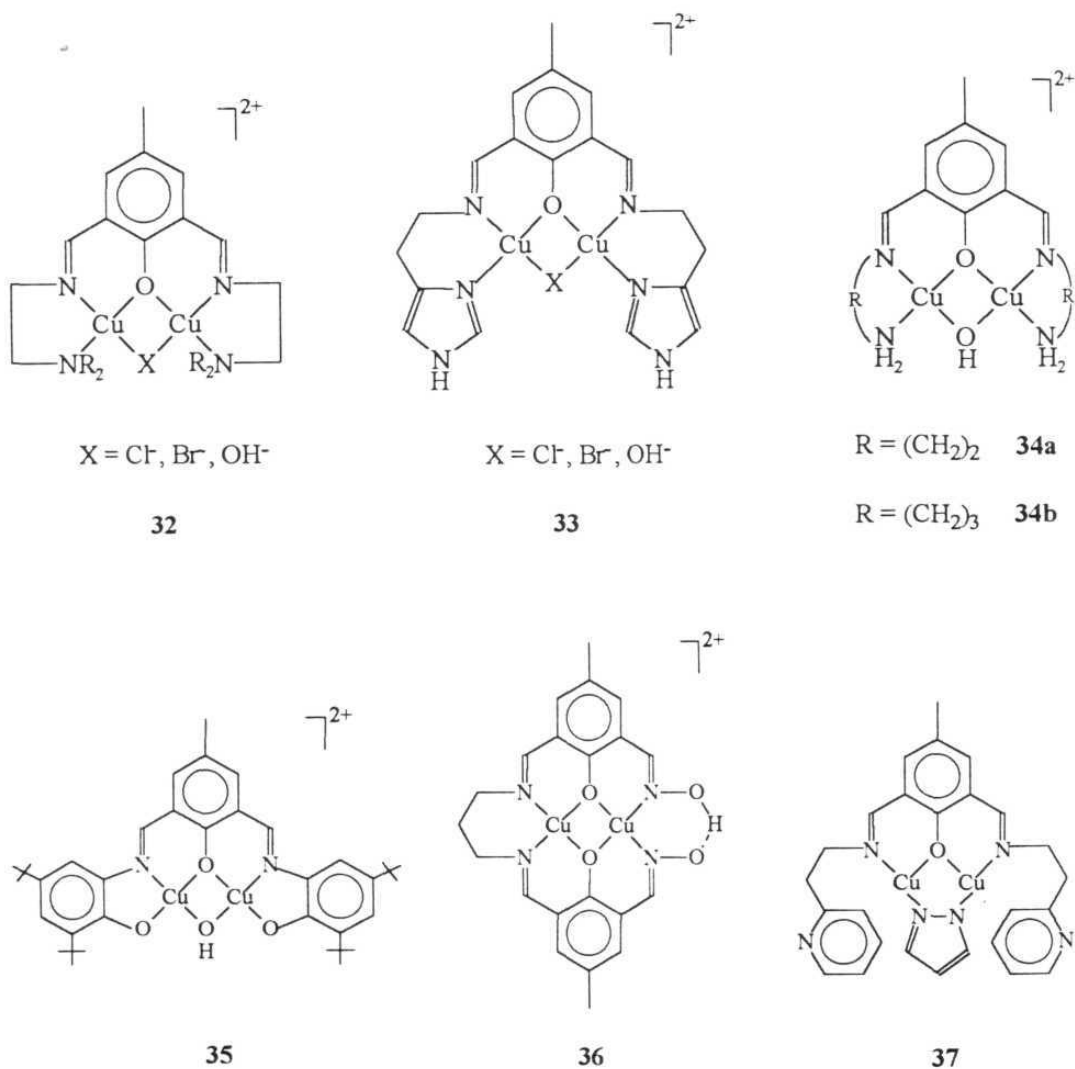
the EPR and electronic spectral data square-planar geometry was proposed for the metal center. The room-temperature magnetic moments per copper atom for the dinuclear complexes lie in the range  $\mu_{\text{eff}} = 0.8\text{-}1.2 \mu_{\text{B}}$ , showing antiferromagnetic interactions of varying intensities operative in these systems. The mononuclear complexes undergo quasi-reversible reduction at  $\sim -0.45 \text{ V}$  to  $\sim -0.58 \text{ V}$ . The dinuclear complexes undergo two one-electron reductions at two different potentials. The formal reduction potentials of the complexes are influenced by the nature of the substituents and the reduction occurs more easily with the electron-withdrawing groups.

Dinuclear Cu(II), Ni(II) complexes, **30** and Co(II) complexes, **31** of the ligand  $H_2L^{24}$  are catalytically active for the conversion of 3,5-di-*tert*-butyl catechol to 3,5-di-*tert*-butyl quinone. The redox properties of the homo and heterodinuclear complexes of ligand  $H_2L^{25}$  are influenced by the antiferromagnetic exchange interaction.<sup>48,49</sup>

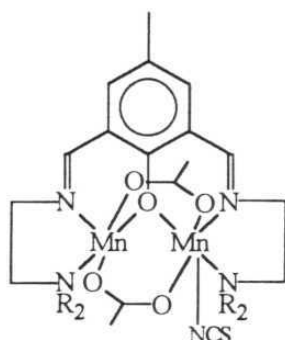


Dinuclear Cu(II) complexes, **32**, **33**, **34** and **35** bridged by OH / Cl or Br have been characterized.<sup>50-54</sup> Magnetic data on complexes **32** showed an increase in the antiferromagnetic interaction in the order OH >> Cl > Br. The lower magnetic moment in **34a** compared to **34b** was explained based on greater flexibility of 1,3-diaminopropane which increases the Cu-O-Cu angle thus influencing the interaction.

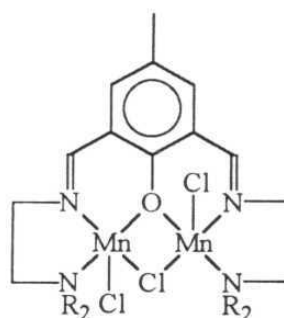
Dinuclear Cu(II) complex,<sup>55</sup> **36** and dinuclear Cu(I) complex, **37** are structurally characterized. The geometry around each copper in complex **37** is distorted pyramidal.<sup>56</sup>



Comparison of the magnetic data on two different types of Mn(II) complexes,  $[\text{Mn}_2\text{L}^{26}(\text{CH}_3\text{COO})_2(\text{NCS})]$ , **38** and  $[\text{Mn}_2\text{L}^{26}\text{Cl}_3]$ , **39** indicated antiferromagnetic exchange ( $J = -2$  to  $-5 \text{ cm}^{-1}$ ) for acetate bridged complexes and no appreciable interaction in the chloride complexes.<sup>57</sup>

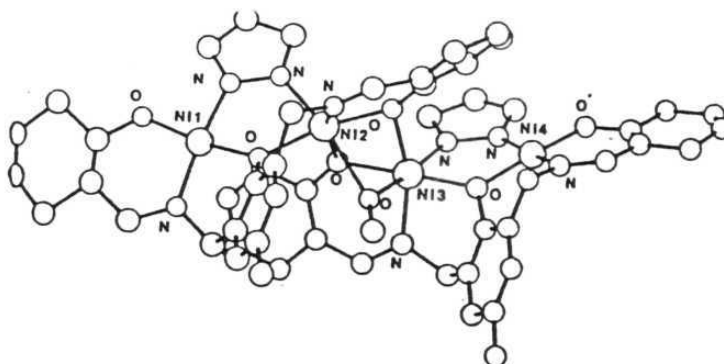


38



39

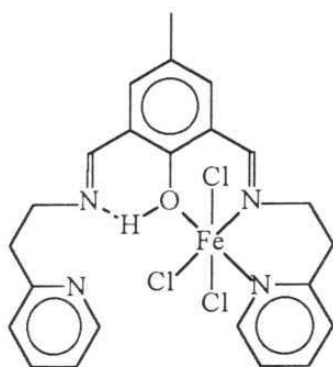
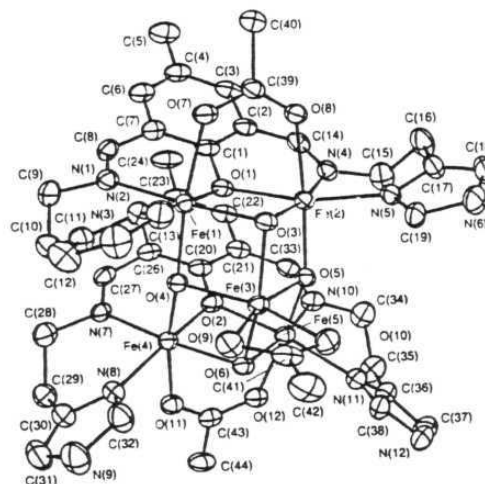
The tetranuclear  $[\text{Co}_2\text{L}^{27}(\text{OH})(\text{CH}_3\text{COO})]_2$  complex with two  $[\text{Co}_2\text{L}^{27}(\text{OH})(\text{CH}_3\text{COO})]$  moieties bridged by two  $\mu_3$ -hydroxo oxygen atoms,<sup>58</sup> a tetranuclear  $[\text{NiL}^{27}(\text{pyrazolate})_2(\text{CH}_3\text{OH})]^{59}$  complex, **40** and a dodecanuclear  $[\text{Mn}_{12}(\text{L}^{27})_6(\text{OH})_4(\text{CH}_3\text{COO})_2]$  complex have been crystallographically characterized.<sup>60</sup> The lower magnetic moment value for the nickel complex, **40** has been explained in terms of magnetic interaction between the two paramagnetic nickel centers.<sup>59</sup>



40



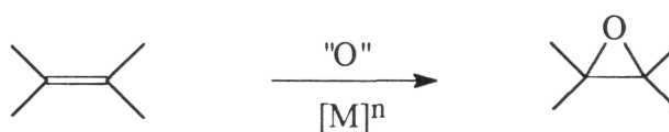
Mononuclear  $[\text{FeHL}^{28}\text{Cl}_3]$  complex, **41** and pentanuclear  $[\text{Fe}_5(\text{L}^{29})_2(\text{O})_4(\text{CH}_3\text{COO})_3](\text{ClO}_4)_2 \cdot 2\text{C}_2\text{H}_5\text{OH} \cdot \text{H}_2\text{O}$  complex, **42** are structurally characterized.<sup>61,62</sup>

**41****42**

### 1.3. Transition metal complexes as catalysts for epoxidation reactions

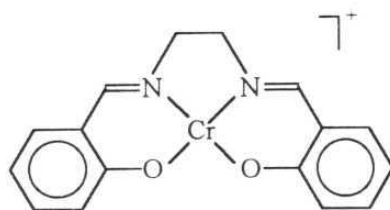
The use of transition metal complexes as catalysts for epoxidation reactions has received increased attention mainly to understand reactions of biological importance, for selective oxidation and for preparation of compounds with specific spatial structures.<sup>63</sup> Metalloporphyrins have been studied extensively owing to their direct relationship to enzymatic oxidation with cytochrome P-450.<sup>63</sup> These catalytic reactions are also mimicked by

non-porphyrin metal complexes of both cyclic and acyclic ligands with oxygen and nitrogen donor atoms. Complexes of Schiff bases, amides, polypyridyls, aminocarboxylates, cyclams and various other ligands have been used as oxidation catalysts.



The type of intermediate that is formed in the catalytic cycle depends on the metal center and the ligands. Quite often, a high-valent oxometal species is proposed as the reactive intermediate and the formation of this oxo species depends on the ability of the metal to acquire variable oxidation states. The shuttling of the metal complex between the two states corresponds to an oxidative addition followed by the reductive elimination. The redox potentials of the metal ion indicate the ease with which a metal ion can be converted from one oxidation state to another. At moderate redox potentials, higher catalytic activity is observed, *i.e.* the oxo species formed is neither stable nor highly reactive, thus enhancing the catalytic efficiency of the system. Catalytic efficiency can be tuned by varying the substituents on the ligands *i.e.* the ligand should stabilize the metal ion in variable oxidation states. As part of the work presented in the thesis deals with non-porphyrin metal complex catalyzed epoxidations, a brief survey on the research carried out in this field is presented.

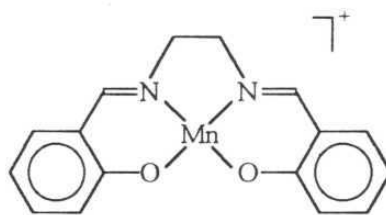
Cr(III) salen complexes, **43** were used as catalysts for epoxidation of various olefins.<sup>64</sup> The oxochromium(V) cation proposed as active intermediate was crystallographically characterized.<sup>65</sup> The stability of the oxo

**43**

species is greatly influenced by the substituents on the salen ligand. The  $\text{O}=\text{Cr}(\text{V})$  species is prone to coordination and addition of pyridine N-oxide immediately formed an adduct  $\text{O}=\text{Cr}(\text{Salen})(\text{PyO})^+$ . This axial ligation leads to the weakening of  $\text{Cr}=\text{O}$  bond, which accounts for the increased reactivity of the six-coordinate cation, relative to coordinatively unsaturated precursor. The mechanism of oxygen atom transfer involves the rate limiting attack on the olefin by the electrophilic oxochromium(V) cation. Formation of benzaldehyde as a byproduct, derived from pyridine oxide promoted  $\text{C}=\text{C}$  cleavage of styrene indicated presence of a transient intermediate during oxygen atom transfer.

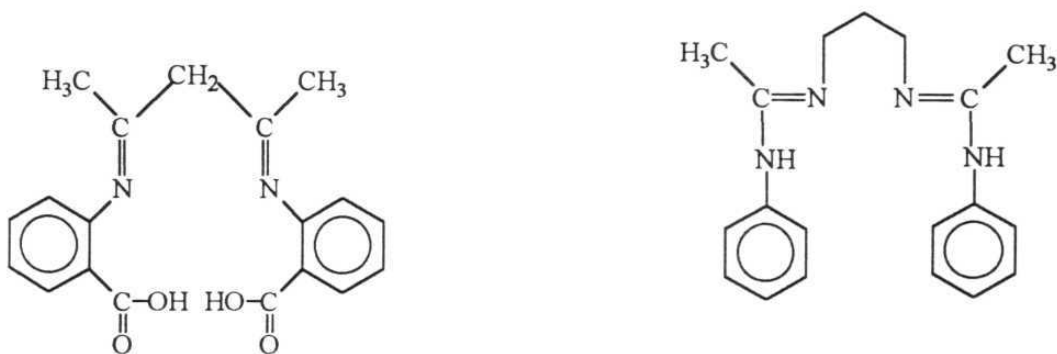
Analogous Mn(III) salen complexes, **44** were also used as catalysts for the epoxidation of various olefins using iodosylbenzene as terminal oxidant. Presence of electron-withdrawing groups on the salen ligand and addition of ligands like pyridine and pyridine N-oxide enhanced the catalytic activity. Based on the spectral data,  $\text{O}=\text{Mn}(\text{V})$  species was proposed as the

active intermediate. However, it was also observed that this species easily gets converted as  $\mu$ -oxo Mn(IV) dimer by ready combination with Mn(III) cations, thus reducing the catalytic efficiency of the system.<sup>66</sup>



44

Similar results were observed for another series of Mn(III) Schiff base complexes<sup>67</sup> using ligands shown in **45**. Cyclohexenol and cyclohexenone

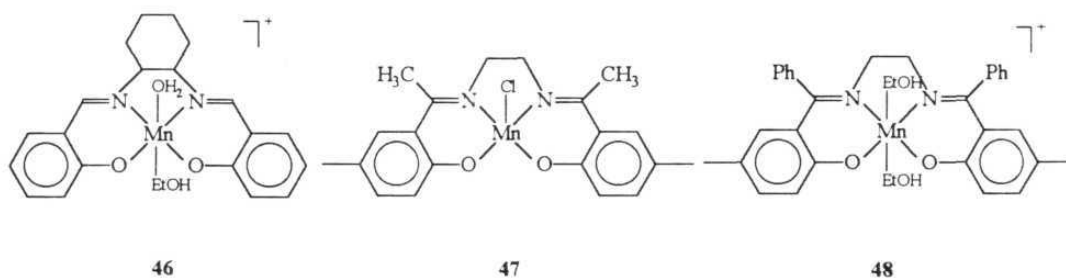


45

were also produced as a result of allylic oxidation. It was concluded that alkene was not rigidly coordinated to the metal center in the rate determining step based on the higher rate of epoxidation observed for norbornene,

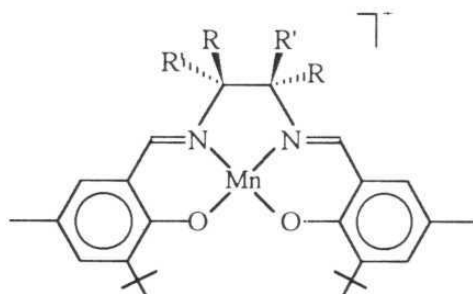
cyclooctene and cycloheptene relative to cyclohexene. Several other Mn(III) Schiff base complexes have also been reported to be active catalysts.<sup>68</sup>

Hodgson *et al.* have synthesized and crystallographically characterized [Mn(salency)(H<sub>2</sub>O)(C<sub>2</sub>H<sub>5</sub>OH)]ClO<sub>4</sub>, **46** [Mn(tetraMe-salen)Cl], **47** and [Mn(MePhsalen)(C<sub>2</sub>H<sub>5</sub>OH)]ClO<sub>4</sub>, **48** complexes. The higher catalytic



activity of six-coordinate complexes compared to five-coordinate complexes was explained based on the weaker axial coordination which would lead to the easy formation of the active intermediate O=Mn(V).<sup>69</sup>

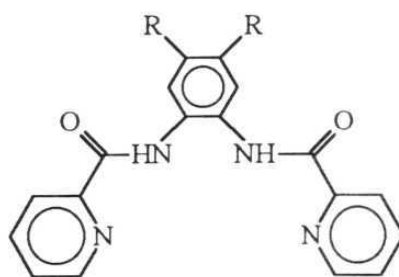
Jacobsen *et al.* synthesized Mn(III) complexes, **49** from chiral Schiff base ligands, obtained by the condensation of salicylaldehyde and (R,R) or (S,S)-1,2-diamino-1,2-diphenylethane. These complexes enantioselectively catalyze epoxidation of alkyl and aryl substituted olefins. Iodosylmesitylene and sodium hypochlorite have been used as oxygen source and enantioselectivity did not differ significantly by changing the oxygen source indicating common oxo intermediate as the active oxidant.<sup>70</sup>



49

Sharpless *et al.* reported epoxidation of allyl alcohols using titanium tetrakisopropoxide, (+) or (-) diethyl tartarate and *tert*-butyl hydroperoxide. This chiral epoxidation system is characterized by high enantioselectivity over a range of substitution patterns.<sup>71</sup>

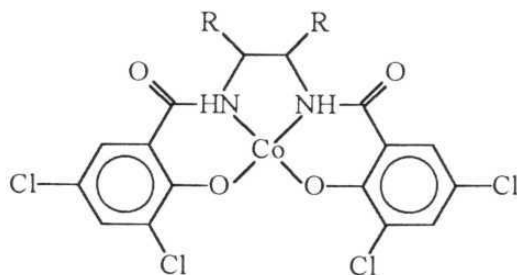
Cr(III) and Mn(III) amide complexes of 1,2-bis(pyridine-2-carboxamido)benzene and its substituents, **50** have been used as catalysts. It



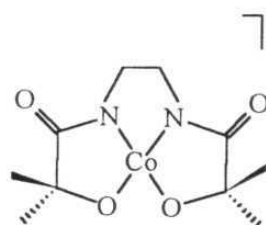
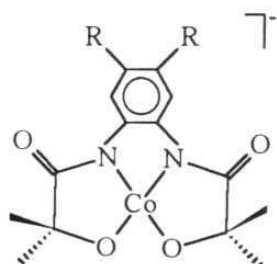
50

is observed that Mn(III) complexes were catalytically more active than Cr(III) complexes. An oxygen rebound mechanism involving O=Cr(V) and O=Mn(V) species was proposed for oxidation reaction.<sup>72</sup>

Cobalt(II) bis-salicylamide complexes, **51** are shown to be catalytically active for epoxidation of olefins using *tert*-butyl hydroperoxide (TBHP) and iodosylbenzene as terminal oxidants. As catalytic oxidation in presence of TBHP was inhibited by ionol (2,6-di-*tert*-butyl-*p*-cresol), it was proposed that a radical chain mechanism is operative where *tert*-butyl hydroperoxy radical adds homolytically to the double bond. Here cobalt catalysis is associated with Co(II)/Co(III) interconversion. With iodosylbenzene as terminal oxidant, an oxocobalt(IV) species was proposed as an active intermediate.<sup>73</sup> Square-planar Co(III) complexes, **52** of polyanionic chelating ligands have shown to be catalytically active for styrene.<sup>74</sup>

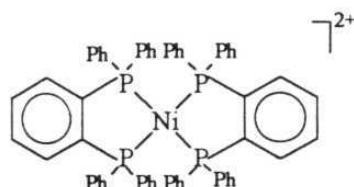
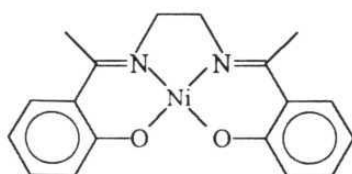
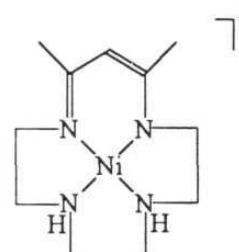
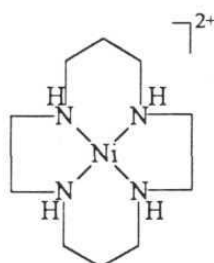
**51**

A wide range of Ni(II) complexes, **53** derived from tetraaza macrocycles, Schiff bases, porphyrins and bidentate phosphines have been examined for their catalytic activity. All the complexes convert iodosylbenzene to iodobenzene but only Ni(II) cyclam complexes, its



52

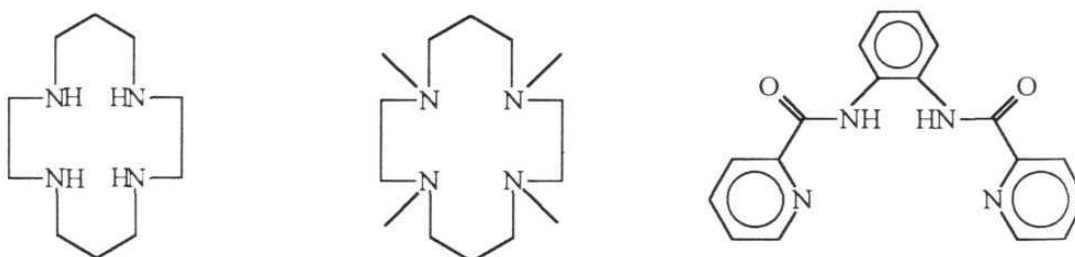
unsaturated analogues and Schiff bases gave modest yields of epoxide. The catalytic activity was ascribed to a reactive oxonickel(IV) intermediate which also reacts with the solvent, ligand system and readily forms the inactive ( $\mu$ -oxo)nickel(III) dimer thus reducing the catalytic efficiency of the system.<sup>75</sup>



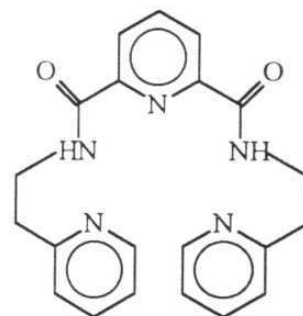
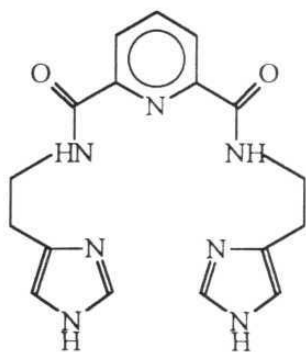
53



Iron(II) complexes of cyclam and related ligands, **54** were used as catalysts using 30%  $\text{H}_2\text{O}_2$  as oxygen source.<sup>76</sup> It was seen that Fe(II) cyclam complexes were effective as oxidation catalysts whereas N-substituted Fe(II) cyclam complexes and amide complexes were ineffective. The epoxidation reactions were stereoselective and only small amounts of allylic oxidation products were isolated.  $\text{HOO}^\cdot$  is proposed as the intermediate. When alkyl hydroperoxide was used as oxygen source, only allylic oxidation products were obtained while iodosylbenzene gave high yields of epoxides.

**54**

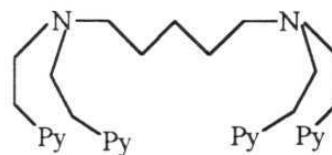
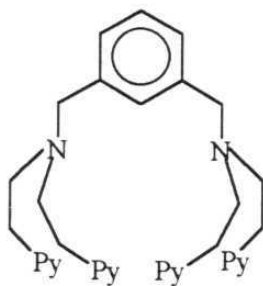
$\text{FeCl}_2$  and  $\text{Co}(\text{CH}_3\text{COO})_2$  with heterocyclic podand ligands  $\text{N,N}'$ -bis{2-(4-imidazolyl)ethyl}-2,6-pyridinedicarboxamide, **55** were used for catalytic epoxidation.<sup>77</sup> Molecular oxygen was used as an oxygen source without a co-reductant. A  $\mu$ -peroxo di-iron species is proposed as intermediate and the flexible heterocyclic multidentate ligand was considered to contribute mainly for the efficiency of the system.



55

Fe(III) complexes of chiral aminoacid-linked bipyridine macrocycle,<sup>78</sup> mono and dinuclear Fe(III) Schiff base complexes<sup>79,80</sup> are also reported to be active catalysts.

Valentine and coworkers examined dinuclear and mononuclear copper(II) complexes of ligands shown in **56** as catalysts.<sup>81</sup> Both the type of complexes react with iodosylbenzene to form iodosylbenzene complexes or

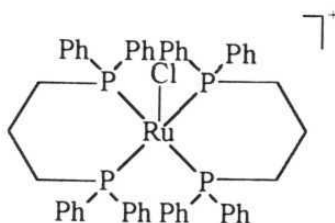


56

related species containing high-valent iodine, but the species formed from the dinuclear complexes only were effective for oxygen transfer to olefin. The active intermediate was not isolated but it was proposed that the dinuclear nature of the complexes played an important role in determining the reactivity of the active species.

$\text{RuCl}_3 \cdot n\text{H}_2\text{O}$  or  $\text{FeSO}_4$  with bipyridyl or phenanthroline ligands catalyze epoxidation of stilbenes by potassium periodate or sodium hypochlorite.<sup>82</sup> It was observed that in the presence of  $\text{RuCl}_3$ , electron rich ligands slow down the rate of reaction and improve the selectivity and yield. With  $\text{FeSO}_4$ , epoxidation of *trans*-stilbene in presence of periodate was observed with lower rate and higher selectivity. It was also observed that electrophilicity and reactivity of an oxoiron intermediate could be markedly enhanced by using diimine ligands bearing electron-withdrawing groups.

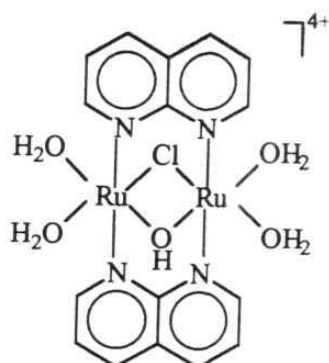
Coordinatively unsaturated complexes of Ru(II) of the type,  $[\text{RuClL}_2]^+$ , **57** where L = 1,3-bis(diphenylphosphino)propane effectively promoted the epoxidation of olefins in the presence of iodosylbenzene.<sup>83</sup>



Competition from oxidative cleavage and allylic cleavage was observed. Coordinating solvents like  $\text{CH}_3\text{CN}$  inactivated the catalyst forming coordinatively saturated  $[\text{RuCl}(\text{CH}_3\text{CN})\text{L}_2]^+$  adducts. A reactive  $\text{O}=\text{Ru}(\text{IV})$  species was proposed as the intermediate which reacts with iodosylbenzene to form iodoxybenzene and with phosphine ligands to give phosphine oxide in addition to epoxides. Kinetic experiments indicated that the alkene binds to oxometal species, forming a relatively stable intermediate, the decomposition of this species represents the rate determining step.

A high-valent paramagnetic ruthenium(IV) complex,<sup>84</sup>  $[\text{Ru}(\text{chbae})(\text{PPh}_3)(\text{py})]$  ( $\text{chbae}$  = 1,2-bis(3,5-dichloro-2-hydroxybenzamido)-ethane and ruthenium(III) complexes,<sup>85</sup> *trans*- $[\text{Ru}(\text{bpy})_2(\text{OH})(\text{H}_2\text{O})](\text{ClO}_4)_2$  and *trans*- $[\text{Ru}(\text{phen})_2(\text{OH})(\text{H}_2\text{O})](\text{ClO}_4)_2$  have also been shown to be catalytically active for epoxidation of cyclohexene, styrene and norbornene.

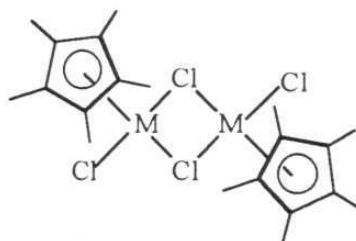
Mono and dinuclear Ru(III) Schiff base complexes,<sup>86,87</sup> Ru(III) amide complex,<sup>88</sup>  $[\text{Ru}(\text{III})(\text{bbpc})(\text{PPh}_3)\text{Cl}]$  ( $\text{bbpc}$  = 1,2-bis(4-*tert*-butyl-pyridine-2-



carboxamido)-4,5-dichlorobenzene),  $[\text{Ru(IV)(bpy)}_2(\text{py})(\text{O})]^{2+}$  complex,<sup>89</sup> chiral monooxoRu(IV) complex,<sup>90</sup>  $[\text{RuL}(\text{bpy})\text{O}]^{2+}$  ( $\text{L} = 2,6\text{-bis}[(4\text{S},7\text{R})\text{-}7,8,8\text{-trimethyl-}4,5,6,7\text{-tetrahydro-}4,7\text{-methanoindazol-}2\text{-yl}]\text{pyridine}$ ) and dinuclear Ru(III) complex,  $[\text{Ru}_2(\text{napy})_2(\text{H}_2\text{O})_4\text{Cl}(\text{OH})](\text{ClO}_4)_4$ ,<sup>91</sup> **58** ( $\text{napy} = 1,8\text{ naphthyridine}$ ) have also been shown to catalyze epoxidation of olefins in presence of various oxygen donors.

#### 1.4. Pentamethylcyclopentadienyl complexes of Rh(III) and Ir(III)

The pentamethylcyclopentadienyl ( $\text{Cp}^*$ ) complexes of rhodium and iridium have been studied extensively because these complexes act as homogenous catalysts for hydrogenation of alkenes and arenes.<sup>92</sup> The first  $\text{Cp}^*$  complex of rhodium was obtained by the reaction of  $\text{RhCl}_3$  with hexamethylbicyclo[2.2.0]hexa-2,5-diene.<sup>93,94</sup> Analogous iridium complex was also synthesized in the similar way. The complexes are crystallographically characterized and the structure is shown in **59**.<sup>95</sup> The complexes are stable and highly reactive. The stability arises from the strong  $\text{Cp}^*\text{-M}$  bond which survives acidic, basic as well as reducing and oxidizing conditions. The steric bulk of  $\text{Cp}^*$  also adds some kinetic stability to the otherwise reactive metal center. The ready cleavage of the halide bridge by various ligands allows preparation of monomeric complexes. As the work presented in chapter 4 deals with  $\text{Cp}^*\text{Rh}$  and  $\text{Cp}^*\text{Ir}$  polypyridyl complexes, a very brief literature survey on  $\text{Cp}^*\text{-Rh}$  and  $\text{Cp}^*\text{-Ir}$  complexes is presented.



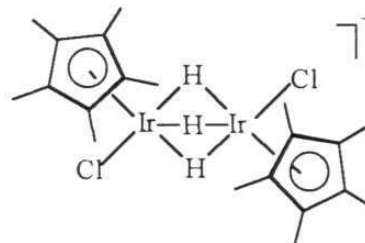
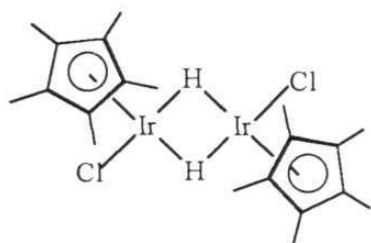
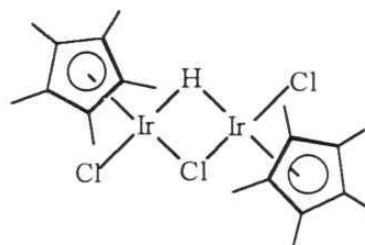
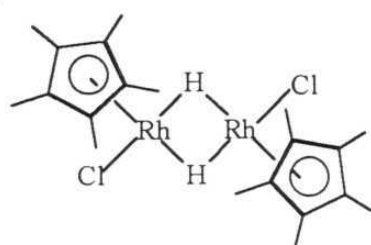
M = Rh(III) or Ir(III)

59

The new Cp\* complexes are generally synthesized from the basic  $[\text{Cp}^*\text{M}(\mu\text{-Cl})\text{Cl}]_2$  complexes. These complexes undergo metathetical replacement of the chloride ligands on reaction with NaBr and NaI in methanol.<sup>96,93</sup> The bromide and iodide complexes are shown to be isostructural with the chloro analog.<sup>97,98</sup> The  $\text{N}_3$ , NCO and SCN bridged complexes are also proposed to have similar structures.<sup>99</sup>

A number of Cp\*Rh(III) and Cp\*Ir(III) complexes of the type  $[\text{Cp}^*\text{MX}_2]$  (M = Rh, Ir, X = Cl, Br, I; M = Rh, X =  $\text{NO}_3$ ) have been used as catalysts for hydrogenation of olefins under ambient conditions.<sup>100</sup>

A range of hydrides have been prepared by the reaction of dimer with ethanolic base.<sup>92,101-103</sup> These complexes catalyze hydrogenation of alkenes and arenes in the presence of co-catalyst like  $\text{Et}_3\text{N}$ . The structure of various hydride complexes are shown in 60. Catalytic activity decreases with increasing hydrogen bridging and was explained in terms of kinetic inertness of bridging hydrides and the mechanism of hydrogenation involving



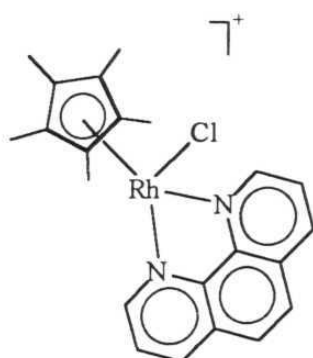
$[\text{Cp}^*\text{M}(\text{H})_2\text{solvent}]$  was proposed. Hydride complexes of the type  $[\text{Cp}^*\text{Rh}(\text{H})_2(\text{PMe}_3)]$  and  $[\text{Cp}^*\text{IrHCl}(\text{PMe}_3)]$  are also reported.<sup>104,92</sup>

Reaction of Rh(III) and Ir(III) dimers with trimethylphosphine and various other substituted phosphines gave adducts of the type  $[\text{Cp}^*\text{MLCl}_2]$  which react with silver acetate to give  $[\text{Cp}^*\text{M}(\text{PMe}_3)(\text{CH}_3\text{COO})_2]$ . The rhodium complex was crystallographically characterized.<sup>105</sup>

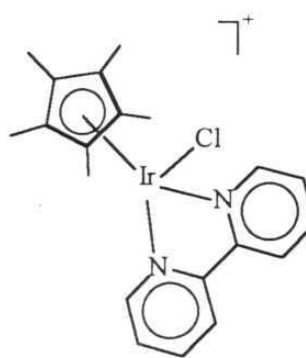
Several Rh(III) and Ir(III) complexes containing N-N donors were synthesized by the reaction of ligands on the dimer. The  $[\text{Cp}^*\text{Rh}(\text{phen})\text{Cl}]\text{Cl}$ , **61** and  $[\text{Cp}^*\text{Ir}(\text{bpy})\text{Cl}]\text{Cl}$ , **62** complexes have been crystallographically characterized.<sup>106</sup> The complex  $[\text{Cp}^*\text{Rh}(\text{bpy})\text{Cl}]\text{Cl}$  is shown to catalyze proton reduction *via* hydride intermediate.<sup>107</sup> Substituted 2,2'-bipyridyl complexes were studied as redox catalysts for chemical and electrochemical  $\text{NAD(P)}^+$

reduction.<sup>108</sup> The electrochemically reduced complexes are proposed to act as hydride ion transfer agents. The catalytic efficiency is decreased by electron-withdrawing substituents on the 2,2'-bipyridyl ligands while it is increased by electron-donating substituents.

The bis-4,4'-[bis(pyrrol-1-ylmethyl)methoxycarbonyl]-2,2'-bipyridine complex of rhodium was electropolymerized on carbon electrode, and the polymer coated electrode catalyzes hydrogen evolution from aqueous



61



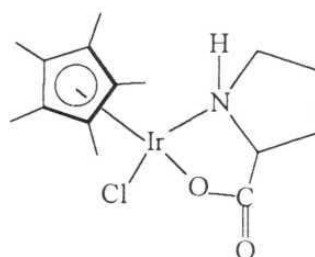
62

solutions.<sup>109</sup> The two electron reduction of  $[\text{Cp}^*\text{Ir}(\text{bpy})\text{Cl}]\text{Cl}$  complex gave a highly reactive  $[\text{Cp}^*\text{Ir}(\text{bpy})]$  which was protonated to  $[\text{Cp}^*\text{Ir}(\text{bpy})\text{H}]^+$ , a presumed intermediate in the photolytic production of hydrogen.<sup>110</sup> The  $[\text{Cp}^*\text{Ir}(\text{bpy})\text{H}]^+$ ,  $[\text{Cp}^*\text{Ir}(\text{phen})\text{Cl}]^+$  and  $[\text{Cp}^*\text{Ir}(\text{bpy})\text{Cl}]^+$  have been shown to be active catalysts for the light driven water gas shift reaction.<sup>111</sup>



In addition to these, complexes from several other N-N donors like 2,2'-bipyrazine, 2,2'-bipyrimidine, *o*-phenylenediamine, ethylenediamine, adenine and  $\text{NAD}^+$  were reported.<sup>112-114</sup>

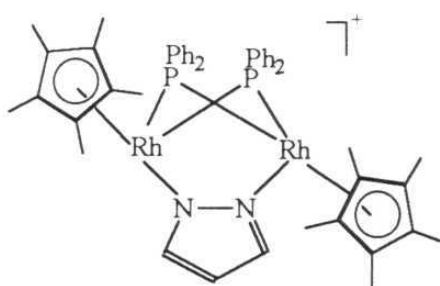
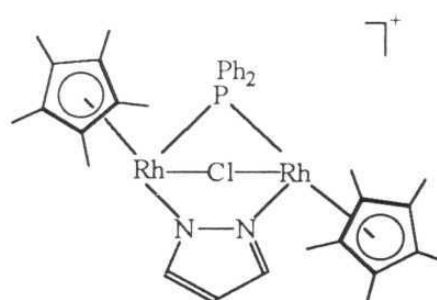
Optically active aminoacid complexes of Rh(III) and Ir(III) where the aminoacid acts as a chelating monoanionic N-O donor were synthesized by the reaction of aminoacid with the dimers. The  $[\text{Cp}^*\text{Ir}(\text{L-proline})\text{Cl}]$ , **63** complex was crystallographically characterized.<sup>115</sup> Complexes were also synthesized and studied from other aminoacids.<sup>116</sup> Air stable unsaturated sixteen electron  $\text{Cp}^*\text{Ir}$  aminoacid complexes were synthesized by the reaction of the dimer with the aminoacid bearing electron-withdrawing groups on nitrogen. The crystal structure of (R)-N-tosylphenylglycine derivative was determined. The short N-Ir and O-Ir bonds suggested stabilization of unsaturated Ir(III) by  $\pi$ -donation. Addition of ligands such as  $\text{PPh}_3$ , CO, primary aliphatic amines and heterocyclic amines gave complexes of the type, where aminoacid side chain and  $\text{Cp}^*$  are *cis* to each other.<sup>117</sup>



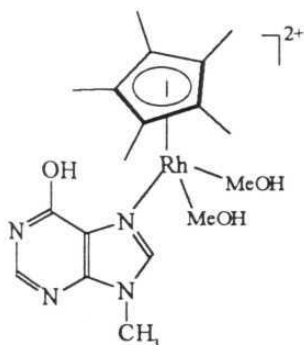
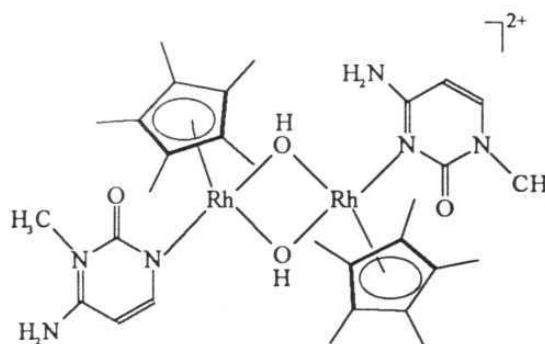
63

Reaction of pyridine-2-carboxylic acid, pyrones and pyridinones with  $[\text{Cp}^*\text{Rh}(\mu\text{-Cl})\text{Cl}]_2$ , in presence of sodium methoxide gave water soluble

complexes of the type  $[\text{Cp}^*\text{RhLCl}]$ .<sup>118</sup> The complexes where L is pyridine-2-carboxylic acid or 2-methylpyran-4-one have been crystallographically characterized. The complexes  $[\{\text{Cp}^*\text{Rh}\}_2(\mu\text{-pz})(\mu\text{-PPh}_2)_2]\text{BF}_4$ , **64** and  $[\{\text{Cp}^*\text{Rh}\}_2(\mu\text{-pz})(\mu\text{-Cl})(\mu\text{-PPh}_2)]\text{BF}_4$ , **65** are structurally characterized.<sup>119</sup>

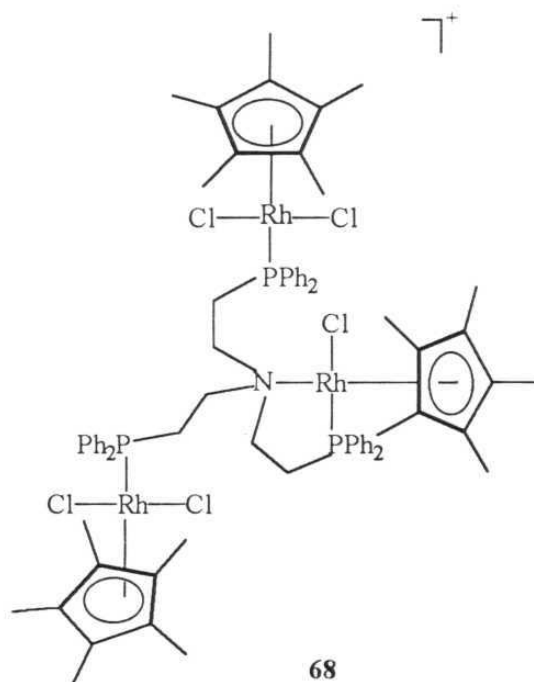
**64****65**

Reaction of aqua complex,  $[\text{Cp}^*\text{Rh}(\text{H}_2\text{O})_2(\text{OTf})_2]_x$  with guanosine and 1-methylcytosine were studied in methanol and aqueous solutions and it

**66****67**

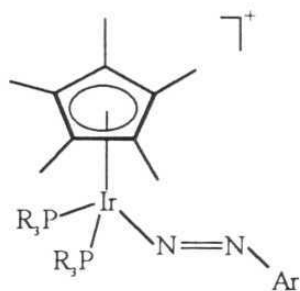
was observed that the structure of Cp\*Rh nucleobase depends on the reaction medium. The complexes  $[\text{Cp}^*\text{Rh}(\eta^1(\text{N}7)\text{-9-methylhypoxanthine})(\text{CH}_3\text{OH})_2](\text{OTf})_2$ , **66** and  $[\text{Cp}^*\text{Rh}(\eta^1(\text{N}3)\text{-1-methylcytosine})(\mu\text{-OH})]_2^{2+}$ , **67** were structurally characterized.<sup>120</sup>

Cationic complexes were synthesized by the reaction of bidentate ligands  $\text{R}_2\text{N}(\text{CH}_2)_n\text{PR}_2$  with  $[\text{Cp}^*\text{Rh}(\mu\text{-X})\text{X}]_2$  in the presence of  $\text{NaBPh}_4$ .<sup>121</sup>

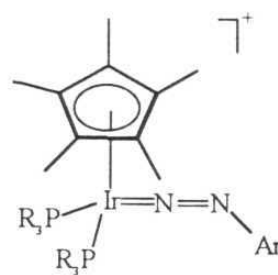


With terdentate ligands  $\text{Y}(\text{CH}_2\text{CH}_2\text{PPh}_2)_3$  ( $\text{Y} = \text{P}$  or  $\text{N}$ ) the trinuclear complex was obtained. Addition of chloride to **68** gave neutral complex. Complexes of aryldiazenido ligands with doubly-bent geometry,  $[\text{Cp}^*\text{Ir}(\text{PMe}_3)_2(\text{N}_2\text{Ar})](\text{BF}_4)$ , **69** and singly-bent geometry,  $[\text{Cp}^*\text{Ir}\{\text{P}(p\text{-tol})_3\}(\text{N}_2\text{Ar})]\text{BF}_4$ , **70** have been structurally characterized.<sup>122</sup>

Reactions of rhodium and iridium dimers with excess  $\text{H}_2\text{S}$  gas gave

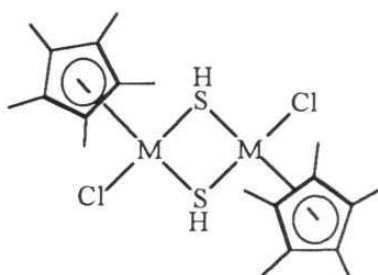


69



70

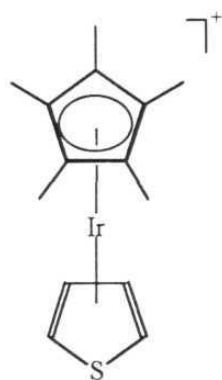
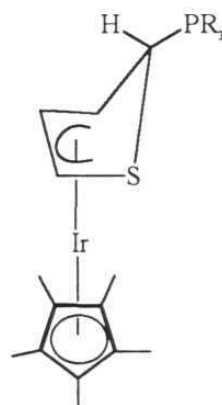
hydrosulfido-bridged dirhodium and diiridium complexes  $[\text{Cp}^*\text{MCl}(\mu_2\text{-SH})_2\text{MCp}^*\text{Cl}]$ , **71**. Treatment of these with  $\text{Et}_3\text{N}$  gave cuboidal sulphido clusters,  $[(\text{Cp}^*\text{M})_4(\mu_3\text{-S})_4]$ .<sup>123</sup>



71

Extensive studies of thiophene bound to  $[\text{Cp}^*\text{Ir}]$  as models for hydrodesulfurization are reported. The triacetone complex,  $[\text{Cp}^*\text{Ir}(\text{acetone})_3]$  reacts with thiophene to give **72** where thiophene is planar.<sup>124</sup> Reaction of **72**

with  $\text{PR}_3$  gave  $\eta\text{-C}_4\text{H}_5\text{S}$  complex, **73**. Similar type of reactions were reported with benzothiophene also.<sup>125</sup>

**72****73**

In addition to these reactions, several other compounds have been reported in the literature.<sup>126,127</sup> These reactions illustrate the diversity of both rhodium and iridium complexes that can be generated from  $[\text{Cp}^*\text{M}(\mu\text{-X})\text{X}]_2$ .

## 1.5. References

1. Fenton, D. E. in Sykes, A. G. (Ed.), *Advances in Inorganic and Bioinorganic Mechanisms* Academic press, London, 1983, Vol. **2**, p 187.
2. Karlin, K. D. and Zubieta, J. *Biological and Inorganic Copper chemistry* Adenine Press, 1986, Vol. **1** and **2**.
3. Urbach, F. L. in Sigel, H. (Ed.), *Metal ions in Biological systems* Marcel Dekker, Basle, 1981, Vol. **13** p 73 and references cited therein.
4. LuBien, C. D.; Winkler, M. E.; Thamann, T. J.; Scott, R. A.; Co, M. S.; Hodgson, K. O.; Solomon, E. I. *J. Am. Chem. Soc.* 1981, **103**, 7014.
5. Calabrese, L.; Cocco, D.; Desideri, A. *FEBS Lett.* 1979, **106**, 142.
6. Mutterties, E. L.; Rhodin, T. N.; Band, E.; Brucker, G. F.; Pretzer, W. *R. Chem. Rev.* 1979, **79**, 91.
7. Guerriero, P.; Tamburini, S.; Vigato, P. A. *Coord. Chem. Rev.* 1995, **139**, 17. Vigato, P. A.; Tamburini, S.; Fenton, D. E. *Coord. Chem. Rev.* 1990, **106**, 25. Zanello, P.; Tamburini, S.; Vigato, P. A.; Mazzocchin, G. A. *Coord. Chem. Rev.* 1987, **77**, 165.
8. Pilkington, N. H.; Robson, R. *Aust. J. Chem.* 1970, **23**, 2225.
9. Lambert, S. L.; Hendrickson, D. N. *Inorg. Chem.* 1979, **18**, 2683.
10. Hoskins, B. F.; Meheod, N. J.; Schaap, H. A. *Aust. J. Chem.* 1976, **29**, 515.

11. Hoskins, B. F.; Williams, G. A. *Aust. J. Chem.* 1975, **28**, 2607.
12. Mandal, S. K.; Thompson, L. K.; Newlands, M. J.; Gabe, E. J.; Nag, K. *Inorg. Chem.* 1990, **29**, 1324.
13. Mandal, S. K.; Thompson, L. K.; Newlands, M. J.; Gabe, E. J. *Inorg. Chem.* 1989, **28**, 3707.
14. Spiro, C. L.; Lambert, S. L.; Smith, T. J.; Duesler, E. N.; Gagne, R. R.; Hendrickson, D. N. *Inorg. Chem.* 1981, **20**, 1229.
15. Okawa, H.; Kida, S. *Bull. Chem. Soc. Jpn.* 1972, **45**, 1759.
16. Rao, R. K. Ch.; Zacharias, P. S. *Polyhedron* 1996, **16**, 1201.
17. Adams, H.; Bailey, N. A.; Bertrand, P.; Rodriguez de Barbarin, C. O.; Fenton, D. E.; Gou, S. *J. Chem. Soc., Dalton Trans.* 1995, 275.
18. Atkins, A. J.; Black, D.; Blake, A. J.; Marin-Becerra, A.; Parsons, S.; Ramirez, I.; Schroder, M. *Chem. Commun.* 1996, 457.
19. Carlisle, W. D.; Fenton, D. E.; Roberts, P. B.; Casellato, U.; Vigato, P. A.; Graziani, R. *Transition Met. Chem.* 1986, **11**, 292.
20. Mandal, S. K.; Nag, K. *J. Chem. Soc., Dalton Trans.* 1983, 2429.
21. Lacroix, P.; Kahn, O.; Theobald, F.; Leroy, J.; Wakselman, C. *Inorg. Chim. Acta.* 1988, **142**, 129.
22. Gagne, R. R.; Spiro, C. L.; Smith, T. J.; Hamann, C. A.; Thies, W. R.; Shiemke, A. K. *J. Am. Chem. Soc.* 1981, **103**, 4073.

23. Gagne, R. R.; Koval, C. A.; Smith, T. J. *J. Am. Chem. Soc.* 1977, **99**, 8367.
24. Gagne, R. R.; Koval, C. A.; Smith, T. J.; Cimolino, M. C. *J. Am. Chem. Soc.* 1979, **101**, 4571.
25. Gagne, R. R.; Henling, L. M.; Kistenmacher, T. J. *Inorg. Chem.* 1980, **19**, 1226.
26. Addison, A. W. *Inorg. Nucl. Chem. Lett.* 1976, **12**, 899.
27. Long, R. C.; Hendrickson, D. N. *J. Am. Chem. Soc.* 1983, **105**, 1513.
28. Tandon, S. S.; Thompson, L. K.; Bridson, J. N.; Mckee, V.; Downward, A. J. *Inorg. Chem.* 1992, **31**, 4635.
29. Downard, A. J.; Mckee, V.; Tandon, S. S. *Inorg. Chim. Acta.* 1990, **173**, 181.
30. Wada, H.; Motoda, K.; Ohba, M.; Sakiyama, H.; Matsumoto, N.; Okawa, H. *Bull. Chem. Soc. Jpn.* 1995, **68**, 1105.
31. Ikawa, Y.; Nagata, T.; Maruyama, K. *Chem. Lett.* 1993, 1049.
32. Timken, M. D.; Marrit, W. A.; Hendrickson, D. N.; Gagne, R. R.; Sinn, E. *Inorg. Chem.* 1985, **24**, 4202.
33. McKee, V.; Tandon, S. S. *J. Chem. Soc., Dalton Trans.* 1991, 221.  
McKee, V.; Tandon, S. S. *J. Chem. Soc., Chem. Commun.* 1988, 385.  
McKee, V.; Tandon, S. S. *Inorg. Chem.* 1989, **28**, 2901.
34. Sakiyama, H.; Motoda, K.; Okawa, H.; Kida, S. *Chem. Lett.* 1991, 1133.



35. Luneau, D.; Savariault, J.-M.; Cassoux, P.; Tuchagues, J.-P. *J. Chem. Soc., Dalton Trans.* 1988, 1225.
36. Mckee, V.; Tandon, S. S. *J. Chem. Soc., Chem. Commun.* 1988, 1334.
37. Sakiyama, H.; Tokuyama, K.; Matsumura, Y.; Okawa, H. *J. Chem. Soc., Dalton Trans.* 1993, 2329.
38. Bell, M.; Edwards, A. J.; Hoskins, B. F.; Kachab, E. H.; Robson, R. *J. Am. Chem. Soc.* 1989, **111**, 3603. Edwards, A. J.; Hoskins, B. F.; Kachab, E. H.; Markiewicz, A.; Murray, K. S.; Robson, R. *Inorg. Chem.* 1992, **31**, 3585.
39. Tandon, S. S.; Thompson, L. K.; Bridson, J. N.; Benelli, C. *Inorg. Chem.* 1995, **34**, 5507.
40. Hoskins, B. F.; Robson, R.; Smith, P. *J. Chem. Soc., Chem. Commun.* 1990, 488.
41. Lambert, S. L.; Spiro, C. L.; Gagne, R. R.; Hendrickson, D. N. *Inorg. Chem.* 1982, **21**, 68.
42. Tadokoro, M.; Okawa, H.; Matsumoto, N.; Koikawa, M.; Kida, S. *J. Chem. Soc., Dalton Trans.* 1991, 1657.
43. Okawa, H.; Nishio, J.; Ohba, M.; Tadokoro, M.; Matsumoto, N.; Koikawa, M.; Kida, S.; Fenton, D. E. *Inorg. Chem.* 1993, **32**, 2949.
44. Ohtsuka, S.; Kodera, M.; Motoda, K.; Ohba, M.; Okawa, H. *J. Chem. Soc., Dalton Trans.* 1995, 2599.

45. Mandal, S. K.; Nag, K. *Inorg. Chem.* 1983, **22**, 2567.
46. Adhikary, B.; Biswas, A. K.; Nag, K.; Zanello, P.; Cinquantini, A. *Polyhedron* 1987, **6**, 897.
47. Adhikary, B.; Mandal, S. K.; Nag, K. *J. Chem. Soc., Dalton Trans.* 1988, 935.
48. Srinivas, B.; Arulsamy, N.; Zacharias, P. S. *Polyhedron* 1991, **10**, 737.
49. Srinivas, B.; Zacharias, P. S. *Can. J. Chem.* 1992, **70**, 2906.
50. Okawa, H.; Tokii, T.; Nonaka, Y.; Muto, Y.; Kida, S. *Bull. Chem. Soc. Jpn.* 1973, **46**, 1462.
51. Mandal, S. K.; Nag, K. *J. Chem. Soc., Dalton Trans.* 1984, 2141.
52. Maekawa, M.; Kitagawa, S.; Munakata, M.; Masuda, H. *Inorg. Chem.* 1989, **28**, 1904.
53. Okawa, H.; Kida, S.; Muto, Y.; Tokii, T. *Bull. Chem. Soc. Jpn.* 1972, **45**, 2480.
54. Bond, A. M.; Haga, M.; Creece, I. S.; Robson, R.; Wilson, J. C. *Inorg. Chem.* 1989, **28**, 559.
55. Rybak-Akimova, E. V.; Busch, D. H.; Kahol, P.; Pinto, N.; Alcock, N.; Clase, H. J. *Inorg. Chem.* 1997, **36**, 510.
56. Gagne, R. R.; Kreh, R. P.; Dodge, J. A. *J. Am. Chem. Soc.* 1979, **101**, 6917.

57. Sakiyama, H.; Tamaki, H.; Koderu, M.; Matsumoto, N.; Okawa, H. *J. Chem. Soc., Dalton Trans.* 1993, 591. Higuchi, C.; Sakiyama, H.; Okawa, H.; Isobe, R.; Fenton, D. E. *J. Chem. Soc., Dalton Trans.* 1994, 1097.
58. Hoskins, B.; Robson, R.; Vince, D. *J. Chem. Soc., Chem. Commun.* 1973, 392.
59. Mikuriya, M.; Nakadera, K.; Kotera, T. *Chem. Lett.* 1993, 637.
60. Luneau, D.; Savariault, J.-M.; Tuchagues, J.-P. *Inorg. Chem.* 1988, **27**, 3912.
61. Mikuriya, M.; Kushida, K.; Nakayama, H.; Mori, W.; Kishita, M. *Inorg. Chim. Acta.* 1989, **165**, 35.
62. Mikuriya, M.; Hashimoto, Y.; Nakashima, S. *Chem. Commun.* 1996, 295.
63. Jorgensen, K. A. *Chem. Rev.* 1989, **89**, 431.
64. Samsel, E. G.; Srinivasan, K.; Kochi, J. K. *J. Am. Chem. Soc.* 1985, **107**, 7606. Srinivasan, K.; Kochi, J. K. *Inorg. Chem.* 1985, **24**, 4671.
65. Siddall, T. L.; Miyaara, N.; Huffman, J. C.; Kochi, J. K. *J. Chem. Soc., Chem. Commun.* 1983, 1185.
66. Srinivasan, K.; Michaud, P.; Kochi, J. K. *J. Am. Chem. Soc.* 1986, **108**, 2309.
67. Agarwal, D. D.; Bhatnagar, R. P.; Jain, R.; Srivatsava, S. *J. Chem. Soc., Perkin Trans. 2* 1990, 989.

68. Trivedi, B. M.; Bhattacharya, P. K.; Ganeshpure, P. A.; Satish, S. *J. Mol. Catal.* 1992, **75**, 109.
69. Oki, A. R.; Hodgson, D. J. *Inorg. Chim. Acta.* 1990, **170**, 65.
70. Zhang, W.; Loebach, J. L.; Wilson, S. R.; Jacobsen E. N. *J. Am. Chem. Soc.* 1990, **112**, 2801. Zhang, W.; Jacobsen, E. N. *J. Org. Chem.* 1991, **56**, 2296.
71. Katsuki, T.; Sharpless, K. B. *J. Am. Chem. Soc.* 1980, **102**, 5974. Gao, Y.; Hanson, R. M.; Klunder, J. M.; Ko, S. Y.; Masamune, H.; Sharpless, K. B. *J. Am. Chem. Soc.* 1987, **109**, 5765. Finn, M. G.; Sharpless, K. B. *J. Am. Chem. Soc.* 1991, **113**, 113.
72. Leung, W. H.; Ma, J.-X.; Yam, V. W.-W.; Che, C.-M.; Ponn, C.-K. *J. Chem. Soc., Dalton Trans.* 1991, 1071. Che, C.-M.; Cheng, W.-K. *J. Chem. Soc., Chem. Commun.* 1986, 1443.
73. Koola, J. D.; Kochi, J. K. *J. Org. Chem.* 1987, **52**, 4545.
74. Collins, T. J.; Ozaki, S.; Richmond, T. G. *J. Chem. Soc., Chem. Commun.* 1987, 803.
75. Koola, J. D.; Kochi, J. K. *Inorg. Chem.* 1987, **26**, 908. Kinneary, J. F.; Albert, J. S.; Burrows, C. J. *J. Am. Chem. Soc.* 1988, **110**, 6124.
76. Nam, W.; Ho, R.; Valentine, J. S. *J. Am. Chem. Soc.* 1991, **113**, 7052.
77. Hirao, T.; Moriuchi, T.; Mikami, S.; Ikeda, I.; Ohshiro, Y. *Tetrahedron. Lett.* 1993, **34**, 1031.

78. Hopkins, R. B.; Hamilton, A. D. *J. Chem. Soc., Chem. Commun.* 1987, 171.
79. Jacob, M.; Bhattacharya, P. K.; Ganeshpure, P. A.; Satish, S.; Sivaram, S. *Bull. Chem. Soc. Jpn.* 1989, **62**, 1325.
80. Agarwal, D. D.; Bhatnagar, R. P.; Jain, R.; Srivastava, S. *J. Mol. Catal.* 1990, **59**, 389.
81. Tai, A. F.; Margerum, L. D.; Valentine, J. S. *J. Am. Chem. Soc.* 1986, **108**, 5006.
82. Eskenazi, C.; Balavoine, G.; Meunier, F.; Riviere, H. *J. Chem. Soc., Chem. Commun.* 1985, 1111. Balavoine, G.; Eskenazi, C.; Meunier, F.; Riviere, H. *Tetrahedron. Lett.* 1984, **25**, 3187.
83. Bressan, M.; Morvillo, A. *Inorg. Chem.* 1989, **28**, 950.
84. Che, C.-M.; Cheng, W.-K.; Leung, W.-H.; Mak, T. C. *J. Chem. Soc., Chem. Commun.* 1987, 418.
85. Che, C.-M.; Leung, W.-H.; Poon, C.-K. *J. Chem. Soc., Chem. Commun.* 1987, 173.
86. Upadhyay, M. J.; Bhattacharya, P. K.; Ganeshpure, P. A.; Satish, S. *J. Mol. Catal.* 1992, **73**, 277.
87. Leung, W.-H.; Che, C.-M. *Inorg. Chem.* 1989, **28**, 4619.
88. Ko, P.-H.; Chen, T.-Y.; Zhu, J.; Cheng, K.-F.; Peng, S.-M.; Che, C.-M. *J. Chem. Soc., Dalton Trans.* 1995, 2215.

89. Stultz, L. K.; Binstead, R. A.; Reynolds, M. S.; Meyer, T. J. *J. Am. Chem. Soc.* 1995, **117**, 2520.
90. Fung, W.-H.; Cheng, W.-C.; Yu, W.-Y.; Che, C.-M.; Mak, T. C. W. *J. Chem. Soc., Chem. Commun.* 1995, 2007.
91. Boelrijk, A. E. M.; Velzen, M. M.; Neenan, T. X.; Reedijk, J. Kooijman, H.; Spek, A. L. *J. Chem. Soc., Chem. Commun.* 1995, 2465.
92. Maitlis, P. M. *Acc. Chem. Res.* 1977, **11**, 301.
93. Kang, J. W.; Mosely, K.; Maitlis, P. M. *J. Am. Chem. Soc.* 1969, **91**, 5970.
94. Booth, B. L.; Haszeldine, R. N.; Hill, M. *J. Chem. Soc. A.* 1969, 1299.
95. Churchill, M. R.; Julis, S. A.; Rotella, F. J. *Inorg. Chem.* 1977, **16**, 1137.
96. Gill D. S.; Maitlis, P. M. *J. Organomet. Chem.* 1975, **87**, 359.
97. Churchill, M. R.; Julis, S. A.; *Inorg. Chem.* 1978, **17**, 3011.
98. Churchill, M. R.; Julis, S. A.; *Inorg. Chem.* 1979, **18**, 2918.
99. Rigby, W.; Bailey, P. M.; McCleverty, J. A.; Maitlis, P. M. *J. Chem. Soc., Dalton Trans.* 1979, 371.
100. Gill, D. S.; White, C.; Maitlis, P. M. *J. Chem. Soc., Dalton Trans.* 1978, 617.
101. White, C.; Gill, D. S.; Kang, J. W.; Lee, H.-B.; Maitlis, P. M. *J. Chem. Soc., Chem Commun.* 1971, 734. White, C.; Oliver, A. J.; Maitlis, P. M. *J. Chem. Soc., Dalton Trans.* 1973, 1901. Churchill, M. R.; Ni, S. W. *J. Am. Chem. Soc.* 1973, **95**, 2150.

102. Maitlis, P. M. *Chem. Soc. Rev.* 1981, **10**, 1.
103. Robertson, D. R.; Stephenson, T. A. *J. Chem. Soc., Dalton Trans.* 1978, 486.
104. Periana, R. A.; Bergman, R. G. *J. Am. Chem. Soc.* 1986, **108**, 7332. Jones, W. D.; Kuykendall, V. L. *Inorg. Chem.* 1991, **30**, 2615. Jones, W. D.; Feher, F. J. *J. Am. Chem. Soc.* 1984, **106**, 1650.
105. Isobe, K.; Bailey, P. M.; Maitlis, P. M. *J. Chem. Soc., Dalton Trans.* 1981, 2003.
106. Youinou, M.-J.; Zeissel, R. *J. Organomet. Chem.* 1989, **363**, 197.
107. Koella, U.; Graetzel, M.; *Angew. Chem. Int. Ed. Engl.* 1987, **26**, 567.
108. Steckhan, E.; Herrmann, S.; Ruppert, R.; Dietz, E.; Frede, M.; Spika, E. *Organometallics*, 1991, **10**, 1568. Steckhan, E.; Herrmann, S.; Thoemmes, J.; Wandray, C.; Ruppert, R. *Angew. Chem. Int. Ed. Engl.* 1990, **29**, 388.
109. Cosnier, S.; Deronzier, A.; Vlachopoulos, N.; *J. Chem. Soc., Chem. Commun.* 1989, 1229.
110. Ladwig, M.; Kaim, W. *J. Organomet. Chem.* 1992, **439**, 79.
111. Zeissel, R. *J. Chem. Soc., Chem. Commun.* 1988, 16.
112. Ladwig, M.; Kaim, W. *J. Organomet. Chem.* 1991, **419**, 233.
113. Garcia, G.; Sanchez, G.; Romero, I.; Solano, I.; Santana, M. D.; Lopez, G. *J. Organomet. Chem.* 1991, **408**, 241.

114. Ryabov, A. D.; Menglet, D. L.; Levi, M. D. *J. Organomet. Chem.* 1991, **421**, C16.
115. Carmona, D.; Mendoza, A.; Lahoz, F. J.; Oro, L. A.; Lamata, M. P.; Jose, E. S. *J. Organomet. Chem.* 1990, **396**, C17.
116. Kraemer, R.; Polborn, K.; Wanjek, H.; Zahn, I.; Beck, W. *Chem. Ber.* 1990, **123**, 767. Kraemer, R.; Polborn, K.; Beck, W. *Chem. Ber.* 1991, **124**, 2429. Zahn, I.; Polborn, K.; Wagner, B.; Beck, W. *Chem. Ber.* 1991, **124**, 1065. Zahn, I.; Wagner, B.; Polborn, K.; Beck, W. *J. Organomet. Chem.* 1990, **394**, 601.
117. Grotjahn, D. B.; Groy, T. L. *Organometallics* 1995, **14**, 3669.
118. Abbott, A. P.; Capper, G.; Davies, D. L.; Fawcett, J.; Russel, D. R. *J. Chem. Soc., Dalton Trans.* 1995, 3709.
119. Carmona, D.; Lamata, M. P.; Esteban, M.; Lahoz, F. J.; Oro, L. A.; Apreda, M. C.; Foces-Foces, C.; Cano, F. H. *J. Chem. Soc., Dalton Trans.* 1994, 159.
120. Smith, D. P.; Griffin, M. T.; Olmstead, M. M.; Maestre, M. F.; Fish, R. H. *Inorg. Chem.* 1993, **32**, 4677. Smith, D. P.; Olmstead, M. M.; Noll, B. C.; Maestre, M. F.; Fish, R. H. *Organometallics* 1993, **12**, 593.
121. Stoppioni, P.; Di Vaira, M.; Maitlis, P. M. *J. Chem. Soc., Dalton Trans.* 1982, 1147.



122. Kim, G. C.-Y.; Batchelor, R. J.; Yan, X.; Einstien, F. W. B.; Sutton, D. *Inorg. Chem.* 1995, **34**, 6163.
123. Tang, Z.; Nomura, Y.; Ishii, Y.; Mizobe, Y.; Hidai, M.; *Organometallics* 1997, **16**, 151.
124. Hockett, S. C.; Miller, L. L.; Jacobson, R. A.; Angelici, R. J. *Organometallics* 1988, **7**, 686. Hockett, S. C.; Angelici, R. J. *Organometallics* 1988, **7**, 1491.
125. Chen, J.; Su, Y.; Jacobson, R. A.; Angelici, R. J. *J. Organomet. Chem.* 1992, **428**, 415.
126. Hughes, R. P. in Wilkinson, G.; Stone, F. G. A.; Abel, E. W. (Ed), *Comprehensive Organometallic Chemistry*, Pergamon Press, NewYork, 1982, Vol. **5**, 277. Leigh, G. J.; Richards, R. L. in Wilkinson, G.; Stone, F. G. A.; Abel, E. W. (Ed), *Comprehensive Organometallic Chemistry*, Pergamon Press, NewYork, 1982, Vol. **5**, 541.
127. Sharp, P. R. in Wilkinson, G.; Abel, E. W.; Stone, F. G. A. (Ed), *Comprehensive Organometallic Chemistry II*, Pergamon Press, NewYork, 1995, Vol. **5**, 115. Atwood, J. D. in Wilkinson, G.; Abel, E. W.; Stone, F. G. A. (Ed), *Comprehensive Organometallic Chemistry II* Pergamon Press, NewYork, 1995, Vol. **5**, 303.

## CHAPTER 2

### Synthesis and Molecular Structure of Di- and Mononuclear Schiff base Phenolate Complexes: Facile Formation of Cyclometallated Ruthenium Complexes\*

#### 2.1. Abstract

Condensation of 2,6-diformyl-4-methylphenol with aliphatic diamines,  $\text{NH}_2(\text{CH}_2)_n\text{NH}_2$  ( $n = 2, 3, 4$ ) in presence of  $[\text{Ru}(\text{dmsO})_4\text{Cl}_2]$  form ruthenium(II) complexes. These complexes have been characterized by analytical, spectral and magnetic data. They are shown to be acyclic, dinuclear six-coordinate ruthenium(II) complexes. The crystal structure of the representative complex **2**,  $[\text{Ru}_2\text{L}^2(\text{dmsO})_4\text{Cl}_4]$  confirms this structure. It crystallizes in orthorhombic space group  $\text{Pbca}$ ,  $a = 15.070(1) \text{ \AA}$ ,  $b = 23.112(1) \text{ \AA}$ ,  $c = 25.240(1) \text{ \AA}$  and  $Z = 8$ . The general structure of these complexes is shown in Figure 2.2. However, these reactions in the presence of triphenylphosphine give four membered cyclometallated dinuclear complexes.

---

\*Part of the work presented in this chapter appeared in J. Chem. Soc. Dalton Trans. 1997, 1697.

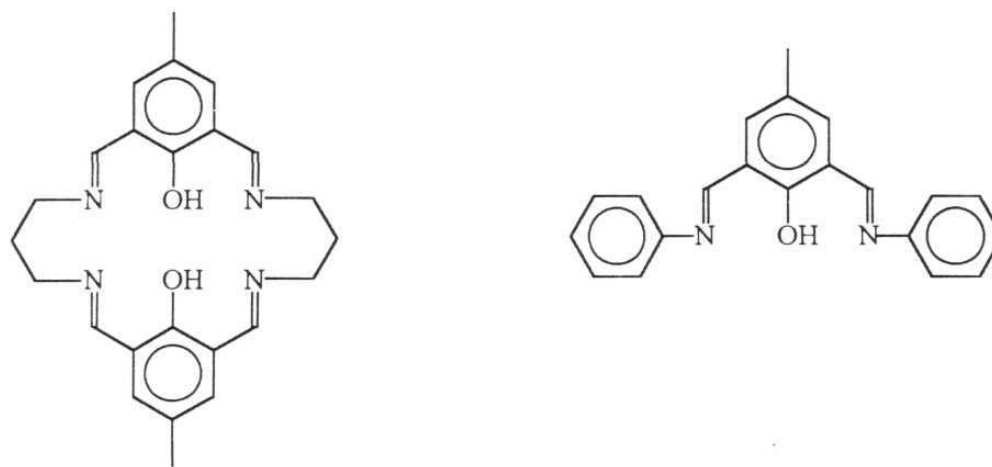
They have been characterized by analytical and spectral methods. The structure is given in Figure 2.10. The ligands of 2,6-diformyl-4-methylphenol with aromatic monoamines,  $L^4$ - $L^8$ , react with  $[Ru(dmsO)_4Cl_2]$  /  $PPh_3$  to give cyclometallated mononuclear ruthenium(II) complexes. The structure is confirmed from the crystal structure of the representative complex **5**,  $[RuL^{5'}(PPh_3)_2(CO)Cl]$ . It crystallizes in monoclinic space group  $C2/c$ ,  $a = 34.263$  (10) Å,  $b = 9.855$  (7) Å,  $c = 26.710$  (7) Å,  $\beta = 102.67$  (2)° and  $Z = 8$ . The generalized structure of these complexes is shown in Figure 2.8. The facile formation of cyclometallated ruthenium complexes is rationalized. Attempts to synthesize macrocyclic complexes by transmetallation reactions results only in the formation of acyclic complexes.

## 2.2. Introduction

The chemistry of ruthenium phenolates has attracted considerable attention because of the remarkable effect of phenolate coordination on the oxidation state of the metal ion. A series of 17-electron ruthenium(III) complexes with phenolate coordination have been isolated by Chakravorty *et al.*<sup>1</sup> Studies on tris chelate complexes of Ru(salicylaldehyde)<sub>3</sub>,<sup>2</sup> Ru(8-quinolinol)<sub>3</sub>,<sup>3</sup> Ru(N-arylsalicylaldimines)<sub>3</sub>,<sup>3</sup> divalent and trivalent ruthenium salen complexes<sup>4</sup> and various other substituted salicylaldimine complexes are reported.<sup>5</sup> Dinuclear Schiff base phenolate complexes,<sup>6</sup> Ru(II) and Ru(III) complexes of the type<sup>7</sup> [RuL<sub>2</sub>(PPh<sub>3</sub>)<sub>2</sub>], [RuL<sub>2</sub>(PPh<sub>3</sub>)<sub>2</sub>]PF<sub>6</sub> (L = 8-quinolinol), Ru(II) quinone-semiquinonate-catecholate complexes,<sup>8</sup> bis phenolate Ru(II) and Ru(III) complexes,<sup>9</sup> and mixed ligand complexes have also been studied.<sup>10,11</sup>

2,6-dicarbonyl-4-methylphenol and the various Schiff bases formed from it have been studied mainly as dinucleating ligands. Template condensation of 2,6-diformyl-4-methylphenol with various diamines is known to form macrocyclic dinuclear complexes with metal ions in close proximity. Synthesis and studies on such macrocyclic dinuclear complexes has received considerable attention because of their interesting spectral, magnetic, redox and catalytic properties.<sup>12</sup> Pilkington and Robson, first reported the 'direct' template synthesis of a dinucleating macrocycle,<sup>13</sup> by the condensation of 2,6-diformyl-4-methylphenol and 1,3-diaminopropane in 2:2 ratio. However, such condensation reactions with monoamines in 1:2 ratio provide acyclic ligands.<sup>14</sup> The dinucleating ability of these ligands stems from the readiness of

the phenolic proton to deprotonate and bridge two metal ions in close proximity. Homo and heterodinuclear complexes of  $3d$  metal ions from these ligands and related systems have been investigated in detail.<sup>15,16</sup>



The role of ruthenium as a template ion in such condensation reactions is not well understood.<sup>17</sup> One example of cyclometallation reaction in presence of ruthenium ions involving acyclic dinucleating ligands has been reported.<sup>18</sup> Hence, condensation reactions of 2,6-diformyl-4-methylphenol with different diamines and monoamines in presence of ruthenium salts are investigated to study the pattern of product formation. Under proper reaction conditions, acyclic dinuclear ruthenium complexes, **1-3** are obtained. They are structurally characterized. These complexes are then converted to the analogous cyclometallated complexes, **9-11** by varying the reaction conditions. Mononuclear cyclometallated ruthenium complexes, **4-8** are also synthesized and structurally characterized. The facile formation of cyclometallated ruthenium complexes is rationalized.

## 2.3. Experimental

Ruthenium trichloride was obtained from Sisco chemicals and was activated by treating with concentrated hydrochloric acid and evaporating it to dryness two to three times. The adducts  $[\text{Ru}(\text{dmsO})_4\text{Cl}_2]^{19}$  and  $[\text{RuCl}_3(\text{PPh}_3)_2(\text{CH}_3\text{OH})]^{20}$  were prepared as reported in the literature. 2,6-diformyl-4-methylphenol was also prepared according to the literature procedure.<sup>21</sup> The ligands  $\text{L}^1\text{-L}^3$  and  $\text{L}^4\text{-L}^8$  were synthesized by the known procedures.<sup>22,14</sup> All the solvents were dried prior to use by the standard procedures.<sup>23,24</sup> Dichloromethane was purified by treatment with  $\text{NaHCO}_3$  and anhydrous calcium chloride. Triphenylphosphine was recrystallized from hexane. The amines were purified by distillations. All the other solvents and chemicals were of reagent grade and were used without further purification.

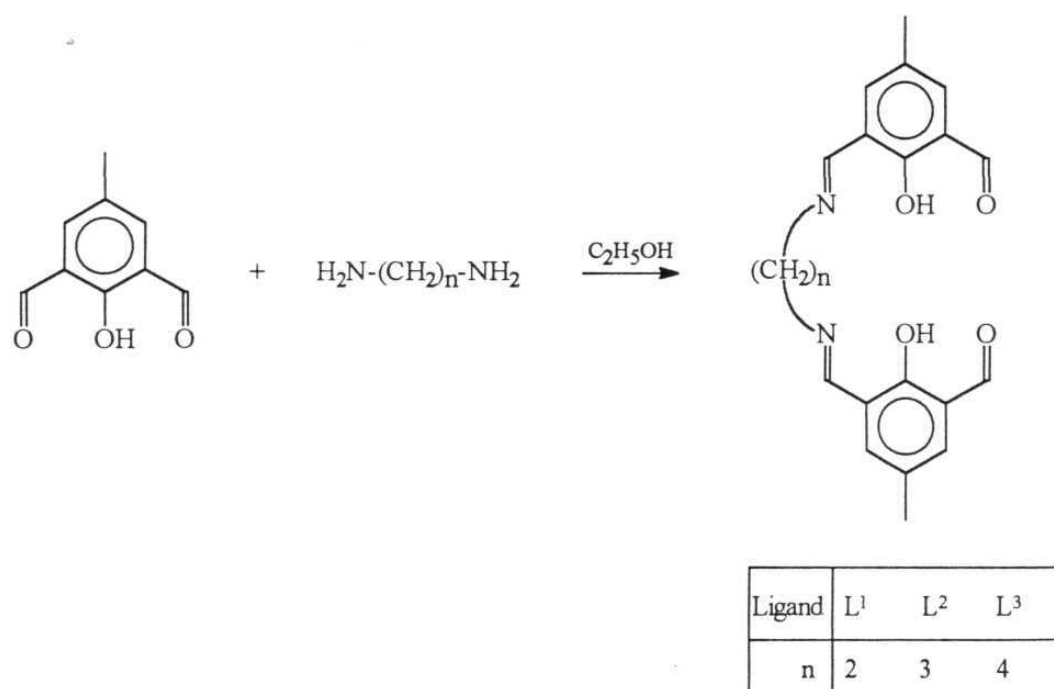
### 2.3.1. Synthesis of ligands

The ligands  $\text{L}^{1-3}$  were synthesized by following a general procedure represented in Scheme 2.1. Details are given for a representative ligand  $\text{L}^2$ .

To a solution of 2,6-diformyl-4-methylphenol (0.820 g, 5 mmol) in 20 mL of ethanol, was added 1,3-diaminopropane (0.285 g, 2.5 mmol) in 10 mL of ethanol. The reaction mixture was heated on steam-bath for 10 min. Yellow solid deposited on cooling and was collected by filtration.

Yield : 80-90%.

**Selected IR bands :** (KBr disc;  $\nu$ ,  $\text{cm}^{-1}$ ) C=O 1680, C=N 1630.



Scheme 2.1

**<sup>1</sup>H NMR data :** (CDCl<sub>3</sub>; δ, ppm)

L<sup>1</sup> : 13.85 (b, 2H, OH); 10.50 (s, 2H, H-C=O); 8.45 (s, 2H, H-C=N); 7.75 (s, 2H, Ar); 7.31 (s, 2H, Ar); 3.56 (s, 4H, N-CH<sub>2</sub>); 2.32 (s, 6H, CH<sub>3</sub>)

L<sup>2</sup> : 14.18 (b, 2H, OH); 10.49 (s, 2H, H-C=O); 8.41 (s, 2H, H-C=N); 7.68 (s, 2H, Ar); 7.30 (s, 2H, Ar); 3.78 (t, 4H, N-CH<sub>2</sub>); 2.32 (s, 6H, CH<sub>3</sub>); 2.15 (q, 2H, CH<sub>2</sub>)

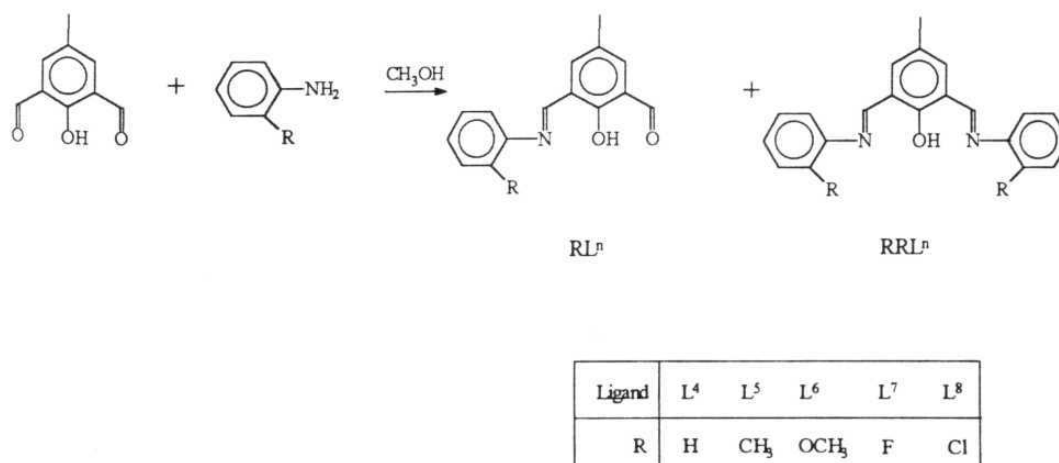
$L^3$  : 14.38 (b, 2H, OH); 10.51 (s, 2H, H-C=O); 8.45 (s, 2H, H-C=N); 7.75 (s, 2H, Ar); 7.28 (s, 2H, Ar); 3.75 (m, 4H, N-CH<sub>2</sub>); 2.31 (s, 6H, CH<sub>3</sub>); 1.85 (q, 2H, CH<sub>2</sub>)

The ligands  $L^{4-8}$  were synthesized by following the general procedure given below. The synthetic sequence is shown in Scheme 2.2.

To a solution of 2,6-diformyl-4-methylphenol (0.492 g, 3 mmol) in 20 mL of methanol, aromatic monoamine (9 mmol) was added in 10 mL of methanol. The reaction mixture was refluxed for 6-8 h. On cooling orange-red crystalline solid deposited. It was collected by filtration and dried.

Yield : 80%.

The  $^1\text{H}$  NMR spectra of the compounds indicated that they are mixture of two products, one side condensed and two side condensed Schiff bases in 40:60 ratio.



**Scheme 2.2**



### 2.3.2. Synthesis of complexes

#### $[\text{Ru}_2\text{L}^n(\text{dmso})_4\text{Cl}_4]$ complexes ( $n = 1-3$ )

The complexes **1-3** were synthesized following a general method. Detailed procedure is given for the representative complex **2**. To a solution of 2,6-diformyl-4-methylphenol (0.082 g, 0.5 mmol) in 20 mL of dry methanol,  $[\text{Ru}(\text{dmso})_4\text{Cl}_2]$  (0.242 g, 0.5 mmol) was added under nitrogen and the reaction mixture was stirred for 10 min. To this mixture, 1,3-diaminopropane (0.037 g, 0.5 mmol) in 10 mL of methanol was added and the reaction mixture was refluxed for 4 h. Cooling the reaction mixture to room temperature resulted in the deposition of red microcrystalline solid **2**. This was washed with small quantities of cold methanol and dried in *vacuum*. Yield : 50-60%

Complexes **1-3** were also obtained by the reaction of the preformed ligands,  $\text{L}^1\text{-L}^3$ , with  $[\text{Ru}(\text{dmso})_4\text{Cl}_2]$ . To a solution of ligand  $\text{L}^n$  ( $n = 1-3$ ) (0.5 mmol) in 25 mL of dry methanol,  $[\text{Ru}(\text{dmso})_4\text{Cl}_2]$  (1 mmol) was added and the mixture was refluxed for 4 h under dry nitrogen. This was cooled to room temperature and red microcrystalline solid which deposited was filtered, washed with small quantities of cold methanol and dried in *vacuum* for 4 h.

#### $[\text{RuL}^{n'}(\text{PPh}_3)_2\text{COCl}]$ ( $n = 4-8$ )

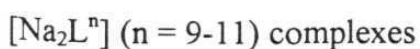
The complexes **4-8** were synthesized by following a general procedure. Details are given for the representative complex **5**. To a solution of  $\text{L}^5$  (0.215 g) in 30 mL of dry methanol was added  $[\text{Ru}(\text{dmso})_4\text{Cl}_2]$  (0.242 g, 0.5 mmol) and  $\text{PPh}_3$  (0.262 g, 1 mmol). The reaction mixture was

refluxed for 1 h by which time red microcrystalline solid separated out in quantitative yield.



The complexes **9-11** were synthesized by the following general procedure. To a solution of ligand  $\text{L}^n$  ( $n = 1-3$ ) (0.5 mmol) in 30 mL of dry methanol,  $[\text{Ru}(\text{dmsO})_4\text{Cl}_2]$  (0.484 g, 1 mmol) and  $\text{PPh}_3$  (0.524 g, 2 mmol) were added together under nitrogen and the reaction mixture was refluxed for 2 h by which time orange microcrystalline solid separated out. It was filtered and washed repeatedly with warm hexane to remove any excess triphenylphosphine. The complex was dried in *vacuum* for 3 h. Yield : 55-65%.

The complexes **4-11** were also obtained by the reaction of ligands with  $[\text{Ru}(\text{PPh}_3)_2\text{Cl}_3(\text{CH}_3\text{OH})]$ .



The disodium complexes were synthesized by the following general procedure.<sup>25</sup> Diamine  $\text{H}_2\text{N}-(\text{CH}_2)_n-\text{NH}_2$  ( $n = 2, 3, 4$ ,  $\text{L}^9\text{-L}^{11}$ ) (1 mmol) in 10 mL of ethanol was added slowly to a suspension of sodium 2,6-diformyl-4-methylphenolate (1 mmol) in 20 mL of ethanol. The mixture was refluxed for 1 h and the resulting yellow product was filtered and dried under *vacuum*. Yield : 80%.

#### Transmetallation of $\text{Na}_2\text{L}^n$ ( $n = 9-11$ ) with $[\text{Ru}(\text{dmsO})_4\text{Cl}_2]$

To a suspension of disodium complex,  $[\text{Na}_2\text{L}^n]$  ( $n = 9-11$ ) (0.112 g, 0.25 mmol) in 20 mL of ethanol was added  $[\text{Ru}(\text{dmsO})_4\text{Cl}_2]$  (0.242 g, 0.5 mmol) and the reaction mixture was refluxed for 20-30 min. It was filtered hot and on cooling the microcrystalline ruthenium complex precipitated in 50-60% yield.

#### Transmetallation of $\text{Na}_2\text{L}^n$ ( $n = 9-11$ ) with $[\text{Ru}(\text{dmsO})_4\text{Cl}_2]$ in presence of $\text{PPh}_3$

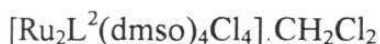
To a suspension of disodium complex,  $\text{Na}_2\text{L}^n$  ( $n = 9-11$ ) (0.112 g, 0.25 mmol) in 20 mL of ethanol was added  $[\text{Ru}(\text{dmsO})_4\text{Cl}_2]$  (0.242 g, 0.5 mmol) and triphenylphosphine (0.262 g, 1 mmol). The reaction mixture was refluxed for 1 h. The orange product deposited in 30-40% yield.

## 2.4. Physical measurements

The carbon, hydrogen and nitrogen analysis were carried out on Perkin-Elmer 240C elemental analyzer. IR spectra were recorded on Jasco FT/IR-5300 spectrophotometer in KBr pellets.  $^1\text{H}$  and  $^{31}\text{P}$  NMR spectra were recorded on Bruker ACF-200 spectrometer at 200 MHz and 81 MHz. Electronic absorption spectra were recorded on Jasco model 7800 UV-vis spectrophotometer. Magnetic susceptibility measurements were carried out on CAHN magnetic balance set-up. Fast atom bombardment (FAB) mass spectra were recorded on JEOL SX 102/DA-6000 mass spectrometer/data

system using Xenon (6KV, 10 mA) as the FAB gas and *m*-nitrobenzyl alcohol was used as the matrix. Cyclic voltammograms were recorded on cypress systems model CS-1090/CS-1087 computer-controlled electroanalytical system. All the experiments were performed under dry nitrogen in dichloromethane solvent.  $1 \times 10^{-3}$  M solutions were used with 0.1 M  $\text{NBu}_4\text{ClO}_4$  as supporting electrolyte using platinum working electrode, Ag-AgCl as reference electrode and platinum wire as auxiliary electrode. Ferrocene-ferrocenium couple was used as the redox standard.

#### 2.4.1. X-ray crystallography



A red plate of dimensions  $0.04 \times 0.20 \times 0.20$  mm, obtained by diffusion of ether into dichloromethane solution, was mounted on a fiber. A total of 8850 reflections were measured with Rigaku RAXIS IIC diffractometer using graphite-monochromated Mo  $K\alpha$  radiation ( $2\theta_{\text{max}} = 55^\circ$ ). An empirical absorption correction was applied<sup>26</sup> (transmission factor 0.747, 1.040). The structure was solved using Siemens SHELXTL PLUS (PC version)<sup>27,28</sup> by direct methods in orthorhombic space group  $\text{Pbca}$  (#61) with eight molecules in a unit cell. All non-hydrogen atoms were refined anisotropically and hydrogen atoms were fixed at calculated positions and were refined using riding model. The carbon atoms C(24), C(25) and C(28), C(29) of two dmsO ligands were disordered and were refined with 0.5 site occupation factor. 5233 reflections with  $F > 6\sigma F$  were used for structure

solution. Refinement converged at  $R = 4.03\%$ ,  $R_w = 4.72\%$  (509 variable parameters).



A red prism of dimensions  $0.25 \times 0.33 \times 0.33$  mm, obtained by diffusion of hexane into dichloromethane solution, was mounted on a fiber. A total of 7073 reflections were measured with a Rigaku AFC7S diffractometer using graphite-monochromated Mo  $K\alpha$  radiation ( $2\theta_{\text{max}} = 47^\circ$ ). An empirical absorption correction was applied (transmission factor 0.9044, 1.00). Cell constants and orientation matrix for data collection, obtained from a least-squares refinement using the setting angles of 25 carefully centered reflections in the range  $15.18^\circ < 2\theta < 26.96^\circ$  corresponded to a C-centered monoclinic cell. All the calculations were performed using the TEXSAN<sup>29</sup> crystallographic software package of Molecular Structure Corporation and solved by direct methods<sup>30,31</sup> in C2/c (#15) space group with eight molecules in a unit cell. The phenyl ring on one of the  $\text{PPh}_3$  units is disordered and was refined as such. In the final cycles, all non-hydrogen atoms were refined anisotropically except those in the disordered phenyl ring and all hydrogen atoms were fixed at idealized positions. The anisotropic displacement parameters for the carbons C(47) to C(56) were not calculated due to disorder. There were 6935 unique reflections of which 4644 with  $F > 6\sigma F$  were used for structure solution. Refinement converged at a final  $R = 4.5\%$  and  $R_w = 5.2\%$  (518 variable parameters).

## 2.5. Results and Discussion

### 2.5.1. Acyclic dinuclear ruthenium (II) complexes

Synthetic details of the ruthenium complexes **1-3** are given in the experimental section 2.3.2.

IR spectra of the complexes exhibit C=N stretching band at  $\sim 1616\text{ cm}^{-1}$ . The C=O stretching frequency of 2,6-diformyl-4-methylphenol at  $1680\text{ cm}^{-1}$  is shifted to  $1655\text{ cm}^{-1}$  in the complexes indicating the presence of coordinated C=O group. The relevant IR frequencies are presented in Table 2.1. The  $^1\text{H}$  NMR spectrum of a representative complex **2** is shown in Figure 2.1. The aldehydic proton signal at 10.4 ppm in 2,6-diformyl-4-methylphenol is shifted upfield to 9.4 ppm and appears as a singlet (2H). The azomethine protons give two signals each corresponding to one proton. The broad signal in the range of 13.3-13.7 ppm is due to phenolic hydrogen bonded to nitrogen (N---O---H). The two aromatic protons of 2,6-diformyl-4-methylphenol appear as two separate signals in the complex. In addition to these, resonances due to coordinated dmso molecules are seen as two sharp singlets at 3.6 ppm and at 3.4 ppm corresponding to twelve protons each, indicating the presence of four dmso molecules in two different environments. The relevant data are presented in Table 2.2. The IR and the  $^1\text{H}$  NMR data suggest the presence of both C=N and C=O groups in the ruthenium complexes. This implies that the condensation has proceeded in 2:1 fashion with two molecules of 2,6-diformyl-4-methylphenol and one molecule of diamine resulting in an acyclic system.

The analytical data (C, H, N) show the composition of the complexes to be  $[\text{Ru}_2\text{L}^n(\text{dmso})_4\text{Cl}_4]$ . Presence of dmso molecules has already been inferred from the  $^1\text{H}$  NMR signals. Analytical data are presented in Table 2.1. The FAB mass spectrum of the complex **2**, (MF :  $\text{C}_{29}\text{H}_{46}\text{N}_2\text{O}_8\text{S}_4\text{Cl}_4\text{Ru}_2$ , MW : 1022) shows molecular ion peak at  $m/z$  1022. In addition to this, several prominent fragments are seen at  $m/z$  987, 944, 909, 830, 866, 790, 753, 640. The species with  $m/z$  987 is assigned to the loss of one chloride ion and that with  $m/z$  944 to loss of one dmso molecule. The other fragments correspond to the progressive loss of dmso or chloride units.

Room-temperature magnetic susceptibility measurements show that the complexes are diamagnetic with  $t_{2g}^6$  ground state. The electronic spectra of the complexes in  $\text{CH}_2\text{Cl}_2$  exhibit high intensity charge-transfer transitions at 480 nm and at 400 nm besides a band at  $\sim 315$  nm of the ligand.<sup>2</sup> The electronic spectral data are collected in Table 2.3.

Based on these experimental data, the complexes, **1-3** are assigned a dimeric structure as shown in Figure 2.2. Each ruthenium(II) is coordinated by aldehydic and phenolic oxygens, two chloride ions and two molecules of dmso in an octahedral geometry. Owing to the bulky groups around the ruthenium centers, the metal ions will move away facilitating the arrangements shown in Figure 2.2. Flexibility of the bridging diamine helps this arrangement. The complexes do not coordinate on further addition of  $[\text{Ru}(\text{dmso})_4\text{Cl}_2]$  *via* phenolate and azomethine nitrogen. Also further condensation of coordinated aldehyde groups in these complexes with aromatic monoamines is unsuccessful.

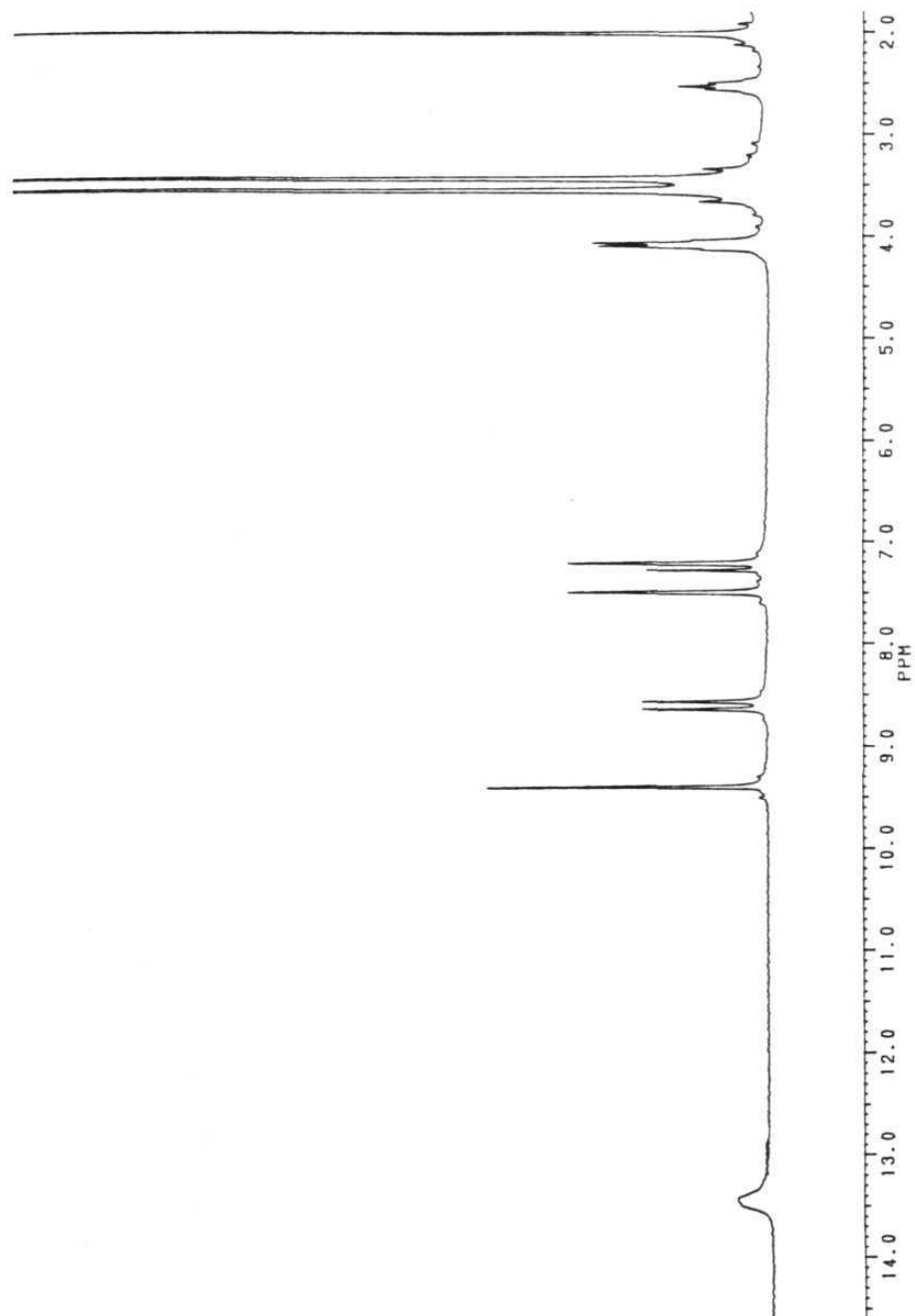


**Figure 2.1.**  $^1\text{H}$  NMR spectrum of a representative complex, **2**  $[\text{Ru}_2\text{L}^2(\text{dmso})_4\text{Cl}_4]$



**Table 2.1.** Analytical and selected IR data for ruthenium(II) complexes.

Complex	Analysis <sup>a</sup> (%)			IR (cm <sup>-1</sup> )		
	C	H	N	C=O	C=N	C≡O
[1] Ru <sub>2</sub> L <sup>1</sup> (dmsO) <sub>4</sub> Cl <sub>4</sub>	33.0 (33.3)	4.2 (4.4)	2.6 (2.8)	1655	1616	
[2] Ru <sub>2</sub> L <sup>2</sup> (dmsO) <sub>4</sub> Cl <sub>4</sub>	33.9 (34.1)	4.4 (4.3)	2.5 (2.7)	1655	1616	
[3] Ru <sub>2</sub> L <sup>3</sup> (dmsO) <sub>4</sub> Cl <sub>4</sub>	34.6 (34.7)	4.3 (4.6)	2.5 (2.7)	1649	1618	
[4] RuL <sup>4'</sup> (PPh <sub>3</sub> ) <sub>2</sub> (CO)Cl	67.6 (68.1)	4.7 (4.7)	1.4 (1.6)		1630	1905
[5] RuL <sup>5'</sup> (PPh <sub>3</sub> ) <sub>2</sub> (CO)Cl	68.5 (68.4)	4.9 (4.8)	1.4 (1.5)		1628	1907
[6] RuL <sup>6'</sup> (PPh <sub>3</sub> ) <sub>2</sub> (CO)Cl	66.5 (67.2)	4.6 (4.7)	1.6 (1.5)		1628	1907
[7] RuL <sup>7'</sup> (PPh <sub>3</sub> ) <sub>2</sub> (CO)Cl	65.8 (66.8)	4.2 (4.5)	1.7 (1.5)		1618	1910
[8] RuL <sup>8'</sup> (PPh <sub>3</sub> ) <sub>2</sub> (CO)Cl	66.8 (65.6)	4.9 (4.4)	1.3 (1.5)		1618	1908
[9] Ru <sub>2</sub> L <sup>9'</sup> (PPh <sub>3</sub> ) <sub>4</sub> (CO) <sub>2</sub> Cl <sub>2</sub>	65.9 (66.1)	4.6 (4.7)	1.7 (1.7)		1630	1907
[10] Ru <sub>2</sub> L <sup>10'</sup> (PPh <sub>3</sub> ) <sub>4</sub> (CO) <sub>2</sub> Cl <sub>2</sub>	66.0 (66.2)	4.8 (4.8)	1.6 (1.7)		1630	1911
[11] Ru <sub>2</sub> L <sup>11'</sup> (PPh <sub>3</sub> ) <sub>4</sub> (CO) <sub>2</sub> Cl <sub>2</sub>	65.8 (66.4)	4.8 (4.8)	1.7 (1.7)		1633	1898

<sup>a</sup>calculated values in parenthesis.

Table 2.2.  $^1\text{H}$  and  $^{31}\text{P}$  NMR data of ruthenium(II) complexes<sup>a</sup>

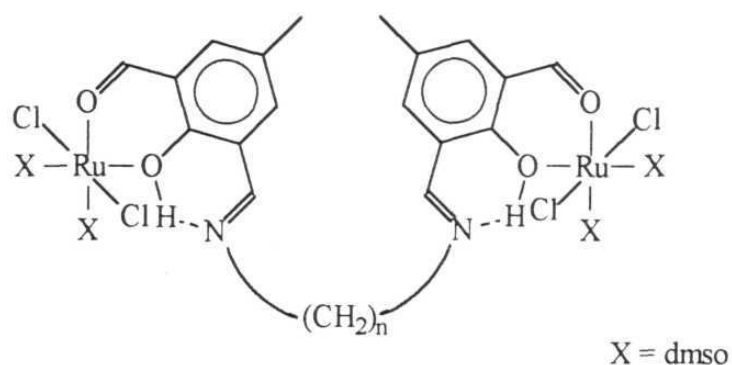
Complex	NMR data <sup>b</sup> ( $\delta$ )	
	$^1\text{H}$	$^{31}\text{P}$
1	13.68 (b 2H OH); 9.38 (s 2H H-C=O); 8.25 (d 2H H-C=N); 7.63 (d 2H Ar); 7.52 (d 2H Ar); 4.09 (s 4H N-CH <sub>2</sub> ); 3.56 (s 12H CH <sub>3</sub> -dmso); 3.43 (s 12H CH <sub>3</sub> -dmso); 2.06 (s 6H CH <sub>3</sub> )	--
2	13.41 (b 2H OH); 9.39 (s 2H H-C=O); 8.64 (d 2H H-C=N); 7.48 (d 2H Ar); 7.19 (d 2H Ar); 4.10 (t 4H N-CH <sub>2</sub> ); 3.56 (s 12H CH <sub>3</sub> -dmso); 3.44 (s 12H CH <sub>3</sub> -dmso); 2.56 (q 4H CH <sub>2</sub> ); 2.01 (s 6H CH <sub>3</sub> )	--
3	13.42 (b 2H OH); 9.36 (s 2H H-C=O); 8.64 (d 2H H-C=N); 7.45 (d 2H Ar); 7.31 (d 2H Ar); 3.86 (m 4H N-CH <sub>2</sub> ); 3.52 (s 12H CH <sub>3</sub> -dmso); 3.44 (s 12H CH <sub>3</sub> -dmso); 2.18 (m 4H CH <sub>2</sub> ); 2.05 (s 6H CH <sub>3</sub> )	--
4	12.63 (b 1H OH); 7.69 (m 12H PPh <sub>3</sub> ); 7.57 (s 1H H-C=N); 7.24 (m 18H PPh <sub>3</sub> ); 7.22 (d 2H Ar); 6.98 (d 2H Ar); 6.89 (s 1H Ar); 6.03 (s 1H Ar); 5.98 (s 1H Ar); 1.69 (s 3H CH <sub>3</sub> ).	37.7
5	12.58 (b 1H OH); 7.77 (m 12H PPh <sub>3</sub> ); 7.58 (s 1H H-C=N); 7.22 (m 18H PPh <sub>3</sub> ); 7.24 (m 2H Ar); 6.98 (m 2H Ar); 6.02 (s 1H Ar); 5.98 (s 1H Ar); 2.39 (s 3H CH <sub>3</sub> ); 1.70 (s 3H CH <sub>3</sub> ).	36.9
6	12.48 (b 1H OH); 7.71 (m 12H PPh <sub>3</sub> ); 7.45 (s 1H H-C=N); 7.20 (m 18H PPh <sub>3</sub> ); 7.12 (s 2H Ar); 7.03 (s 2H Ar); 5.85 (s 1H Ar); 5.83 (s 1H Ar); 4.13 (s 3H OCH <sub>3</sub> ); 1.66 (s 3H CH <sub>3</sub> ).	36.7
7	12.68 (b 1H OH); 7.69 (m 12H PPh <sub>3</sub> ); 7.51 (s 1H H-C=N); 7.24 (m 18H PPh <sub>3</sub> ); 6.99 (m 4H Ar); 6.02 (s 1H Ar); 5.98 (s 1H Ar); 1.69 (s 3H CH <sub>3</sub> )	37.2
8	11.48 (b 1H OH); 7.73 (m 12H PPh <sub>3</sub> ); 7.53 (m 18H PPh <sub>3</sub> ); 7.45 (s 1H H-C=N); 7.23 (m 4H Ar); 5.96 (s 1H Ar); 5.94 (s 1H Ar); 1.67 (s 1H CH <sub>3</sub> ).	36.4
10	11.38 (b 2H OH); 7.65 (m 12H PPh <sub>3</sub> ); 7.45 (s 2H H-C=N); 7.19 (m 18H PPh <sub>3</sub> ); 5.99 (s 2H Ar); 5.88 (s 2H Ar); 2.83 (t 4H N-CH <sub>2</sub> ); 1.76 (m 2H CH <sub>2</sub> ) 1.65 (s 6H CH <sub>3</sub> ).	37.2

<sup>a</sup>CDCl<sub>3</sub>; <sup>b</sup>NMR spectra of complexes 9 and 11 are not recorded.

**Table 2.3.** UV-vis and electrochemical data of ruthenium complexes

Complex	UV-vis <sup>a</sup> $\lambda_{\text{max}}$ , ( $\epsilon$ , $\text{M}^{-1} \text{cm}^{-1}$ )	CV data <sup>b</sup> $E_{1/2}/\text{V}$ ( $\Delta E/\text{mV}$ ) Ru(II) to Ru(III)
1	470 (6890), 407 (11070) 310 (2850)	0.900 (66)
2	480 (6775), 407 (10815) 314 (3690)	0.876 (100)
3	476 (7175), 406 (12090) 313 (3970)	0.845 (75)
4	538 (4580), 411(11330)	0.648 (77)
5	539 (4360), 412 (11080)	0.639 (93)
6	531 (5475), 419 (12050)	0.591 (84)
7	548 (3480), 414 (9535)	-
8	555 (4290), 419 (12525)	0.649 (93)
9	504 (6810), 374 (9890)	0.688 (62)
10	495 (6485), 370 (10145)	0.663 (71)
11	490 (4950), 370 (6025)	0.651 (78)

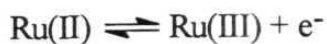
<sup>a</sup>in  $\text{CH}_2\text{Cl}_2$ , <sup>b</sup>CV experiments were carried out in  $\text{CH}_2\text{Cl}_2$  at 298 K using 0.1 M  $\text{NBu}_4\text{ClO}_4$  as supporting electrolyte at platinum working electrode Ag-AgCl reference electrode and platinum wire as auxiliary electrode.



n	2	3	4
Complex	1	2	3

**Figure 2.2.** Generalized structure of complexes **1-3**.

Cyclic voltammetric profiles of complexes **1-3** in dichloromethane solvent show an oxidation peak at  $\sim 0.92$  V and a corresponding reduction peak at  $\sim 0.82$  V at a scan rate of 100 mV / sec. The anodic and cathodic peak heights are equal and peak to peak separation ( $\Delta E_p$ ) lie in the range of 70-100 mV suggesting nearly reversible redox process which corresponds to oxidation of the ruthenium(II) center.



A representative profile is shown in Figure 2.3 and the  $E_{1/2}$  values for the complexes are given in Table 2.3.

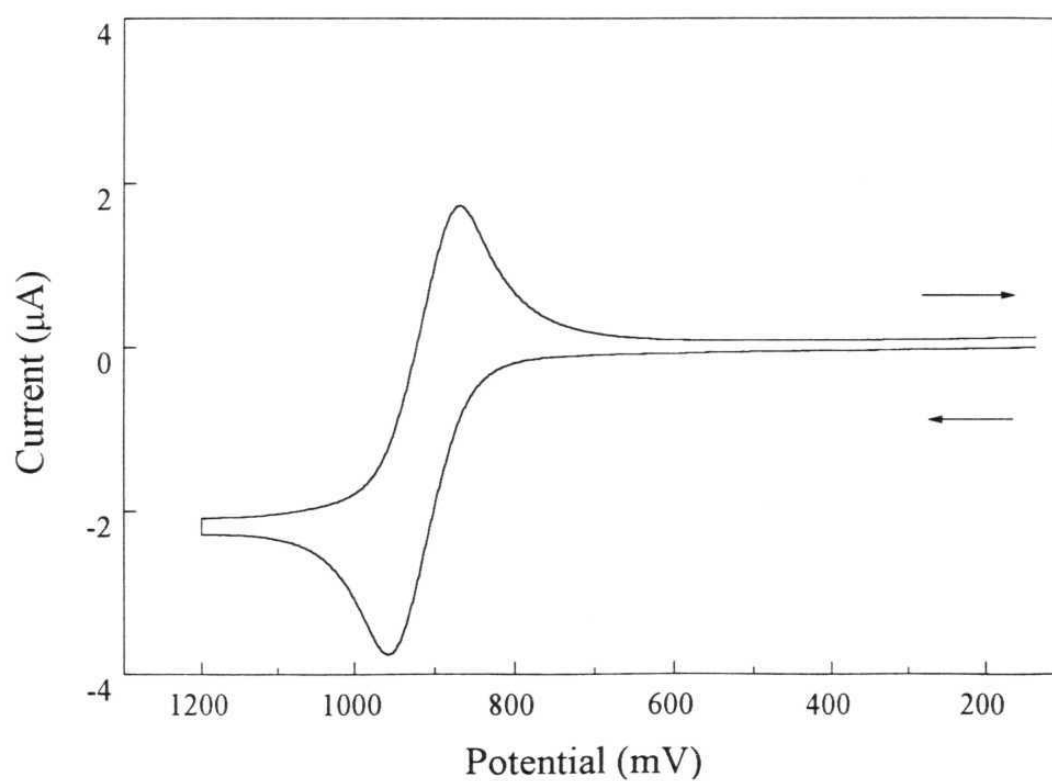


**Figure 2.3.** Cyclic voltammogram of  $[\text{Ru}_2\text{L}^2(\text{dmso})_4\text{Cl}_4]$  complex in  $\text{CH}_2\text{Cl}_2$  (0.1 M TBAP) at platinum electrode at a scan rate of  $100 \text{ mV s}^{-1}$

### Crystal structure of $[\text{Ru}_2\text{L}^2(\text{dmsO})_4\text{Cl}_2]\cdot\text{CH}_2\text{Cl}_2$ complex

To confirm the proposed dinuclear structure shown in Figure 2.2., the crystal structure of representative complex **2** was solved.

The compound crystallizes in orthorhombic *Pbca* space group with eight molecules per unit cell. The crystallographic parameters are summarized in Table 2.4. The positional parameters along with isotropic thermal parameters are given in Table 2.5. The anisotropic thermal parameters, hydrogen atom coordinates, bond lengths and bond angles are given in Appendix Tables A1-A4. The ORTEP drawing of the molecule **2** and the atom-numbering scheme is displayed in Figure 2.4. Selected bond parameters are listed in Table 2.6. The asymmetric unit consists of two ruthenium ions bridged by the Schiff base ligand. Both the metal ions are in identical environment. The Schiff base ligand acts as a tetradentate  $\text{O}_4$  donor, each ruthenium coordinated by phenolate and carbonyl oxygen, two sulphur atoms from dimethylsulphoxide and two chloride ions in the *trans* position. The metal coordination sphere is almost close to octahedral geometry. Slight deviation in the bond angles results because of the bulky dmsO molecules. Ru(1), O(1), O(2), S(1), S(2); Ru(1), S(2), O(1) Cl(1), Cl(2) and Ru(1), O(2), S(1), Cl(1), Cl(2), separately define three least-square planes with no atom deviating more than 0.09 Å and the maximum deviation between the planes is 1.39°. Similar deviations from the least-square planes were also observed for the three orthogonal planes around the other ruthenium center.

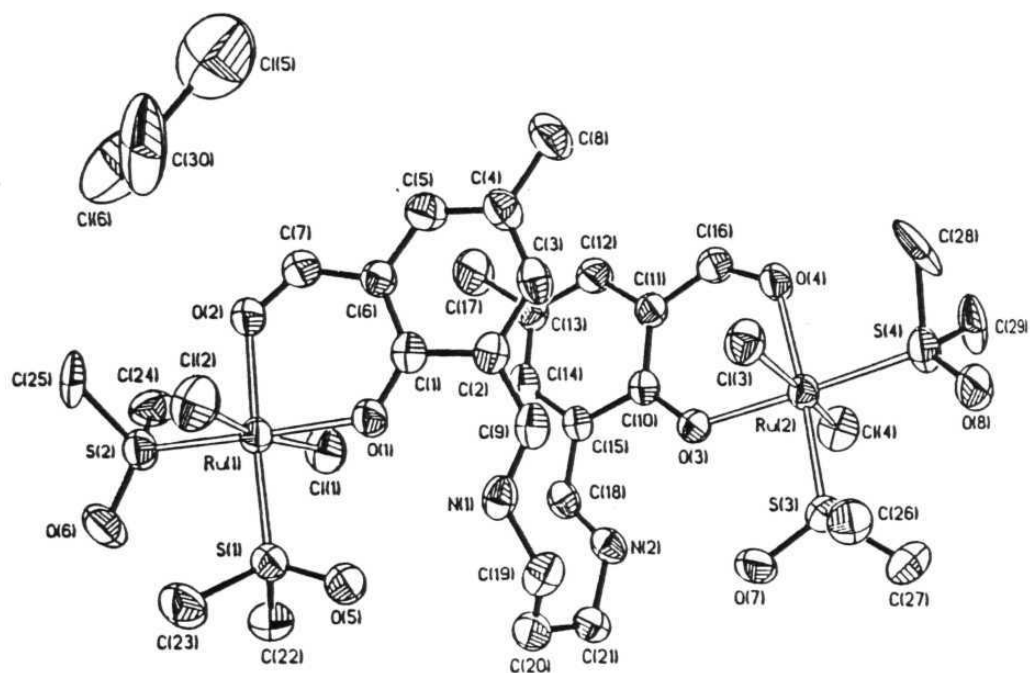


**Figure 2.4.** ORTEP drawing of the molecular structure of  $[\text{Ru}_2\text{L}^2(\text{dmsO})_4\text{Cl}_4]\cdot\text{CH}_2\text{Cl}_2$  showing the thermal ellipsoids at the 35% probability level with atom-labeling scheme.

**Table 2.4.** Crystallographic data for  $[\text{Ru}_2\text{L}^2(\text{dmsO})_4\text{Cl}_4]\cdot\text{CH}_2\text{Cl}_2$ 


---

chemical formula	$\text{C}_{30}\text{H}_{48}\text{N}_2\text{O}_8\text{Cl}_6\text{S}_4\text{Ru}_2$
fw	1107.816
space group	Pbca (#61)
a, Å	15.070 (1)
b, Å	23.112 (1)
c, Å	25.240 (1)
V, Å <sup>3</sup>	8791 (4)
Z	8
D calcd, g cm <sup>-3</sup>	1.692
T, °C	21
$\lambda$ (Mo K $\alpha$ ), Å	0.71073
$\mu$ (Mo K $\alpha$ ), cm <sup>-1</sup>	12.88
F(000)	4576
transm. coeff.	0.747-1.04
R <sup>a</sup>	0.0403
R <sub>w</sub> <sup>b</sup>	0.0472

---

$$^a\text{R} = \sum ||\text{Fo}| - |\text{Fc}|| / \sum |\text{Fo}| ; ^b\text{R}_w = [\sum w(|\text{Fo}| - |\text{Fc}|)^2 / \sum w\text{Fo}^2]^{1/2}$$



**Table 2.5.** Atomic coordinates ( $\times 10^5$  for Ru;  $\times 10^4$  for others) and equivalent isotropic displacement coefficients ( $\text{\AA}^2 \times 10^4$  for Ru,  $\text{\AA}^2 \times 10^3$  for others) with estimated standard deviations in parentheses for  $[\text{Ru}_2\text{L}^2(\text{dmsO})_4\text{Cl}_4] \cdot \text{CH}_2\text{Cl}_2$

Atom	x	y	z	$U_{\text{eq}}^a$
Ru(1)	31571(3)	22604(2)	32520(2)	553(3)
Ru(2)	75610(3)	-4541(2)	41773(2)	526(3)
Cl(1)	2594(1)	1426(1)	3696(1)	86(1)
Cl(2)	3911(1)	3000(1)	2745(1)	96(1)
Cl(3)	7931(1)	287(1)	3555(1)	73(1)
Cl(4)	6966(1)	-1192(1)	4737(1)	81(1)
S(1)	3456(1)	2714(1)	4003(1)	69(1)
S(2)	1810(1)	2644(1)	3160(1)	71(1)
S(3)	7978(1)	931(1)	4859(1)	63(1)
S(4)	8878(1)	-874(1)	4088(1)	71(1)
O(1)	4385(3)	1859(2)	3317(2)	66(1)
O(2)	2939(3)	1818(2)	2546(2)	69(1)
O(3)	6324(3)	-73(2)	4235(1)	60(1)
O(4)	7082(3)	-936(2)	3535(2)	65(1)
O(5)	4362(3)	2607(2)	4215(2)	88(1)
O(6)	1431(3)	3034(2)	3561(2)	106(1)
O(7)	7264(3)	465(2)	5080(2)	88(1)
O(8)	9684(3)	-600(2)	4285(2)	88(1)

....cont.

....cont. Table 2.5

N(1)	5675(3)	1719(2)	4001(2)	60(1)
N(2)	5482(3)	685(2)	4812(2)	58(1)
C(1)	4710(4)	1470(3)	3017(2)	56(1)
C(2)	5541(4)	1208(3)	3165(2)	58(1)
C(3)	5922(4)	796(3)	2829(3)	68(1)
C(4)	5540(4)	606(3)	2371(3)	71(1)
C(5)	4735(4)	841(3)	2244(3)	70(1)
C(6)	4304(4)	1268(3)	2548(2)	57(1)
C(7)	3456(4)	1459(3)	2359(2)	65(1)
C(8)	5983(5)	167(4)	2012(3)	111(2)
C(9)	5967(4)	1350(3)	3659(3)	67(1)
C(10)	5628(4)	-158(2)	3955(2)	49(1)
C(11)	5593(4)	-549(3)	3521(2)	55(1)
C(12)	4797(4)	-606(3)	3230(2)	70(1)
C(13)	4045(4)	-287(3)	3340(3)	75(1)
C(14)	4076(4)	90(3)	3765(3)	68(1)
C(15)	4841(4)	162(3)	4078(2)	53(1)
C(16)	6317(4)	-908(3)	3350(2)	64(1)
C(17)	3216(4)	-330(4)	3004(3)	114(2)
C(18)	4814(4)	569(3)	4507(2)	58(1)
C(19)	6103(4)	1828(3)	4514(2)	73(1)
C(20)	5465(4)	1745(3)	4976(2)	70(1)
C(21)	5451(4)	1147(3)	5213(2)	65(1)

....cont.

....cont. Table 2.5

C(22)	2725(5)	2562(3)	4524(3)	95(1)
C(23)	3328(5)	3479(3)	3972(3)	99(1)
C(24)	1139(11)	2020(8)	3075(7)	96(2)
C(25)	1840(11)	2917(8)	2496(6)	90(2)
C(24')	983(7)	21685(5)	3013(7)	131(2)
C(25')	1596(10)	3027(8)	2612(6)	202(2)
C(26)	8876(4)	557(3)	4719(3)	77(1)
C(27)	8438(5)	-293(3)	5397(2)	90(1)
C(28)	9203(13)	-846(9)	3411(7)	147(2)
C(29)	8845(11)	-1635(6)	4126(8)	98(2)
C(28')	9031(8)	-1122(7)	3467(5)	149(2)
C(29')	8966(8)	-1493(5)	4484(6)	130(2)
C(30)	3947(9)	2611(4)	1123(6)	247(2)
Cl(5)	4473(4)	2016(2)	760(2)	238(1)
Cl(6)	2896(4)	2366(2)	1260(2)	263(1)

<sup>a</sup>Equivalent isotropic U defined as one third of the trace of the orthogonalized  $U_{ij}$  tensor

**Table 2.6.** Selected bond distances (Å) and bond angles (°) in  $[\text{Ru}_2\text{L}^2(\text{dmso})_4\text{Cl}_4]\cdot\text{CH}_2\text{Cl}_2$

Bond lengths

Ru(1)-Cl(1)	2.386(2)	Ru(1)-Cl(2)	2.418(2)
Ru(1)-S(1)	2.211(2)	Ru(1)-S(2)	2.228(2)
Ru(1)-O(1)	2.076(4)	Ru(1)-O(2)	2.081(4)
Ru(2)-Cl(3)	2.389(2)	Ru(2)-Cl(4)	2.389(2)
Ru(2)-S(3)	2.225(2)	Ru(2)-S(4)	2.221(2)
Ru(2)-O(3)	2.066(4)	Ru(2)-O(4)	2.095(4)
O(1)-C(1)	1.274(7)	O(2)-C(7)	1.232(8)
O(3)-C(10)	1.280(7)	O(4)-C(16)	1.245(7)
N(1)-C(9)	1.290(8)	N(1)-C(19)	1.468(8)
N(2)-C(18)	1.294(8)	N(2)-C(21)	1.474(7)

....cont.

....cont. Table 2.6

## Bond angles

---

Cl(1)-Ru(1)-Cl(2)	170.6(1)	Cl(1)-Ru(1)-S(1)	93.0(1)
Cl(2)-Ru(1)-S(1)	91.3(1)	Cl(1)-Ru(1)-S(2)	92.7(1)
Cl(2)-Ru(1)-S(2)	95.3(1)	S(1)-Ru(1)-S(2)	95.0(1)
Cl(1)-Ru(1)-O(1)	85.4(1)	Cl(2)-Ru(1)-O(1)	86.4(1)
S(1)-Ru(1)-O(1)	87.9(1)	S(2)-Ru(1)-O(1)	176.7(1)
Cl(1)-Ru(1)-O(2)	87.1(1)	Cl(2)-Ru(1)-O(2)	88.2(1)
S(1)-Ru(1)-O(2)	177.2(1)	S(2)-Ru(1)-O(2)	87.8(1)
O(1)-Ru(1)-O(2)	89.4(2)	Cl(3)-Ru(2)-Cl(4)	171.0(1)
Cl(3)-Ru(2)-S(3)	92.0(1)	Cl(4)-Ru(2)-S(3)	93.1(1)
Cl(3)-Ru(2)-S(4)	92.2(1)	Cl(4)-Ru(2)-S(4)	94.8(1)
S(3)-Ru(2)-S(4)	94.3(1)	Cl(3)-Ru(2)-O(3)	87.2(1)
Cl(4)-Ru(2)-O(3)	85.6(1)	S(3)-Ru(2)-O(3)	87.6(1)
S(4)-Ru(2)-O(3)	178.1(1)	Cl(3)-Ru(2)-O(4)	87.3(1)
Cl(4)-Ru(2)-O(4)	87.1(1)	S(3)-Ru(2)-O(4)	175.9(1)
S(4)-Ru(2)-O(4)	89.8(1)	O(3)-Ru(2)-O(4)	88.3(2)

---

The average Ru-O(phenolate) distance is 2.071 (4) Å and the average Ru-O(carbonyl) length is 2.088 (4) Å. Ruthenium(II)-O(carbonyl) distances are close to 2.12 Å.<sup>32</sup> In Ru(III)(salicylaldehyde)<sub>3</sub> complex,<sup>2</sup> the average Ru-O(phenolate) distance is 1.981 (2) Å and the average Ru-O(carbonyl) length is 2.031 (2) Å. The near equivalence in the Ru-O(carbonyl) and the Ru-O(phenolate) bond length in the present complex suggest electron delocalization involving these centers. In *cis*-[Ru(dmso)<sub>4</sub>Cl<sub>2</sub>]<sup>33,34</sup> complex, the mean Ru-S distance is reported at 2.268 (1) Å and is the result of d<sub>π</sub>-d<sub>π</sub> back donation from the central metal to the sulphur atom. In *trans*-[Ru(dmso)<sub>4</sub>Cl<sub>2</sub>]<sup>34,35</sup> complex, the average Ru-S(dmso) distance is close to 2.35 Å and the increase in the bond length is explained based on greater *trans* influence of S compared to Cl and the greater π bonding competition among the dmso ligands. The average Ru-S(dmso) distance (2.221 Å) in the present complex is less than that in *cis* or *trans*-[Ru(dmso)<sub>4</sub>Cl<sub>2</sub>] complexes which indicates greater d<sub>π</sub>-d<sub>π</sub> backbonding. The average Ru-Cl bond length of 2.395 (2) Å is comparable to the Ru-Cl bond lengths in octahedral complexes with *trans* chlorides.<sup>34</sup> The distance between O(1)-N(1) and O(3)-N(2) is 2.62 and 2.61 Å respectively indicating N---H---O interaction involving hydrogen atoms on O(1) and O(3). The hydrogens, though, not located on difference map, are added according to the calculated position with 0.85 Å to O atoms. Analogous hydrogen bonding interaction of phenolic hydrogen with adjacent nitrogen in a ruthenium complex has been crystallographically established.<sup>18</sup>

The molecular geometry of the non-disordered dmso ligands is identical to that in  $[\text{Ru}(\text{dmso})_4\text{Cl}_2]$ <sup>33</sup> and free dmso.<sup>36</sup> The average C-S-O angles ( $106.3^\circ$ ) and the average C-S-C angles ( $99.3^\circ$ ) in the present complex are comparable to the average C-S-O and C-S-C angles in  $[\text{Ru}(\text{dmso})_4\text{Cl}_2]$  ( $106.6^\circ$ ,  $99^\circ$ ) and free dmso molecule ( $107^\circ$ ,  $98^\circ$ ). The mean C-S bond lengths are also comparable. In the disordered dmso molecules, 2 to  $3^\circ$  deviation is observed for the average C-S-C angles. Deviations in the bond lengths are within the standard deviations.

The crystal structure of complex **2** supports the proposed generalized structure shown in Figure 2.2. It is clear from the structure that template condensation in presence of ruthenium ions has proceeded in a 2:1 fashion (aldehyde:amine) to provide acyclic dinuclear complexes. This is in contrast to 2:2 condensation in presence of  $3d$  metal ions which result in dinuclear macrocyclic complexes. Preference of ruthenium for oxygen coordination might have directed the condensation reaction in this fashion.

### 2.5.2. Cyclometallated mononuclear ruthenium(II) complexes

2,6-diformyl-4-methylphenol is known to condense with aromatic monoamines in 1:2 ratio to the corresponding Schiff bases which form dinuclear complexes of  $[\text{M}_2\text{L}_2]^{2-}$  composition with  $3d$  metal ions.<sup>14,37,38</sup> Structural deviations of ruthenium complexes compared to the  $3d$  metal complexes as discussed in the previous section prompted us to explore the structural features of the ruthenium complexes of ligands  $\text{L}^4$ - $\text{L}^8$ . These ligands were obtained as mixtures of mono and dicondensed Schiff bases. Efforts to

complete the condensation of both carbonyl groups or separate the two products were not successful. Hence the ligands were used as such for further complexation.

Reaction of  $[\text{Ru}(\text{dmsO})_4\text{Cl}_2]$  with slight excess of these ligands in dry methanol gave dark red microcrystalline products. It was not possible to assign structure for these complexes based on the analytical and spectral data. Attempts to grow single crystals of these complexes were also unsuccessful. But reactions of these ligands with  $[\text{Ru}(\text{dmsO})_4\text{Cl}_2]$  in the presence of triphenylphosphine yielded complexes **4-8**.

The analytical data of the complexes **4-8** do not correspond to dinuclear structures. IR spectra of the complexes show an intense band at  $\sim 1900\text{ cm}^{-1}$  indicating the presence of carbonyl group besides the characteristic band due to C=N stretching. Absorptions due to coordinated triphenylphosphine molecules at  $\sim 1500, 1480, 740$  and  $690\text{ cm}^{-1}$  are present. The characteristic IR bands are given in Table 2.1. All the complexes are diamagnetic which indicates  $t_{2g}^6$  ground state configurations. The  $^1\text{H}$  NMR spectra of the complexes show the two phenolic ring protons shifted upfield to 6.0 ppm and 5.8 ppm. The azomethine proton is also shifted upfield from the usual 8.5 ppm to 7.5 ppm. Two complex set of signals at 7.2 ppm and 7.7 ppm are observed due to the coordinated triphenylphosphine units. A representative  $^1\text{H}$  NMR spectrum is shown in Figure 2.5. The  $^{31}\text{P}$  NMR spectra of the complexes show a sharp singlet at 37 ppm indicating phosphines to be in *trans* position. The  $^1\text{H}$  and  $^{31}\text{P}$  NMR data of the complexes **4-8** are presented in Table 2.2. The electronic spectra of the complexes recorded in dichloromethane solvent show high intensity charge-



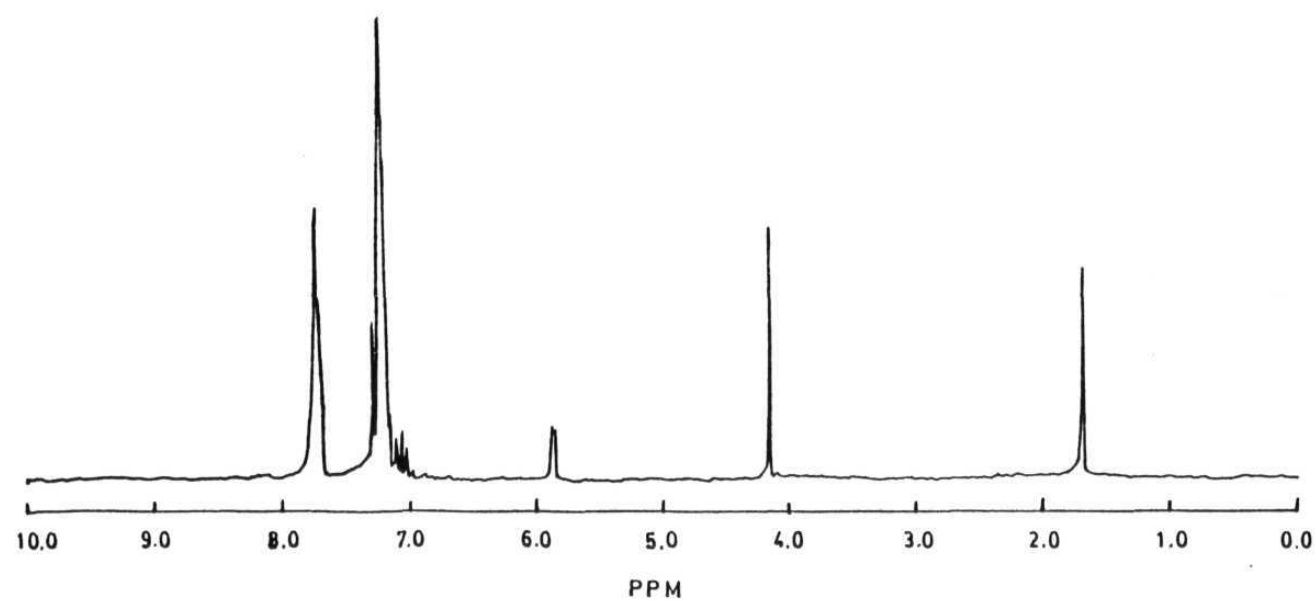


**Figure 2.5.**  $^1\text{H}$  NMR spectrum of a representative complex **6**,  $[\text{RuL}^{6'}(\text{PPh}_3)_2(\text{CO})\text{Cl}]$

transfer bands at 530 nm and 410 nm. These data are presented in Table 2.3.

The cyclic voltammograms of the complexes in dichloromethane solvent, at platinum electrode show one-electron nearly reversible couple in the range 0.6 V - 0.65 V at the scan rate of 100 mV / s. corresponding to metal oxidation



At this scan rate the anodic and cathodic peak heights are equal. On increasing the scan rate, the anodic response becomes progressively prominent and the cathodic response appears with a diminished height. Representative voltammograms of complex **8** at various scan rates are shown in Figure 2.6. The electrochemical data are presented in Table 2.3.

The analytical and spectral data indicate the formation of cyclometallated ruthenium complexes.

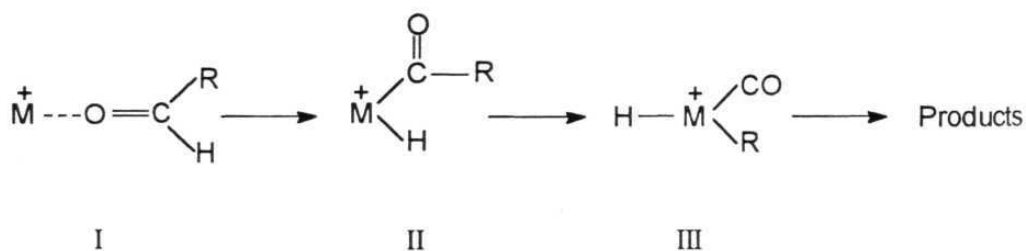
### **Crystal and molecular structure of [RuL<sup>5'</sup>(PPh<sub>3</sub>)<sub>2</sub>(CO)Cl]**

The X-ray structure of representative complex **5** was solved to establish the structure of complexes **4-8**.

The compound crystallizes in monoclinic C2/c space group with eight molecules in a unit cell. The crystallographic parameters are summarized in Table 2.7. The positional parameters along with isotropic thermal parameters are given in Table 2.8. The anisotropic thermal parameters, hydrogen atom coordinates, bond lengths and bond angles are given in Appendix Tables A5-A8. An ORTEP drawing of the molecule **5** and the atom-numbering scheme

is displayed in Figure 2.7. Selected bond lengths and bond angles are given in Table 2.9. The geometry around Ru(II) is distorted octahedral. Ruthenium ion is coordinated by phenolate oxygen O(1) and C(2) carbon to form planar four-membered metallacycle. In addition to this, the ruthenium ion is coordinated to carbonyl carbon (C16) which is *cis* to C(2) carbon and a chloride ion. The two phosphines are coordinated *trans* to each other. The Ru(II)-O(phenolate) distance in four-membered chelate ring is longer than that of five-membered rings<sup>39</sup> and ruthenium(II) semiquinonates.<sup>40,8</sup> The O(1)-Ru-C(2) angle and Cl-Ru-C(2) angle deviate from the optimum values.

From the structure of the complex, it appears that the reaction of  $[\text{Ru}(\text{dmsO})_4\text{Cl}_2]$  with ligands  $\text{L}^{4,8}$  in presence of triphenylphosphine proceeds *via* decarbonylation of the aldehyde group resulting in the cyclometallation of phenyl ring forming a four-membered metallacycle.<sup>41</sup> The proposed mechanism of cyclometallation in conformity with the known similar reactions proceeds through the intermediates shown in Scheme 2.3.



**Scheme 2.3**

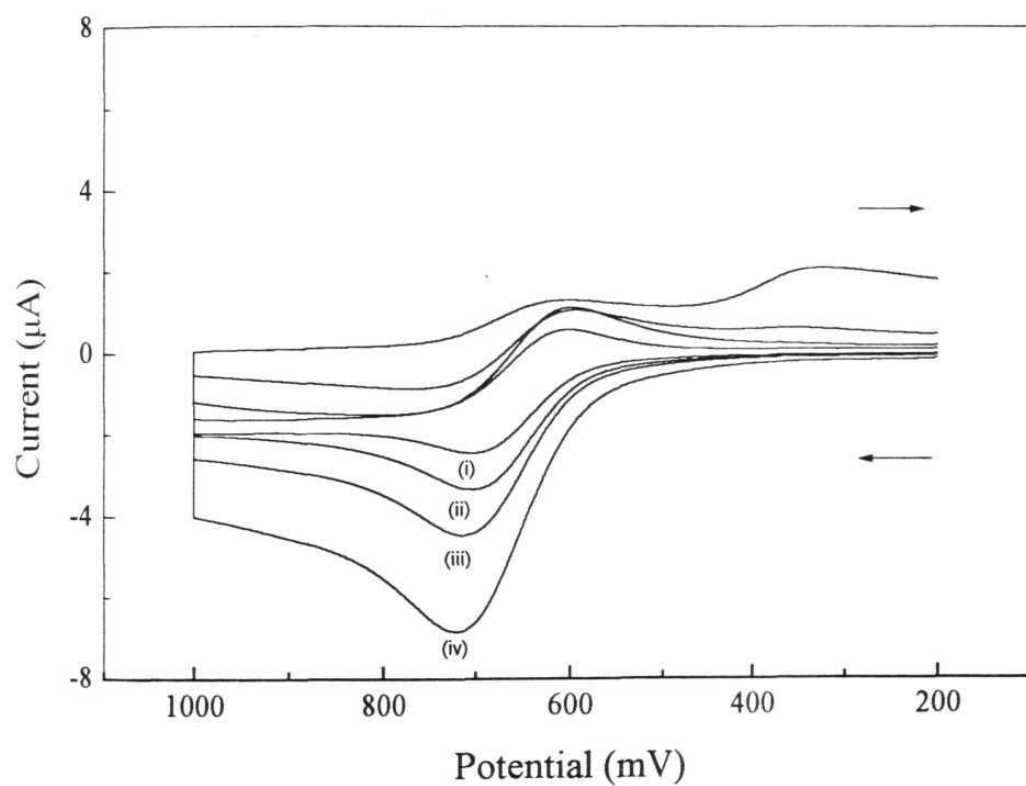


**Figure 2.6.** Cyclic voltammograms of  $[\text{Ru}_2\text{L}^{8'}(\text{PPh}_3)_2(\text{CO})\text{Cl}]$  complex in  $\text{CH}_2\text{Cl}_2$  (0.1 M TBAP) at platinum electrode at scan rates of (i) 50 (ii) 100 (iii) 200 (iv) 500  $\text{mV s}^{-1}$

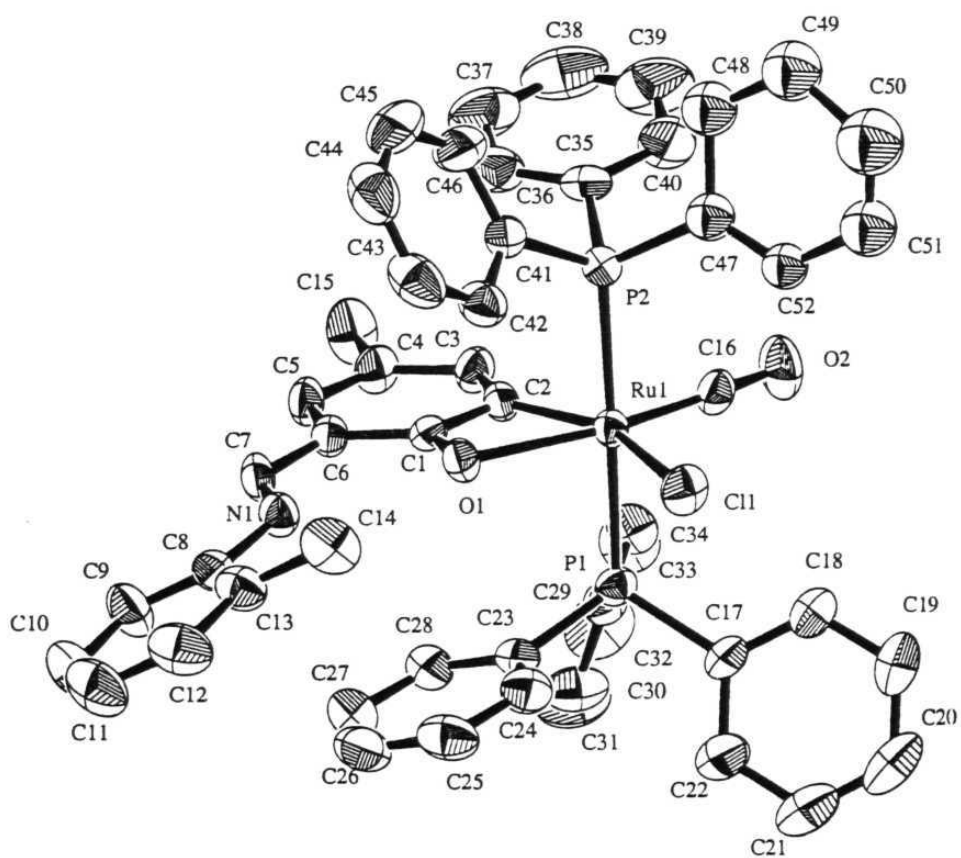
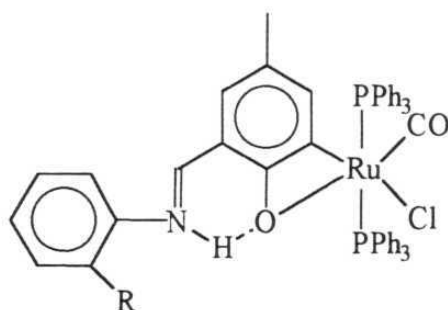


**Figure 2.7.** ORTEP drawing of the molecular structure of  $[\text{Ru}_2\text{L}^{5'}(\text{PPh}_3)_2\text{COCl}]$  showing the thermal ellipsoids at the 50% probability level with atom-numbering scheme.

These reaction steps involve oxidative addition followed by reductive elimination. In the present reaction, the product formed after the oxidative addition step is a stable orthometallated phenolate chelate ring and hence reductive elimination proceeds by  $H^+$  elimination assisted by azomethine nitrogen.<sup>42</sup>

The preference of ruthenium for oxygen coordination is the key factor for the formation of intermediate I with ligands  $L^4$ - $L^8$  which in turn provide the cyclometallated ruthenium complexes as the final product. The generalized structure of the complexes are shown in Figure 2.8.



R	H	CH <sub>3</sub>	OCH <sub>3</sub>	F	Cl
Complex	4	5	6	7	8

**Figure 2.8.** Generalized structure of complexes 4-8.

**Table 2.7.** Crystallographic data for [RuL<sup>5'</sup>(PPh<sub>3</sub>)<sub>2</sub>(CO)(Cl)]

---

chemical formula	C <sub>52</sub> H <sub>43</sub> NClO <sub>2</sub> P <sub>2</sub> Ru
fw	912.39
space group	C2/c (#15)
a, Å	34.263 (10)
b, Å	9.855 (7)
c, Å	26.710 (7)
β, deg	102.67 (2)
V, Å <sup>3</sup>	8799 (6)
Z	8
D calcd, g cm <sup>-3</sup>	1.377
T, °C	24.0
λ (Mo Kα), Å	0.71073
μ (Mo Kα), cm <sup>-1</sup>	5.32
F(000)	3752
transm. coeff.	0.90-1.00
R <sup>a</sup>	0.045
R <sub>w</sub> <sup>b</sup>	0.052

---

$$^a R = \sum ||F_o| - |F_c|| / \sum |F_o|, \quad ^b R_w = [\sum w(|F_o| - |F_c|)^2 / \sum w F_o^2]^{1/2}$$

**Table 2.8.** Atomic coordinates ( $\times 10^5$  for Ru, Cl(1), P(1), P(2), O(1),  $\times 10^4$  for others) and isotropic thermal parameters with estimated standard deviations in parentheses for  $[\text{RuL}^{5'}(\text{PPh}_3)_2(\text{CO})(\text{Cl})]$

Atom	x	y	z	$B_{\text{eq}}^a$
Ru	13598(1)	4443(4)	15067(2)	2.30(1)
Cl	8588(4)	2171(2)	11092(6)	3.57(4)
P(1)	10378(4)	324(2)	22085(6)	2.67(3)
P(2)	17088(4)	472(2)	8278(6)	2.85(3)
O(1)	9596(10)	-1245(4)	1134(1)	2.68(9)
O(2)	2031(1)	2059(5)	2108(2)	4.9(1)
N(1)	514(1)	-3451(5)	872(2)	3.0(1)
C(1)	1224(2)	-2110(6)	1385(2)	2.4(1)
C(2)	1567(1)	-1473(5)	1689(2)	2.5(1)
C(3)	1866(2)	-2272(6)	1956(2)	3.2(1)
C(4)	1837(2)	-3725(6)	1942(2)	3.3(1)
C(5)	1504(2)	-4322(6)	1655(2)	3.2(1)
C(6)	1181(2)	-3540(6)	1370(2)	2.8(1)
C(7)	825(2)	-4156(6)	1114(2)	3.4(2)
C(8)	123(2)	-3982(6)	682(2)	3.2(1)
C(9)	12(2)	-5233(7)	840(3)	4.3(2)
C(10)	-377(2)	-5687(8)	671(3)	5.5(2)
C(11)	-649(2)	-4897(9)	348(3)	5.7(2)
C(12)	-539(2)	-3647(8)	195(3)	5.0(2)

....cont.



....cont. Table 2.8

C(13)	-146(2)	-3158(7)	-354(2)	3.8(2)
C(14)	-31(2)	-1820(7)	177(3)	5.0(2)
C(15)	2184(2)	-4555(7)	2240(3)	5.0(2)
C(16)	1764(2)	1443(6)	1875(2)	3.0(1)
C(17)	875(2)	1920(6)	2459(2)	3.0(1)
C(18)	1087(2)	3079(7)	2428(3)	4.4(2)
C(19)	1000(2)	4279(7)	2654(3)	5.7(2)
C(20)	691(3)	4292(8)	2914(3)	6.1(2)
C(21)	476(2)	3148(9)	2944(3)	5.5(2)
C(22)	566(2)	1947(7)	2715(3)	4.4(2)
C(23)	582(2)	-671(6)	2031(2)	3.1(1)
C(24)	241(2)	-74(7)	1718(2)	3.8(2)
C(25)	-96(2)	-872(8)	1538(3)	4.6(2)
C(26)	-100(2)	-2219(8)	1653(3)	4.9(2)
C(27)	233(2)	-2812(7)	1948(3)	5.0(2)
C(28)	572(2)	-2053(7)	2131(2)	3.9(2)
C(29)	1315(2)	-435(6)	2808(2)	3.2(1)
C(30)	1120(2)	-950(8)	3175(3)	4.7(2)
C(31)	1335(2)	-1460(9)	3632(3)	6.2(2)
C(32)	1747(2)	-1450(8)	3735(3)	5.9(2)
C(33)	1942(2)	-939(8)	3385(3)	5.0(2)
C(34)	1732(2)	-439(7)	2921(2)	3.8(2)
C(35)	2208(2)	-279(7)	1023(2)	3.6(2)

....cont.

....cont. Table 2.8

C(36)	2257(2)	-1674(7)	1028(3)	5.0(2)
C(37)	2634(3)	-2269(9)	1226(3)	6.6(3)
C(38)	2953(2)	-144(1)	1418(3)	7.1(3)
C(39)	2908(2)	-6(1)	1414(4)	7.4(3)
C(40)	2537(2)	527(8)	1227(3)	5.3(2)
C(41)	1479(2)	-410(6)	240(2)	3.4(2)
C(42)	1063(2)	-326(7)	73(2)	3.7(2)
C(43)	879(2)	-878(8)	-398(3)	5.2(2)
C(44)	1095(3)	-1504(8)	-704(3)	6.0(2)
C(45)	1508(3)	-1604(9)	-540(3)	6.4(2)
C(46)	1694(2)	-1068(8)	-78(3)	5.2(2)
C(47)	1811(2)	2148(7)	575(2)	3.7(1)
C(48)	2121(4)	211(1)	237(5)	4.8(3)
C(49)	2204(4)	339(2)	52(6)	5.7(4)
C(50)	1969(3)	4672(9)	188(4)	7.4(2)
C(51)	1756(5)	460(2)	513(6)	5.2(3)
C(52)	1677(4)	328(1)	713(5)	3.4(3)
C(53)	1733(4)	240(2)	50(6)	5.7(3)
C(54)	1794(5)	372(2)	-155(7)	6.9(4)
C(55)	1945(4)	455(2)	717(6)	4.5(3)
C(56)	1868(4)	328(2)	909(6)	4.6(3)

$$^aB_{eq} = 8/3 \pi^2 (U_{11}(aa^*)^2 + (U_{22}(bb^*)^2 + (U_{33}(cc^*)^2 + 2U_{12}aa^*bb^* \cos\gamma + 2U_{13}aa^*cc^*\cos\beta + 2U_{23}bb^*cc^*\cos\alpha)$$

**Table 2.9.** Selected bond distances (Å) and bond angles (°) in  $[\text{RuL}^{5'}(\text{PPh}_3)_2(\text{CO})(\text{Cl})]$

Bond lengths

Ru-Cl(1)	2.484(2)	Ru-P(1)	2.377(2)
Ru-P(2)	2.381(2)	Ru-O(1)	2.246(4)
Ru-C(2)	2.040(5)	Ru-C(16)	1.805(6)
C(1)-O(1)	1.316(6)	C(16)-O(2)	1.158(6)
N(1)-C(7)	1.317(7)	N(1)-C(8)	1.427(7)

Bond angles

Cl-Ru-P(1)	88.54(5)	Cl-Ru-P(2)	94.71(6)
Cl-Ru-O(1)	91.22(10)	Cl-Ru-C(2)	155.3(1)
Cl-Ru-C(16)	103.6(2)	P(1)-Ru-P(2)	176.75(6)
P(1)-Ru-O(1)	88.2(1)	P(1)-Ru-C(2)	87.8(2)
P(1)-Ru-C(16)	91.8(2)	P(2)-Ru-O(1)	91.79(10)
P(2)-Ru-C(2)	89.2(2)	P(2)-Ru-C(16)	87.4(2)
O(1)-Ru-C(2)	64.2(2)	O(1)-Ru-C(16)	165.2(2)
C(2)-Ru-C(16)	100.9(2)	C(7)-N-C(8)	125.2(5)

### 2.5.3. Cyclometallated dinuclear ruthenium(II) complexes

The results of the previous section clearly indicate the facile formation of cyclometallated ruthenium complexes *via*  $[M^{+} \cdots O=C-R]$  intermediate. The dinuclear ruthenium complexes **1-3** are shown to contain two ruthenium centers of the type  $[Ru \cdots O=C-R]$  which can be recognized as the prerequisite for the cyclometallation reaction. Therefore *in situ* cyclometallation reactions of  $L^1-L^3$  were attempted to test the product formation.

Reaction of  $[Ru(dmsO)_4Cl_2]$  with ligands  $L^{1-3}$  in presence of triphenylphosphine yielded orange microcrystalline complexes **9-11**. The IR spectra of the complexes show characteristic absorptions at  $1630\text{ cm}^{-1}$  corresponding to  $C=N$  stretching. A sharp absorption at  $\sim 1910\text{ cm}^{-1}$  corresponding to  $C\equiv O$  is observed for these complexes. In addition to these, absorptions due to coordinated triphenylphosphine ligands are also seen at  $1500, 1480, 740$  and  $690\text{ cm}^{-1}$ . The characteristic IR bands are given in Table 2.1.

The  $^1H$  NMR spectra of the complexes show sharp singlets at  $6.0\text{ ppm}$  and at  $5.8\text{ ppm}$  in addition to a singlet due to azomethine protons at  $7.5\text{ ppm}$ , all of them corresponding to two protons each. Two complex set of signals at  $7.2\text{ ppm}$  and at  $7.7\text{ ppm}$  corresponding to the protons of triphenylphosphine are observed. The signals due to the coordinated dmso molecules are absent. The upfield shift of ring protons is similar as observed in the case of complexes **4-8**. The  $^1H$  NMR spectrum of complex **10** is shown in Figure 2.9. A sharp signal at  $\sim 37\text{ ppm}$  is observed in the  $^{31}P$  NMR spectra

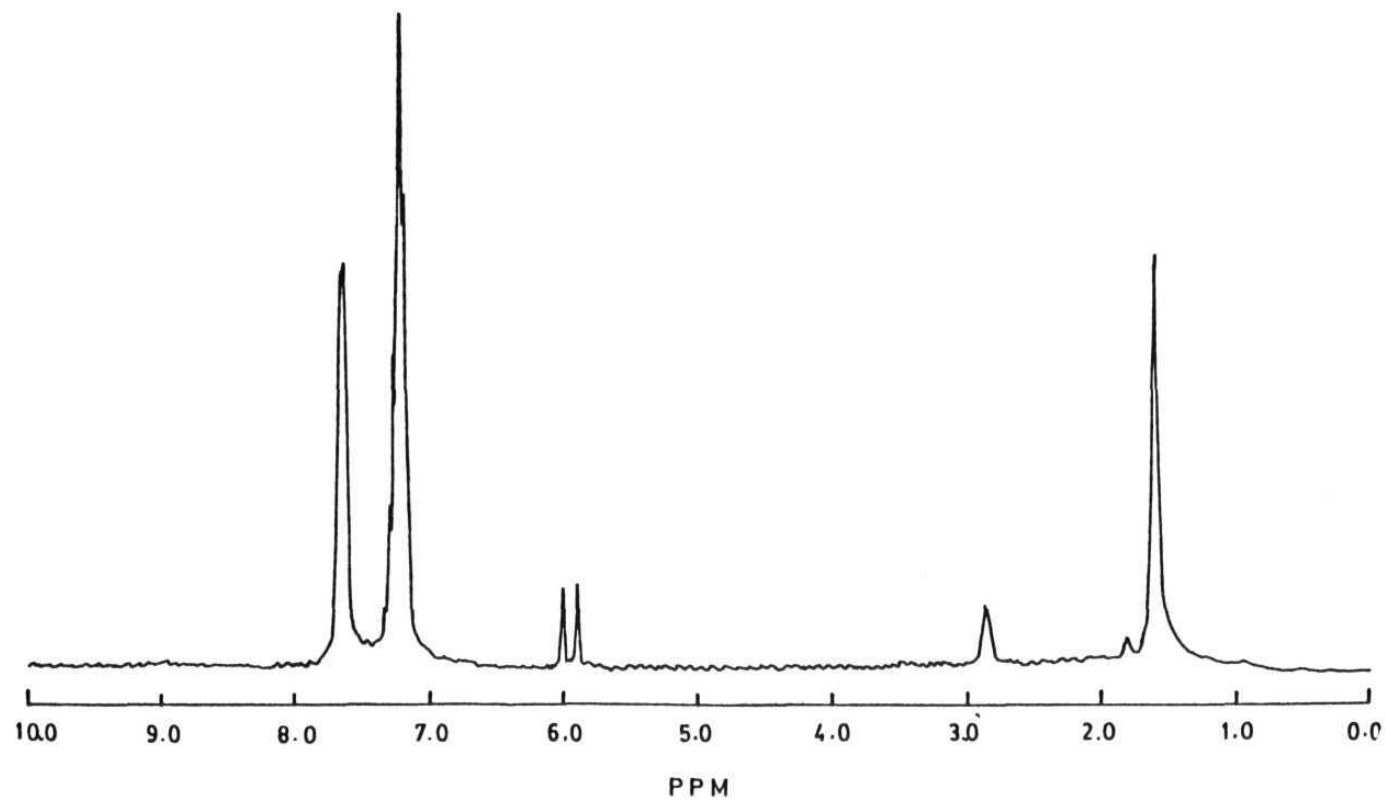
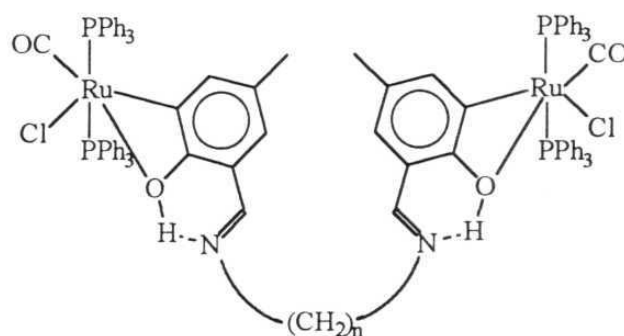


**Figure 2.9.**  $^1\text{H}$  NMR spectrum of a representative complex **10**,  $[\text{Ru}_2\text{L}^{2'}(\text{PPh}_3)_4(\text{CO})_2\text{Cl}_2]$

indicating  $\text{PPh}_3$  to be in the *trans* position. The  $^1\text{H}$  and  $^{31}\text{P}$  NMR data are presented in Table 2.2.

The analytical data (C, H, N) show the composition of the complexes to be  $[\text{Ru}_2\text{L}^n(\text{PPh}_3)_4(\text{CO})_2\text{Cl}_2]$ . The FAB mass spectrum of the complex **10** (MF :  $\text{C}_{93}\text{H}_{88}\text{N}_2\text{O}_4\text{P}_4\text{Cl}_2\text{Ru}_2$ ; MW : 1685) exhibit molecular ion peak at  $m/z$  1685. The intense fragments at  $m/z$  1650, 1614, 1388, 1126, 1090 are due to the progressive loss of chloride or triphenylphosphine units. The spectral and analytical data on complexes **9-11** are quite different from those of the complexes **1-3** and in many respects comparable to those of cyclometallated complexes **4-8**. Possible structure of these products in agreement with the experimental data is given in Figure 2.10. This was



n	2	3	4
Complex	9	10	11

**Figure 2.10.** Generalized structure of complexes **9-11**.

deduced from comparison with structure of cyclometallated  $[\text{RuL}^{5'}(\text{PPh}_3)_2(\text{CO})\text{Cl}]$  complex (*vide supra*). Each Ru(II) is six-coordinated, where the two phosphines are *trans* to each other, the other positions are occupied by phenyl ring carbon, phenolic oxygen, CO and Cl<sup>-</sup> ion.

The complexes **9-11** are obtained only when the ligands are reacted with  $[\text{Ru}(\text{dmsO})_4\text{Cl}_2]$  and  $\text{PPh}_3$  in stoichiometric ratio at a time. The active reagent in the reaction mixture can be presumed to be  $\text{Ru}(\text{PPh}_3)_2\text{Cl}_2$  which is shown to initiate cyclometallation reaction. Addition of  $\text{PPh}_3$  in the later stages of the reaction leads to the formation of mixture of complexes **1-3** and **9-11**. Once formed, the complexes **1-3** do not react further with  $\text{PPh}_3$  implying that  $\text{PPh}_3$  does not replace the coordinated dmsO molecules.

Electronic spectra of the complexes show bands at  $\sim 495$  nm and at  $\sim 370$  nm. These low energy transitions with high intensities are due to the metal to ligand charge-transfer transitions. Magnetic susceptibility experiments indicate the complexes to be diamagnetic and thus confirm the +2 state for ruthenium.

The complexes **9-11** undergo one-electron reversible redox process in the range 0.66 V - 0.69 V in dichloromethane at platinum electrode. The  $\Delta E_p$  values lie in the range of 60-80 mV. The redox potentials of complexes  $[\text{Ru}_2\text{L}^n(\text{PPh}_3)_4(\text{CO})_2\text{Cl}_2]$ , **9-11** are comparable with those of the complexes, **4-8** but quite different from those of the  $[\text{Ru}_2\text{L}^n(\text{dmsO})_4\text{Cl}_4]$ , **1-3** complexes. This further supports the structural similarity of complexes **9-11** and complexes **4-8**. The electrode process corresponds to metal oxidation to Ru(III) state. The CV profile of a representative complex **10** is shown in Figure 2.11 and the data are presented in Table 2.3. Comparison of the

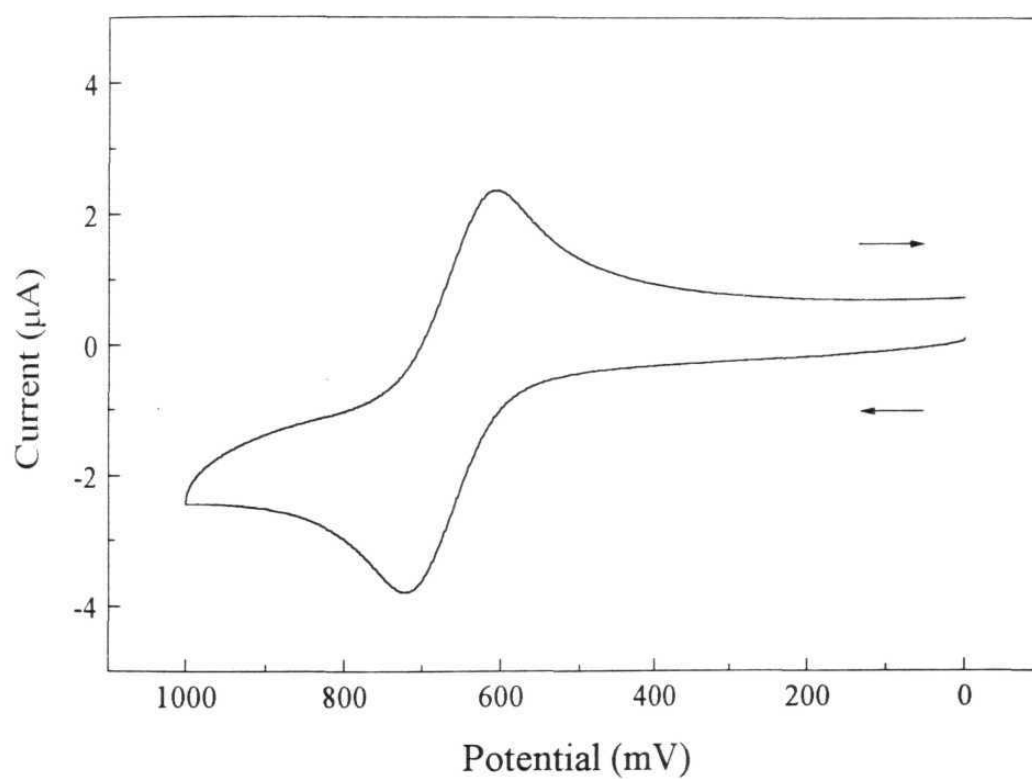


**Figure 2.11.** Cyclic voltammogram of  $[\text{Ru}_2\text{L}^{2'}(\text{PPh}_3)_4(\text{CO})_2\text{Cl}_2]$  complex in  $\text{CH}_2\text{Cl}_2$  (0.1 M TBAP) at platinum electrode at a scan rate of  $100 \text{ mV s}^{-1}$



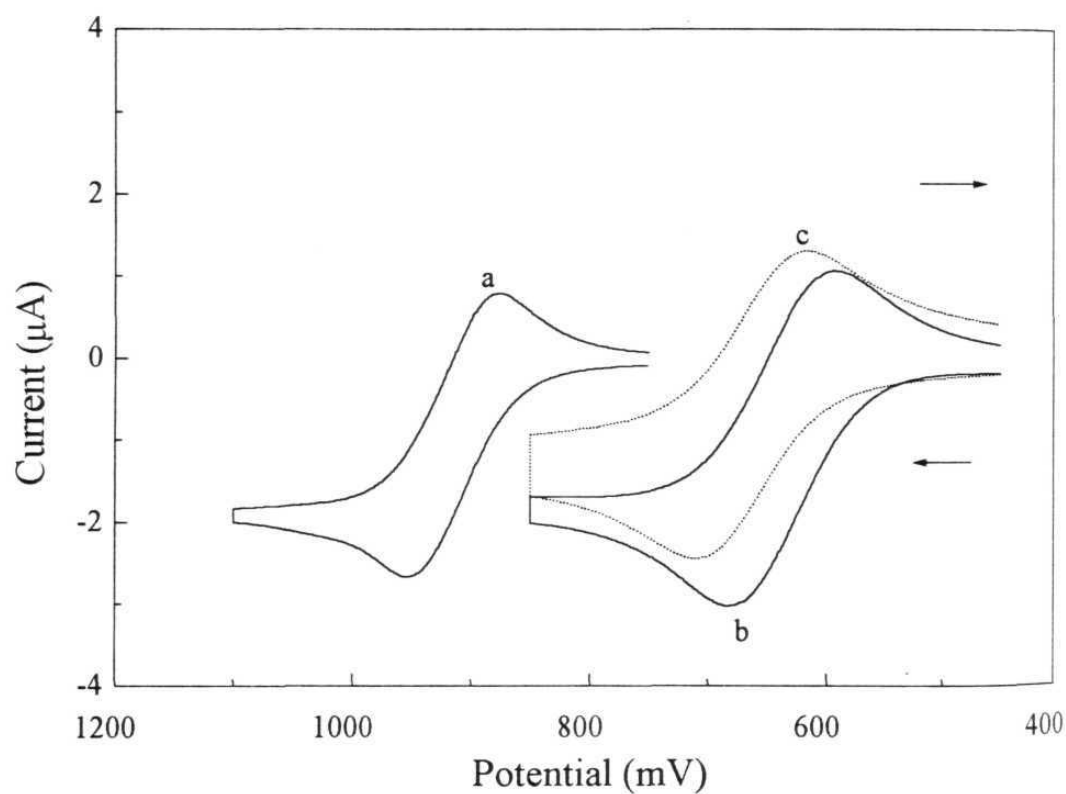
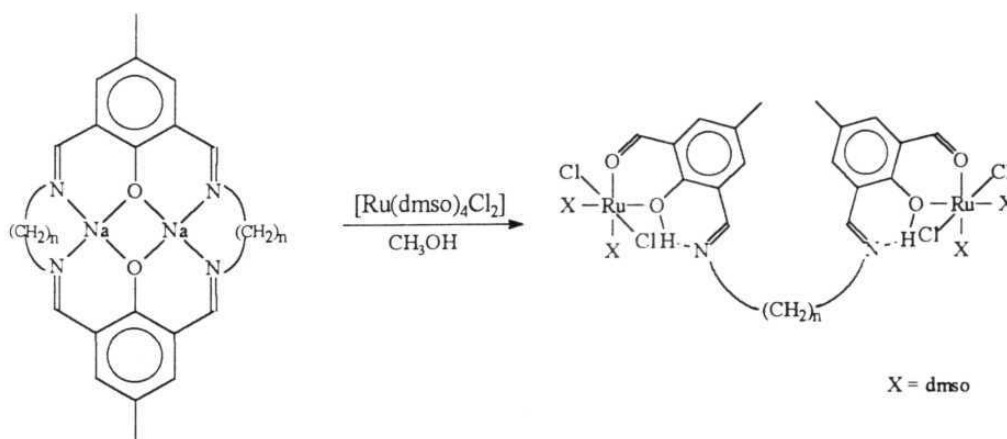


**Figure 2.12.** Cyclic voltammograms in  $\text{CH}_2\text{Cl}_2$  (0.1 M TBAP) at a platinum electrode of complexes **2** (a) **5** (b) and **10** (c) at a scan rate of  $100 \text{ mV s}^{-1}$

electrochemical data of complexes **1-3** with complexes **4-11** show that Ru(II) state is stabilized in complexes **1-3**. Complexes **4-11** undergo oxidation to Ru(III) state more easily owing to the coordination of electron rich triphenylphosphine groups. Comparative cyclic voltammograms of complexes **2**, **5** and **10** are shown in Figure 2.12.

#### 2.5.4. Transmetallation reactions

Attempts to synthesize macrocyclic complexes by template procedure has resulted only in the formation of acyclic dinuclear complexes. Therefore synthesis of macrocyclic complexes by transmetallation reactions was adapted. Sodium phenolate readily reacts with diamines and forms macrocyclic [2+2] Schiff base complexes,  $[\text{Na}_2\text{L}^n]$  ( $n = 9-11$ ). This disodium



n	2	3	4
Complex	$\text{Na}_2\text{L}^9$	$\text{Na}_2\text{L}^{10}$	$\text{Na}_2\text{L}^{11}$

complex of the Robson macrocycle,  $H_2L^n$  ( $n = 9-11$ ) then readily undergoes transmetallation by various transition metal ions to form dinuclear macrocyclic complexes.<sup>25</sup> Reaction of disodium complex with  $[Ru(dmsO)_4Cl_2]$  in  $CH_3OH$  gave dark red microcrystalline solid. Analytical, spectral and redox data of the complexes confirmed the formation of acyclic dinuclear complexes.

This implies the cleavage of the imine function of the macrocycle by hydrolysis to generate acyclic ligands  $H_2L^n$  shown in Scheme 2.1. The Schiff base hydrolysis by addition of water to imine function leading to an  $\alpha$ -hydroxy amine moiety as represented in Scheme 2.4 is proposed.<sup>43</sup>



**Scheme 2.4**

Reaction of disodium complex with  $[Ru(dmsO)_4Cl_2]$  in presence of triphenylphosphine results in the formation of complexes **9-11** *i.e* Schiff base hydrolysis (Scheme 2.4) followed by decarbonylation of the aldehyde function as represented in Scheme 2.3., generating the acyclic ligand system which reacts with ruthenium salts to form the complexes.<sup>41,43</sup>

## 2.6. Conclusions

Template Schiff base condensations of dicarbonyl systems in presence of ruthenium salts like  $[\text{Ru}(\text{dmsO})_4\text{Cl}_2]$  proceeds with the condensation of one carbonyl group while the second carbonyl group is involved in the coordination with ruthenium salts generating acyclic dinuclear complexes. When condensation reactions are performed in presence of triphenylphosphine, cyclometallated complexes are the final products. Attempts to synthesize macrocyclic complexes by transmetallation reactions result in the hydrolysis of Schiff base macrocycle and only acyclic dinuclear complexes are isolated.

## 2.7. References

1. Lahiri, G. K.; Bhattacharya, S.; Mukherjee, M.; Mukherjee, A. K.; Chakravorty, A. *Inorg. Chem.* 1987, **26**, 3359.
2. Bag, N.; Lahiri, G. K.; Bhattacharya, S.; Falvello, L. R.; Chakravorty, A. *Inorg. Chem.* 1988, **27**, 4396.
3. Lahiri, G. K.; Bhattacharya, S.; Ghosh, B. K.; Chakravorty, A. *Inorg. Chem.* 1987, **26**, 4324.
4. Taqui Khan, M. M.; Srinivas, D.; Kureshy, R. I.; Khan, N. H. *Inorg. Chem.* 1990, **29**, 2320. Leung, W.-H.; Che, C.-M. *Inorg. Chem.* 1989, **28**, 4619. Murray, K. S.; Bergen, A. M.; West, B. O. *Aust. J. Chem.* 1978, **31**, 203. Thornback, J. R.; Wilkinson, G. *J. Chem. Soc., Dalton Trans.* 1978, 110.
5. El-Hendawy, A. M.; Alkubaise, A. H.; El-Kourashy, A. El-G.; Shanab, M. M. *Polyhedron* 1993, **12**, 2343. El-Hendawy, A. M.; El-Kourashy, A. El-G.; Shanab, M. *Polyhedron* 1992, **11**, 523.
6. Doine, H.; Stephens, F. F.; Cannon, R. D. *Inorg. Chim. Acta.* 1984, **82**, 149.
7. Menon, M.; Pramanik, A.; Bag, N.; Chakravorty, A. *J. Chem. Soc., Dalton Trans.* 1995, 1417.
8. Bag, N.; Lahiri, G. K.; Partha, B.; Chakravorty, A.; *J. Chem. Soc., Dalton Trans.* 1992, 113. Boone, S. R.; Pierpont, C. G. *Inorg. Chem.* 1987, **26**, 1769. Bhattacharya, S.; Boone, S. R.; Fox, G. A.; Pierpont, C. G. *J. Am. Chem. Soc.* 1990, **112**, 1088.

9. Chakravarty, J.; Bhattacharya, S. *Polyhedron* 1996, **15**, 257.
10. Pramanik, N. C.; Bhattacharya, S. *Polyhedron* 1997, **16**, 1755.
11. Sinha, P. K.; Chakravarty, J.; Bhattacharya, S. *Polyhedron* 1996, **15**, 2931. Chakravarty, J.; Bhattacharya, S. *Polyhedron* 1996, **15**, 1047.
12. Guerriero, P.; Tamburini, S.; Vigato, P. A. *Coord. Chem. Rev.* 1995, **139**, 17. Vigato, P.; Tamburini, S.; Fenton, D. E. *Coord. Chem. Rev.* 1990, **106**, 25. Zanello, P.; Tamburini, S.; Vigato, P. A.; Mazzocchin, G. A. *Coord. Chem. Rev.* 1987, **77**, 165.
13. Pilkington, N. H.; Robson, R. *Aust. J. Chem.* 1970, **23**, 2225. Hoskins, B. F.; Williams, G. A. *Aust. J. Chem.* 1975, **28**, 2607. Hoskins, B. F.; Mcleod, N. J.; Schaap, H. A. *Aust. J. Chem.* 1976, **29**, 515.
14. Adhikary, B.; Mandal, S. K.; Nag, K. *J. Chem. Soc., Dalton Trans.* 1988, 935.
15. Rao, Ch. R. K.; Zacharias, P. S. *Polyhedron* 1996, **16**, 1201. Wada, H.; Motoda, K.; Ohba, M.; Sakiyama, H.; Matsumoto, N.; Okawa, H. *Bull. Chem. Soc. Jpn.* 1995, **68**, 1105. Ikawa, Y.; Nagata, T.; Maruyama, K. *Chem. Lett.* 1993, 1049. Mandal, S. K.; Thompson, L. K.; Newlands, M. J.; Gabe, E. J.; Nag, K. *Inorg. Chem.* 1990, **29**, 1324. Downard, A. J.; Mckee, V.; Tandon, S. S. *Inorg. Chim. Acta.* 1990, **173**, 181. Mandal, S. K.; Thompson, L. K.; Newlands, M. J.; Gabe, E. J. *Inorg. Chem.* 1989, **28**, 3707. Spiro, C. L.; Lambert, S. L.; Smith, T. J.; Duesler, E. N.; Gagne, R. R.; Hendrickson, D. N. *Inorg. Chem.* 1981, **20**, 1229. Gagne, R. R.; Koval, C. A.; Smith, T. J.; Cimolino, C. M. *J. Am. Chem. Soc.* 1979, **101**, 4571.

16. Ohtsuka, S.; Koderu, M.; Motoda, K.; Ohba, M.; Okawa, H. *J. Chem. Soc., Dalton Trans.* 1995, 2599. Okawa, H.; Nishio, J.; Ohba, M.; Tadokoro, M.; Matsumoto, N.; Koikawa, M.; Kida, S.; Fenton, D. E. *Inorg. Chem.* 1993, **32**, 2949. Timken, M. D.; Marrit, W. A.; Hendrickson, D. N.; Gagne, R. R.; Sinn, E. *Inorg. Chem.* 1985, **24**, 4202. Lambert, S. L.; Spiro, C. L.; Gagne, R. R.; Hendrickson, D. N. *Inorg. Chem.* 1982, **21**, 68.
17. Atkins, A. J.; Black, D.; Blake, A. J.; Marin-Becerra, A.; Parsons, S.; Ramirez, I.; Schroder, M. *Chem. Commun.* 1996, 457.
18. Bag, N.; Choudhury, S. B.; Pramanik, A.; Lahiri, G. K.; Chakravorty, A. *Inorg. Chem.* 1990, **29**, 5013. Bag, N.; Choudhury, S. B.; Lahiri, G. K.; Chakravorty, A. *J. Chem. Soc., Chem. Commun.* 1990, 1624.
19. Evans, I. P.; Spencer, A.; Wilkinson, G. *J. Chem. Soc., Dalton Trans.* 1973, 203.
20. Stephenson, T. A.; Wilkinson, G. *J. Inorg. Nucl. Chem.* 1966, **28**, 945.
21. Gagne, R. R.; Spiro, C. L.; Smith, T. J.; Hamann, C. A.; Thies, W. R.; Shiemke, A. K. *J. Am. Chem. Soc.* 1981, **103**, 4073.
22. Okawa, H.; Kida, S. *Bull. Chem. Soc. Jpn.* 1972, **45**, 1759.
23. Vogel, A. I. *Text Book of Practical Organic Chemistry*, ELBS and Longman, 4th Ed. 1978.
24. Perrin, D. D.; Armarego, W. L. F.; Perrin, D. R. *Purification of Laboratory Chemicals* Pergamon press, London 1966.
25. Adams, H.; Bailey, N. A.; Bertrand, P.; Rodriguez de Barbarin, C. O.; Fenton, D. E.; Gou, S. *J. Chem. Soc., Dalton Trans.* 1995, 275.

26. Higashi, T. ABSCOR, An empirical absorption correction based on Fourier coefficient fitting, Rigaku corporation, Tokyo, 1995.
27. Sheldrick, G. M. SHELXTL-PLUS PC Manual Siemens Analytical X-ray Instruments, Madison, Wisconsin, 1990.
28. Sheldrick, G. M. in *Computational Crystallography* Ed. Sayre, S. Oxford University Press, New York, 1982, p. 506.
29. TEXSAN: Crystal Structure Analysis Package, Molecular Structure Corporation, Houston, TX, 1985 and 1992.
30. SIR 92: Altomare, A.; Burla, M. C.; Camalli, M.; Cascarano, M.; Giacovazzo, A.; Polidori, G. *J. Appl. Crystallogr.* 1994, **27**, 1045.
31. Beurskens, P. T.; Admiraal, G.; Beurskens, G.; Bosman, W. P.; de Gelder, R.; Israel, R.; Smits, J. M. M. DIRDIF 94 Report of the Crystallography Laboratory, University of Nijmegen, Netherlands 1994.
32. McGuiggan, M. F.; Pignolet, L. H. *Inorg. Chem.* 1982, **21**, 2523.  
Abraham, F.; Nowogrocki, G.; Sueur, S.; Bremard, C. *Acta Crystallogr. Sect. B.* 1980, **36**, 779; Bennett, M. A.; Matheson, T. W.; Robertson, G. B.; Steffen, W. L.; Turney, T. W. *J. Chem. Soc., Chem. Commun.* 1979, 32.
33. Mercer, A.; Trotter, J. J. *J. Chem. Soc., Dalton Trans.* 1975, 2480.
34. Alessio, E.; Mestroni, G.; Nardin, G.; Attia, M. W.; Calligaris, M.; Sava, G.; Zorzet, S. *Inorg. Chem.* 1988, **27**, 4099.
35. Jaswal, J. S.; Retting, S. J.; James, B. R. *Can. J. Chem.* 1990, **68**, 1808.
36. Reynolds, W. L. *Progr. Inorg. Chem.* 1970, **12**, 1.
37. Srinivas, B.; Arulsamy, N.; Zacharias, P. S. *Polyhedron* 1991, **10**, 731.
38. Srinivas, B.; Zacharias, P. S. *Transition Met. Chem.* 1991, **16**, 521.



39. Pizzotti, M.; Crotti, C.; Demartin, F. *J. Chem. Soc., Dalton Trans.* 1984, 735.
40. Lever, A. B. P.; Auburn, P. R.; Dodsworth, E. S.; Haga, M.; Liu, W.; Meln, M.; Nevin, A. *J. Am. Chem. Soc.* 1988, **110**, 8076.
41. Sonnenfroh, D. M.; Farrar, J. M. *J. Am. Chem. Soc.* 1986, **108**, 3521.
42. Ashworth, T. V.; Singleton, E. *J. Chem. Soc., Chem. Commun.* 1976, 705.
43. Kayser, R. H.; Pollack, R. M. *J. Am. Chem. Soc.* 1977, **99**, 3379.  
Menon, M.; Pramanik, A.; Chakravorty, A. *Inorg. Chem.* 1995, **34**, 3310.  
Dirghangi, B. K.; Menon, M.; Pramanik, A.; Chakravorty, A. *Inorg. Chem.* 1997, **36**, 1095.

## CHAPTER 3

### Synthesis, Characterization and Catalytic Activity of Dinuclear Fe(III) and Ru(III) Complexes\*

#### 3.1. Abstract

A number of dinuclear Fe(III) and Ru(III) complexes of triazene-1-oxide and Schiff base ligands are synthesized and characterized. Based on the analytical, spectral and magnetic data, square-pyramidal geometry is assigned to the Fe(III) complexes and octahedral geometry to Ru(III) complexes. The generalized structures of the complexes are given in Figure 3.1 and Figure 3.2. The complexes are catalytically active for the epoxidation of olefins.

---

\*Part of the work presented in this chapter appeared in *Polyhedron* 1994, **13**, 2659 and *Polyhedron* 1996, **15**, 2445.

### 3.2. Introduction

Metal-catalyzed conversion of olefins to epoxides has received attention because of its chemical and biochemical significance. Several transition-metal complexes with various ligands have been used as catalysts for epoxidation because of their selectivity in oxidation reactions and the flexibility in the synthesis of complexes with specific structural characteristics.<sup>1</sup> In general, the utility of these catalytic systems for effective epoxidation is very limited, but they are useful for mechanistic studies to demonstrate the role of the oxometal intermediate in the oxidation process.

Several mononuclear Fe(II) cyclam complexes,<sup>2</sup> chiral Fe(III) bipyridine macrocyclic complexes<sup>3</sup> and mono and dinuclear Fe(III) Schiff base complexes<sup>4,5</sup> have been used as epoxidation catalysts in presence of various terminal oxidants. FeSO<sub>4</sub><sup>6</sup> in presence of bipyridine and phenanthroline ligands, FeCl<sub>2</sub> with N,N'-bis[2-(4-imidazolyl)ethyl]-2,6-pyridine-dicarboxamide<sup>7</sup> have also been shown to catalyze epoxidations.

Ru(II) phosphine complexes,<sup>8,9</sup> Ru(III) bipyridine and phenanthroline complexes,<sup>10</sup> Ru(III) and Ru(IV) amide complexes<sup>11,12</sup> and some Ru(III) Schiff base complexes<sup>13,14</sup> have been studied as catalysts for epoxidations. In addition to these complexes, several other ruthenium complexes with various ligand structures are shown to catalyze oxidation of olefins.<sup>6,15-18</sup>

In most of the catalytic reactions with iodosylbenzene as oxygen source, a high-valent oxometal species is proposed as an intermediate. Such species is characterized in Ru(III) saloph<sup>19</sup> complexes. The O=Cr(V) salen

complex has been crystallographically characterized.<sup>20</sup> Metal-catalyzed oxidations may also proceed *via* M-O-I-Ph reactive intermediate which is isolated in the manganese porphyrin system.<sup>21</sup> Formation of M-O-M species, decreases the catalytic efficiency of the system.<sup>22</sup> While formation of such species is possible in mononuclear complexes, the feasibility of formation decreases in dinuclear complexes, which in turn should increase the catalytic efficiency of the complexes. To explore this possibility some biphenyl-bridged dinuclear Fe(III) and Ru(III) complexes are synthesized and characterized and their catalytic activity in epoxidation reactions is investigated. The dinucleating ligands used are triazene-1-oxides ( $L^{12-14}$  ; type 1) obtained by the diazo coupling of biphenyl amines with alkyl hydroxyl amine and Schiff bases ( $L^{15-18}$  ; type 2), formed by the condensation of pyridine-2-carboxaldehyde with biphenyl amines. In the ligand,  $L^{14}$  the biphenyl amine moiety is replaced by 4,4'-diaminodiphenylmethane while in ligands,  $L^{17}$  and  $L^{18}$  4,4'-diaminodiphenylmethane and 4,4'-diaminodiphenylether are used. These biphenyl-bridged dinuclear complexes behave more like mononuclear complexes since spin delocalization is limited.

### 3.3. Experimental

The diamines, 4,4'-diamino-3,3'-dimethylbiphenyl, 4,4'-diamino-3,3'-dimethoxybiphenyl, 4,4'-diaminodiphenylmethane and 4,4'-diaminodiphenylether were recrystallized from methanol prior to use. All the solvents were

dried by standard procedures<sup>23,24</sup> and were stored over molecular sieves.  $[\text{Ru}(\text{dmsO})_4\text{Cl}_2]$  and  $\text{Ru}(\text{PPh}_3)_2\text{Cl}_3(\text{CH}_3\text{OH})$  were synthesized by reported methods.<sup>25,26</sup> Iodosylbenzene was synthesized from iodosylbenzene diacetate as reported earlier.<sup>27</sup>

### 3.3.1. Synthesis of ligands

#### Synthesis of triazene-1-oxide ligands ( $\text{L}^{12-14}$ )

The ligands,  $\text{L}^{12-14}$  were obtained by the diazo coupling of diphenylamines with alkyl hydroxylamine as reported in the literature.<sup>28</sup> A generalized procedure is given below. To 10 mmol of diamine in 25 mL of water, 2.1 mL of conc. hydrochloric acid was added. The solution was cooled in an ice bath and further 2.1 mL of hydrochloric acid was added when the temperature of the solution was below 10 °C. This solution was tetra-azotized with 20 mmol of sodium nitrite in 20 mL of water (added in portions) while maintaining the temperature in the range 5-10 °C. A slight excess of nitrous acid is desirable. This tetra-azotized solution was added to a solution of N-ethyl hydroxylamine-hydrochloride (> 20 mmol) in 50 mL of water with magnetic stirring. The pH of the reaction mixture was maintained in the range 5-6 by addition of 10-20 g of sodium acetate in 50 mL of water. A brown precipitate slowly separated out and was filtered at the pump. This compound was dried and recrystallized from acetone. Yield : 75%.

### Synthesis of Schiff base ligands ( $L^{15-18}$ )

These ligands were obtained by the condensation of diamine with pyridine-2-carboxaldehyde in 1:2 ratio. In a typical procedure, 10 mmol of diamine was dissolved in 30 mL of dry ethanol, 20 mmol of freshly distilled pyridine-2-carboxaldehyde dissolved in 20 mL of ethanol was added and the reaction mixture was refluxed for 3 h. The resulting yellow solid was filtered, washed with small amounts of ethanol to obtain pure compound. The synthesis of ligands  $L^{16}$  and  $L^{18}$  by similar procedures gave gummy materials which were difficult to purify. But in presence of metal salts, these reactions gave required complexes in good yields. Hence no further attempts were made to synthesize pure ligands.

### 3.3.2. Synthesis of Complexes

#### $[Fe_2L_nCl_2]$ ( $n = 12-14$ ) complexes

The complexes **12-14** were synthesized by the following general procedure. To a solution of ligand  $L^n$  (1 mmol) in dry ethanol, anhydrous  $FeCl_3$  (0.162 g, 1 mmol) was added and the mixture was refluxed for 3 h. After removal of alcohol, the black gummy mass obtained was dissolved in dichloromethane and was precipitated by addition of hexane. The complex was collected by filtration and dried in *vacuum* for 4 h.

$[\text{Fe}_2\text{L}_2^{\text{n}}\text{Cl}_2]\text{Cl}_4$  ( $n = 15, 17$ ) complexes

The complexes **17** and **19** were synthesized as follows. To a solution of ligand (1 mmol) in 20 mL of dry ethanol, was added 1 mmol of anhydrous  $\text{FeCl}_3$  in 10 mL of ethanol. The reaction mixture was refluxed for 4 h. The precipitated complex was filtered, washed with ethanol and dried in *vacuum* for 2 h.

$[\text{Fe}_2\text{L}_2^{\text{n}}\text{Cl}_2]\text{Cl}_4$  ( $n = 16, 18$ ) complexes

The complexes **18** and **20** were synthesized by the procedure given below. To a solution of amine (0.5 mmol) in 20 mL dry ethanol was added a solution of pyridine-2-carboxaldehyde (1 mmol) in 10 mL of ethanol. The reaction mixture was refluxed for 0.5 h. To the Schiff base formed, anhydrous  $\text{FeCl}_3$  (1 mmol) in ethanol (20 mL) was added under nitrogen. The precipitated complex was collected by filtration, washed with ethanol and dried in *vacuum* for 2 h.

Synthesis of  $\text{Ru}_2\text{L}_2^{\text{n}}(\text{PPh}_3)_2$  complexes ( $n = 12, 14, 15, 17$ )

The complexes **15**, **16**, **21** and **22** were synthesized by the generalized procedure given below. To a solution of ligand  $\text{L}^{\text{n}}$  (1 mmol) in 40 mL of dry ethanol was added  $\text{Ru}(\text{PPh}_3)_2\text{Cl}_3(\text{CH}_3\text{OH})$  (1 mmol) under nitrogen and the reaction mixture was refluxed for 3 h. After removal of solvent, the gummy mass was dissolved in dichloromethane and was precipitated by hexane. The

complex separated was collected by filtration and washed repeatedly with warm hexane to remove any excess of  $\text{PPh}_3$  and dried in *vacuum* for 4 h.

### 3.3.3. Epoxidation of olefins

Epoxidation reactions were carried out in a Schlenk tube under nitrogen. To a solution of catalyst [Fe(III) or Ru(III) complex; 0.005 mmol] in 5 mL of dichloromethane was added the alkene (2.5 mmol). Iodosylbenzene (0.110 g, 0.5 mmol) was added to this mixture over a period of 30 min. The mixture was stirred at ambient temperature for 3 h. The products were distilled off and analyzed by GC using a carbowax 20 column.

### 3.4. Physical measurements

The carbon, hydrogen, and nitrogen analysis were carried out on a Perkin-Elmer 240C elemental analyzer. IR spectra were recorded on a JASCO FT/IR 5300 spectrophotometer in KBr pellets. Electronic absorption spectra were recorded on a JASCO model 7800 UV-vis spectrophotometer. Conductivity experiments were done on CM 82T Elico conductivity meter at 25 °C. Magnetic susceptibility measurements were carried out by Faraday method, at room-temperature using a CAHN magnetic balance set-up. Diamagnetic corrections were made using Pascals constants.<sup>29</sup> Epoxides were estimated using a Shimadzu GS 14A gas chromatograph [GC column (3M),



carbowax 20M, 15 % on chromosorb W, carrier gas, nitrogen, detector, FID, injection temperature 240 °C]. Cyclic voltammograms were recorded on Cypress systems model CS-1090/CS-1087 computer controlled electroanalytical system. All experiments were performed under dry nitrogen in dichloromethane. 0.001 M solution was used with 0.1 M  $\text{NBu}_4\text{ClO}_4$  as supporting electrolyte using a platinum working electrode, Ag-AgCl reference electrode and platinum wire as auxiliary electrode.

### 3.5. Results and Discussion

#### 3.5.1. Fe(III) complexes

Synthetic details of the complexes are given in the experimental section 3.3.2. All the complexes are characterized by C, H and N analytical data and the values are presented in Table 3.1. Analytical data agree with the molecular formula  $\text{Fe}_2\text{L}_2\text{Cl}_2$  for type 1 ligands and  $\text{Fe}_2\text{L}_2\text{Cl}_6$  for type 2 ligands.

The IR spectra of the complexes of type 1 ligands are characterized by bands at  $1610\text{ cm}^{-1}$  due to N=N stretch and at  $1250\text{ cm}^{-1}$  due to N→O stretch. For complexes of type 2 ligands, the C=N stretch was observed at  $1600\text{ cm}^{-1}$ . The characteristic IR frequencies are presented in Table 3.2.

Magnetic moment values per iron at room-temperature are in the range  $\mu_{\text{eff}} = 5.6$  to  $5.8\ \mu_{\text{B}}$  for both the types of complexes. These values are

close to  $\mu_{\text{eff}}$  values for high-spin mononuclear complexes ( $S = 5/2$ ), implying the absence of measurable antiferromagnetic interactions between the iron centers. This ground state configuration of  $S = 5/2$  is possible for both five and six-coordinate geometry. Some of the dinuclear Fe(III) complexes of the biphenyl-bridged system have been shown to be five-coordinate with  $\mu_{\text{eff}}$  values of  $5.8 \mu_{\text{B}}$ .<sup>30</sup>

The conductivity values of the  $\text{Fe}_2\text{L}_2^{\text{n}}\text{Cl}_2$  complexes are low indicating them to be non-electrolytes which suggest that the chloride ions are in the inner coordination sphere. Conductivity values for the complexes of type 2 ligands could not be measured because of their poor solubility. Five-coordinate square-pyramidal geometry is proposed for the iron center based on the experimental data and by comparison with the analogous dinuclear Fe(III) complexes.<sup>30</sup> One chloride ion occupies the fifth coordination position of each iron center. The generalized structures are shown in Figure 3.1.

Electronic spectra of the complexes of type 1 ligands have a shoulder at *ca* 530 nm and for the complexes of type 2 ligands at *ca* 580 nm. Due to the high-intensity ligand transitions in the UV region (360-370 nm), the weak *d-d* transition of the complexes are seen as shoulder. For five-coordinate Fe(III) systems two *d-d* transitions are expected at 500 nm and 400 nm.<sup>31</sup> The positions can vary depending on the ligand systems. For six-coordinate Fe(III) complexes all *d-d* transitions are forbidden and hence absorption bands are generally not observed. The electronic spectral band positions are presented in Table 3.2. The high  $\epsilon$  values show intensity borrowing from the adjacent charge-transfer bands.

**Table 3.1.** Analytical data for Fe(III) and Ru(III) complexes

Complex	Analysis (%) found (calc.)		
	C	H	N
$[\text{Fe}_2\text{L}_2^{12}\text{Cl}_2]$	48.4 (48.5)	4.9 (4.9)	18.7 (18.9)
$[\text{Fe}_2\text{L}_2^{13}\text{Cl}_2]$	45.1 (45.2)	4.5 (4.6)	17.3 (17.6)
$[\text{Fe}_2\text{L}_2^{14}\text{Cl}_2]$	47.3 (47.5)	4.1 (4.6)	19.5 (19.6)
$[\text{Ru}_2\text{L}_2^{12}(\text{PPh}_3)_2\text{Cl}_2]$	57.3 (57.5)	4.7 (4.9)	11.1 (11.2)
$[\text{Ru}_2\text{L}_2^{14}(\text{PPh}_3)_2\text{Cl}_2]$	56.3 (56.8)	4.6 (4.7)	11.2 (11.4)
$[\text{Fe}_2\text{L}_2^{15}\text{Cl}_2]\text{Cl}_4$	56.3 (56.5)	5.4 (4.0)	9.3 (10.1)
$[\text{Fe}_2\text{L}_2^{16}\text{Cl}_2]\text{Cl}_4$	52.8 (53.4)	4.0 (3.8)	9.4 (9.6)
$[\text{Fe}_2\text{L}_2^{17}\text{Cl}_2]\text{Cl}_4$	55.6 (55.7)	3.6 (3.7)	10.3 (10.4)
$[\text{Fe}_2\text{L}_2^{18}\text{Cl}_2]\text{Cl}_4$	53.1 (53.3)	3.2 (3.3)	10.4 (10.4)
$[\text{Ru}_2\text{L}_2^{15}(\text{PPh}_3)_2\text{Cl}_2]\text{Cl}_4$	61.2 (61.4)	4.0 (4.3)	6.1 (6.6)
$[\text{Ru}_2\text{L}_2^{17}(\text{PPh}_3)_2\text{Cl}_2]\text{Cl}_4$	61.2 (61.3)	4.3 (4.1)	6.4 (6.5)

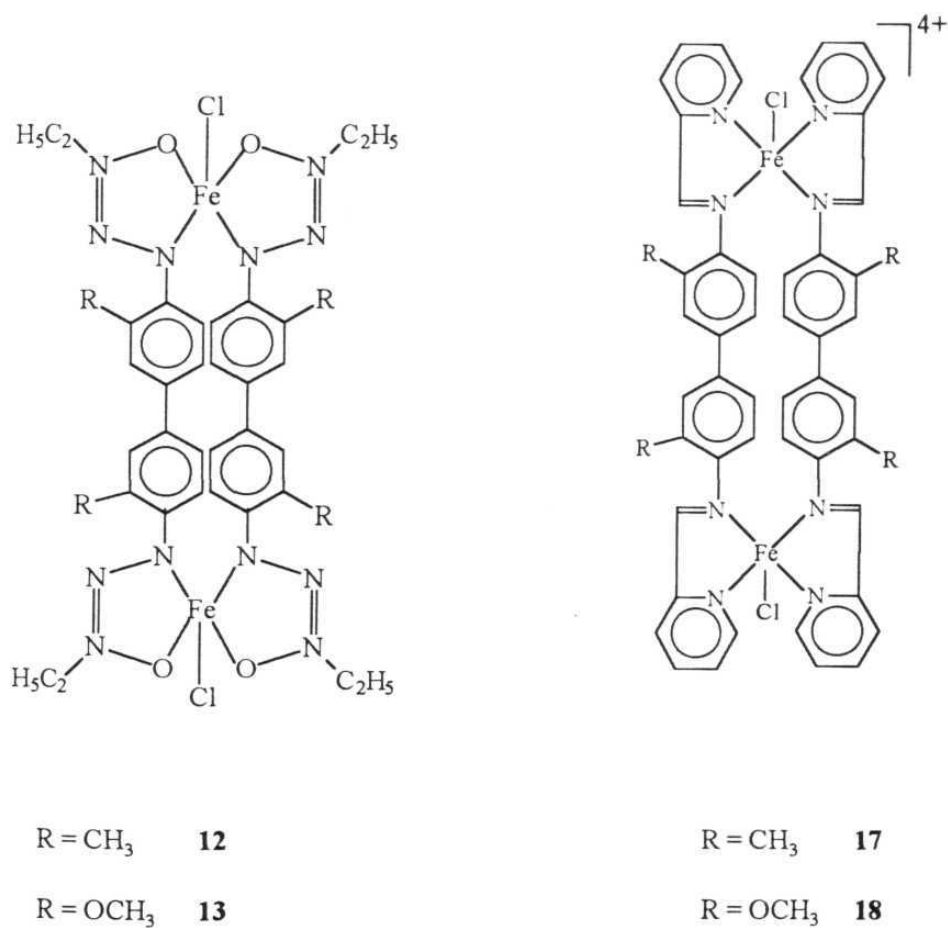


**Figure 3.1.** Generalized structure of Fe(III) complexes.

### 3.5.2. Ruthenium(III) complexes

Ruthenium(III) complexes in general are catalytically more active than Fe(III) complexes. Therefore ruthenium(III) complexes of type 1 and type 2

ligands were synthesized to compare the catalytic activity. These complexes were synthesized by the reaction of  $\text{Ru}(\text{PPh}_3)_2\text{Cl}_3(\text{CH}_3\text{OH})$  with various ligands. The synthetic details are given in experimental section 3.3.2. All the complexes were characterized by C, H, and N analytical data and the values are presented in Table 3.1. The analytical data agree with the general composition of  $\text{Ru}_2\text{L}_2^n(\text{PPh}_3)_2\text{Cl}_2$  for type 1 complexes and  $\text{Ru}_2\text{L}_2^n(\text{PPh}_3)_2\text{Cl}_6$  for type 2 complexes. Attempts to synthesize ruthenium(II) complexes by the reaction of  $[\text{Ru}(\text{dmsO})_4\text{Cl}_2]$  with these ligands resulted in corresponding ruthenium(III) complexes. This is in agreement with the report that triazene-1-oxide ligands do not stabilize the ruthenium(II) oxidation state.<sup>32</sup>

The IR spectra of the complexes show several prominent bands. The Schiff base complexes show the characteristic C=N stretching at  $\sim 1620\text{ cm}^{-1}$  and the triazene-1-oxide complexes show bands in the range of  $1590\text{--}1600\text{ cm}^{-1}$  corresponding to N=N stretching and at  $1275\text{ cm}^{-1}$  due to the N $\rightarrow$ O stretch. In addition, two sets of bands at  $1480$  and  $1435\text{ cm}^{-1}$  and at  $744$  and  $694\text{ cm}^{-1}$  are also observed. These bands originate from the C=C and C-H stretches of the monosubstituted benzene ring of the triphenylphosphine unit. Observation of these bands indicate presence of the triphenylphosphine unit.

The conductivity values for the complexes of type 1 ligands are very low indicating them to be non-electrolytes and for the complexes of type 2 ligands, the values are in the range of 1:4 electrolytes. Based on the experimental data, six-coordinate geometry is proposed for the Ru(III) center

with one chloride and one triphenylphosphine as axial ligands. The structure assigned to these complexes is shown in Figure 3.2.

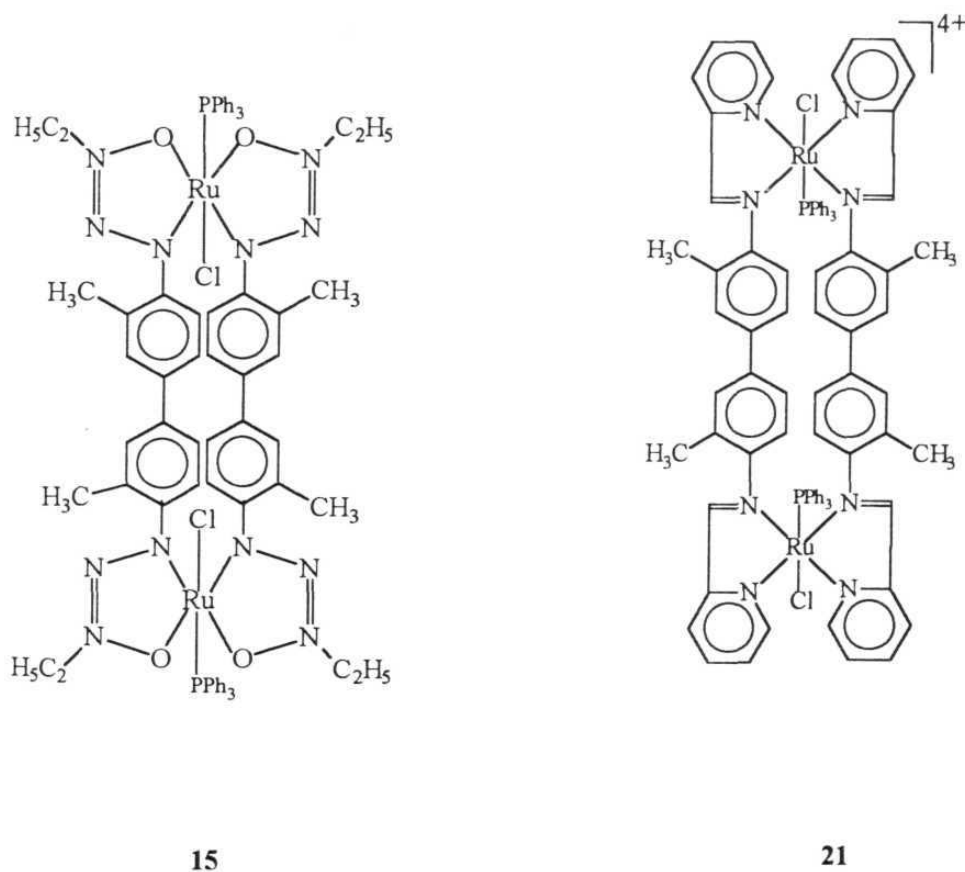


**Figure 3.2.** Generalized structure of Ru(III) complexes.

The magnetic moment values of the complexes at room-temperature are near the spin-only value corresponding to one unpaired electron,

**Table 3.2.** Spectral and magnetic data of Fe(III) and Ru(III) complexes

Complex	Characteristic IR bands (cm <sup>-1</sup> )			UV-vis data <sup>a</sup> λ, nm (ε, M <sup>-1</sup> cm <sup>-1</sup> )	μ <sub>eff</sub> (μ <sub>B</sub> )
	N=N	C=N	N→O		
[Fe <sub>2</sub> L <sub>2</sub> <sup>12</sup> Cl <sub>2</sub> ]	1615		1260	570 (3490)	5.62
[Fe <sub>2</sub> L <sub>2</sub> <sup>13</sup> Cl <sub>2</sub> ]	1615		1260	535 (3005)	5.51
[Fe <sub>2</sub> L <sub>2</sub> <sup>14</sup> Cl <sub>2</sub> ]	1615		1270	520 (1080)	5.72
[Ru <sub>2</sub> L <sub>2</sub> <sup>12</sup> (PPh <sub>3</sub> ) <sub>2</sub> Cl <sub>2</sub> ]	1590		1260	760 (4020)	1.83
[Ru <sub>2</sub> L <sub>2</sub> <sup>14</sup> (PPh <sub>3</sub> ) <sub>2</sub> Cl <sub>2</sub> ]	1600		1275	780 (9860)	1.89
[Fe <sub>2</sub> L <sub>2</sub> <sup>15</sup> Cl <sub>2</sub> ] <sub>4</sub>		1640		500 (sh)	5.84
[Fe <sub>2</sub> L <sub>2</sub> <sup>16</sup> Cl <sub>2</sub> ] <sub>4</sub>		1600		585 <sup>b</sup>	5.86
[Fe <sub>2</sub> L <sub>2</sub> <sup>17</sup> Cl <sub>2</sub> ] <sub>4</sub>		1600		570 <sup>b</sup>	5.88
[Fe <sub>2</sub> L <sub>2</sub> <sup>18</sup> Cl <sub>2</sub> ] <sub>4</sub>		1620		580 <sup>b</sup>	5.60
[Ru <sub>2</sub> L <sub>2</sub> <sup>15</sup> (PPh <sub>3</sub> ) <sub>2</sub> Cl <sub>2</sub> ] <sub>4</sub>		1625		520 (6120)	1.86
[Ru <sub>2</sub> L <sub>2</sub> <sup>17</sup> (PPh <sub>3</sub> ) <sub>2</sub> Cl <sub>2</sub> ] <sub>4</sub>		1620		560 (7410)	1.89

<sup>a</sup>in dichloromethane<sup>b</sup>qualitative because of partial solubility

suggesting a low spin  $d^5$  configuration for ruthenium(III) center with no interaction between the metal ions. The data are given in Table 3.2. The UV-vis spectra of the complexes in dichloromethane showed a high-intensity broad band at *ca* 700 nm for type 1 complexes and at *ca* 500 nm for type 2 complexes. The spectral data are presented in Table 3.2. The high-intensity bands are assigned to ligand to metal charge transfer transitions.<sup>33</sup> Such high-intensity bands generally obscure the weak *d-d* transitions of the metal centers.

### 3.5.3. Electrochemistry

The cyclic voltammetric characteristics of Fe(III) complexes of type 1 ligands showed cathodic peaks at 0.91 V and the corresponding anodic peaks at 0.79 V in the negative potential range. This quasi-reversible process may be due to  $\text{Fe(III)} \rightleftharpoons \text{Fe(II)}$ . In the positive potential range only ill-defined peaks were observed.

The redox properties of the ruthenium complexes have also been investigated in dichloromethane solvent. All the complexes exhibit single redox couple in the range 0.52 V to 0.58 V corresponding to reversible oxidation of  $\text{Ru(III)} \rightleftharpoons \text{Ru(IV)}$  species. The anodic and cathodic peak heights are equal and the  $\Delta E_p$  values lie in the range of 60 - 100 mV. A representative profile at various scan rates is shown in Figure 3.3. The results are presented in Table 3.3. In the negative potential range ill-defined



reduction peaks at *ca* 0.71 V could be observed. However, no oxidation peaks were observed indicating irreversible reduction of Ru(III) species.

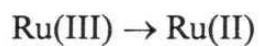


**Table 3.3.** Cyclic voltammetric data for Ru(III) complexes<sup>a</sup>

Complex	Ru(III) to Ru(IV) $E_{1/2}$ (V)	$\Delta E_p$ (mV)
$[\text{Ru}_2\text{L}_2^{12}(\text{PPh}_3)_2\text{Cl}_2]$	0.53	80
$[\text{Ru}_2\text{L}_2^{14}(\text{PPh}_3)_2\text{Cl}_2]$	0.52	60
$[\text{Ru}_2\text{L}_2^{15}(\text{PPh}_3)_2\text{Cl}_2]\text{Cl}_4$	0.55	90
$[\text{Ru}_2\text{L}_2^{17}(\text{PPh}_3)_2\text{Cl}_2]\text{Cl}_4$	0.57	100

<sup>a</sup>potential measured at platinum working electrode in dichloromethane solvent (0.1 M TBAP) with Ag-AgCl as reference electrode

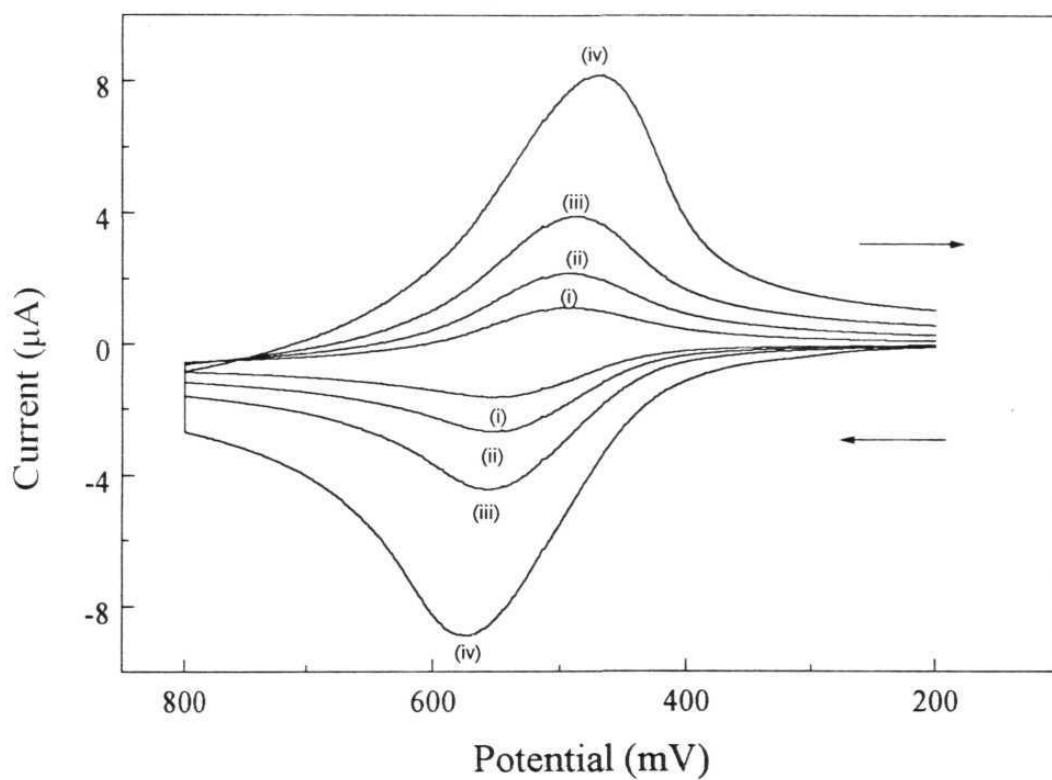
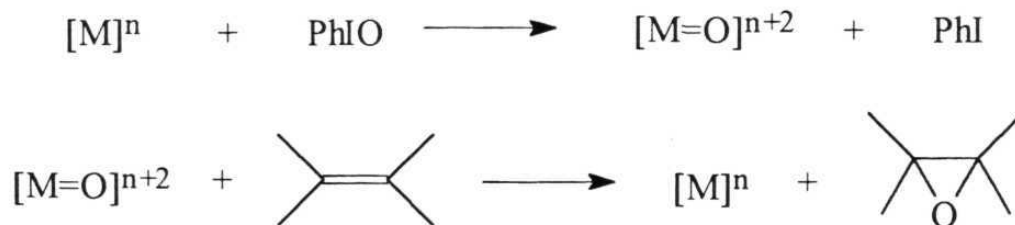


**Figure 3.3.** Cyclic voltammogram of  $[\text{Ru}_2\text{L}_2^{14}(\text{PPh}_3)_2\text{Cl}_2]$  complex in  $\text{CH}_2\text{Cl}_2$  (0.1 M TBAP) at a platinum electrode at a scan rate of (i) 50 (ii) 100 (iii) 200 (iv) 500  $\text{mV s}^{-1}$

### 3.5.4. Epoxidation reactions

The complexes were seen to catalyze epoxidation of olefins using iodosylbenzene as terminal oxidant. The catalytic activity of Fe(III) and Ru(III) complexes were checked using cyclohexene and styrene as substrates under a standard set of conditions. Details are given in the experimental section. The products of oxidation reactions were mainly epoxides with small traces of allylic oxidation products when cyclohexene was substrate. In the absence of metal complexes, no oxidized products were observed. The results of epoxidation studies are given in Table 3.4.

Generally oxometal species is proposed as the intermediate in this type of reactions (Scheme 3.1). Such oxo species have been characterized in the case of [Ru(III)saloph]<sup>19</sup> complexes. Similar type of intermediates are proposed in some Fe(III)<sup>4,5</sup> and Ru(III)<sup>13,14</sup> Schiff base complex-catalyzed epoxidations. In the present study, attempts to isolate such species were unsuccessful, perhaps owing to their poor stability.



Scheme 3.1

**Table 3.4.** Epoxidation data<sup>a</sup> of Fe(III) and Ru(III) complexes

Complex	Yield of epoxide (%) <sup>b</sup>	
	Cyclohexene	Styrene
[Fe <sub>2</sub> L <sub>2</sub> <sup>12</sup> Cl <sub>2</sub> ]	7.5	12.9
[Fe <sub>2</sub> L <sub>2</sub> <sup>13</sup> Cl <sub>2</sub> ]	8.6	12.4
[Fe <sub>2</sub> L <sub>2</sub> <sup>14</sup> Cl <sub>2</sub> ]	6.8	12.3
[Ru <sub>2</sub> L <sub>2</sub> <sup>12</sup> (PPh <sub>3</sub> ) <sub>2</sub> Cl <sub>2</sub> ]	5.6	28.8
[Ru <sub>2</sub> L <sub>2</sub> <sup>14</sup> (PPh <sub>3</sub> ) <sub>2</sub> Cl <sub>2</sub> ]	5.0	22.9
[Fe <sub>2</sub> L <sub>2</sub> <sup>15</sup> Cl <sub>2</sub> ] <sub>4</sub>	6.0	10.3
[Ru <sub>2</sub> L <sub>2</sub> <sup>15</sup> (PPh <sub>3</sub> ) <sub>2</sub> Cl <sub>2</sub> ] <sub>4</sub>	7.0	14.8
[Ru <sub>2</sub> L <sub>2</sub> <sup>17</sup> (PPh <sub>3</sub> ) <sub>2</sub> Cl <sub>2</sub> ] <sub>4</sub>	9.1	14.8

<sup>a</sup>At room-temperature in dichloromethane<sup>b</sup>Yields calculated based on iodosylbenzene consumed.

In presence of  $[\text{Fe}_2\text{L}_2^{\text{n}}\text{Cl}_2]$  complexes as catalysts, the percentage yield of epoxide is in the range of 12 for styrene and 7-9 for cyclohexene. For  $[\text{Fe}_2\text{L}_2^{\text{15}}\text{Cl}_2]\text{Cl}_4$  complex, the percentage yield is 6. For the corresponding mononuclear complex the reported yield was 2%.<sup>4</sup> It has been reported in the case of some iron porphyrins and some iron Schiff base systems that the decrease in catalytic efficiency is due to the formation of  $\mu$ -oxo species of the type  $\text{Fe(IV)-O-Fe(IV)}$ <sup>22</sup> as an intermediate. The possibility of formation of such species is reduced in dinuclear complexes. This may contribute to the enhanced catalytic efficiency of dinuclear complexes compared to the mononuclear analogues.

For Ru(III) complexes, the yield of epoxides based on iodosylbenzene was in the range of 14.8% - 28.8% for styrene and 5% - 9.1% for cyclohexene. In all the systems, iodobenzene was isolated in quantitative yields. For mononuclear Ru(III)salen<sup>14</sup> catalyzed epoxidations, the reported yield was 6% for styrene and 9% for cyclohexene and for analogous dinuclear Ru(III) complexes the reported yields are *ca* 25%.<sup>13</sup> It has been suggested from oxygenation studies of ruthenium(III) complexes that complexes which form less stable ruthenium(IV) superoxo complexes act as better homogenous catalysts in the oxygen atom transfer reactions.<sup>19,34</sup> The formation of less stable intermediate oxometal species may be responsible for the higher catalytic activity of dinuclear ruthenium(III) complexes.

### 3.6. Conclusions

Dinuclear Fe(III) and Ru(III) complexes of biphenyl-bridged ligands are synthesized and characterized. The complexes are seen to be catalytically active in the epoxidation of olefins. Only traces of allylic oxidation products are observed when cyclohexene was substrate. The oxometal species is proposed as an active intermediate, but attempts to isolate such species are unsuccessful.

### 3.7. References

1. Jorgensen, K. A. *Chem. Rev.* 1989, **89**, 431.
2. Nam, W.; Ho, R.; Valentine, J. S. *J. Am. Chem. Soc.* 1991, **113**, 7052.
3. Hopkins, R. B.; Hamilton, A. D. *J. Chem. Soc., Chem. Commun.* 1987, 171.
4. Jacob, M.; Bhattacharya, P. K.; Ganeshpure, P. A.; Satish, S.; Sivaram, S. *Bull. Chem. Soc. Jpn.* 1989, **62**, 1325.
5. Agarwal, D. D.; Bhatnagar, R. P.; Jain, R.; Srivastava, S. *J. Mol. Catal.* 1990, **59**, 385.
6. Eskenazi, C.; Balavoine, G.; Meunier, F.; Riviere, H. *J. Chem. Soc., Chem. Commun.* 1985, 1111.
7. Hirao, T.; Moriuchi, T.; Mikami, S.; Ikeda, I.; Ohshiro, Y. *Tetrahedron Lett.* 1993, **34**, 1031.
8. Turner, J. O.; Lyons, J. E. *Tetrahedron Lett.* 1972, 2903.
9. Bressan, M.; Morvillo, A. *Inorg. Chem.* 1989, **28**, 950.
10. Che, C.-M.; Leung, W.-H.; Poon, C.-K. *J. Chem. Soc., Chem. Commun.* 1987, 173.
11. Ko, P.-H.; Chen, T.-Y.; Zhu, J.; Cheng, K.-F.; Peng, S.-M.; Che, C.-M. *J. Chem. Soc., Dalton Trans.* 1995, 2215.
12. Che, C.-M.; Cheng, W.-K.; Leung, W.-H.; Mak, T. C. W. *J. Chem. Soc., Chem. Commun.* 1987, 418.

13. Upadhyay, M. J.; Bhattacharya, P. K.; Ganeshpure, P. A.; Satish, S. *J. Mol. Catal.* 1992, **73**, 277.
14. Leung, W.-H.; Che, C.-M. *Inorg. Chem.* 1989, **28**, 4619.
15. Fung, W.-H.; Cheng, W.-C.; Yu, W.-Y.; Che, C.-M.; Mak, T. C. W. *J. Chem. Soc., Chem. Commun.* 1995, 2007.
16. Stultz, L. K.; Binstead, R. A.; Reynolds, M. S.; Meyer, T. J. *J. Am. Chem. Soc.* 1995, **117**, 2520.
17. Bennett, S.; Brown, S. M.; Conole, G.; Kessler, M.; Rowling, S.; Sinn, E.; Woodward, S. *J. Chem. Soc., Dalton Trans.* 1995, 367.
18. Boelrijk, A. E. M.; Velzen, M. M.; Neenan, T. X.; Reedijk, J.; Kooijman, H.; Spek, A. L. *J. Chem. Soc., Chem. Commun.* 1995, 2465.
19. Taqui Khan, M. M.; Sreelatha, C.; Mirza, S. A.; Ramachandraiah, G.; Abdi, S. H. R. *Inorg. Chim. Acta.* 1988, **154**, 103.
20. Siddall, T. L.; Miyaura, N.; Huffman, J. C.; Kochi, J. K. *J. Chem. Soc., Chem. Commun.* 1983, 1105.
21. Smegal, J. A.; Hill, C. L. *J. Am. Chem. Soc.* 1983, **105**, 2920. Smegal, J. A.; Hill, C. L. *J. Am. Chem. Soc.* 1983, **105**, 3515.
22. Shardt, B. C.; Hollander, F. J.; Hill, C. L. *J. Am. Chem. Soc.* 1982, **104**, 3964.
23. Vogel, A. I. *Text Book of Practical Organic Chemistry*, ELBS and Longman: 4th Ed.; 1978, 264.
24. Perrin, D. D.; Armarego, W. L. F.; Perrin, D. R. *Purification of Laboratory Chemicals*, Pergamon Press London: 1966.



25. Evans, I. P.; Spencer, A.; Wilkinson, G. *J. Chem. Soc., Dalton Trans.* 1973, 204.
26. Stephenson, T. A.; Wilkinson, G. *J. Inorg. Nucl. Chem.* 1966, **28**, 945.
27. Lucas, H. J.; Kennedy, E. R.; Formo, M. W. *Organic Synthesis*, Wiley, New York: 1955, Collect. Vol. **3**, p 483.
28. Chakravorty, A.; Behra, B.; Zacharias, P. S. *Inorg. Chim. Acta* 1968, **2**, 85. Zacharias, P. S.; Ramachandraiah, A. *Polyhedron* 1985, **4**, 1013.
29. Eranshaw, A. *Introduction to Magnetochemistry*, Academic press, London: 1968.
30. Elizabethe, M. J.; Zacharias, P. S. *Ind. J. Chem.* 1985, **24 A**, 936.
31. Reiff, W. M.; Baker Jr, W. A.; Erickson, N. E. *J. Am. Chem. Soc.* 1968, **90**, 4794. Martin, R. L.; White A. H. *Inorg. Chem.* 1967, **6**, 712.
32. Mukerjee, R.; Chakravorty, A. *J. Chem. Soc., Dalton Trans.* 1983, 955.
33. Murray, K. S.; Vaden Bergen A. M. West, B. O. *Aust. J. Chem.* 1978, **31**, 203.
34. Taqui Khan, M. M.; Sreelatha, C.; Mirza, S. A.; Ramachandraiah, G. *Polyhedron* 1992, **11**, 1821.

## CHAPTER 4

### Synthesis and Characterization of (Pentamethylcyclopentadienyl) Rh(III) and Ir(III) Polypyridyl Complexes: Molecular Structure of $[\text{Cp}^*\text{Rh}(\text{Ph-terpy})\text{Cl}]\text{BF}_4$ Complex

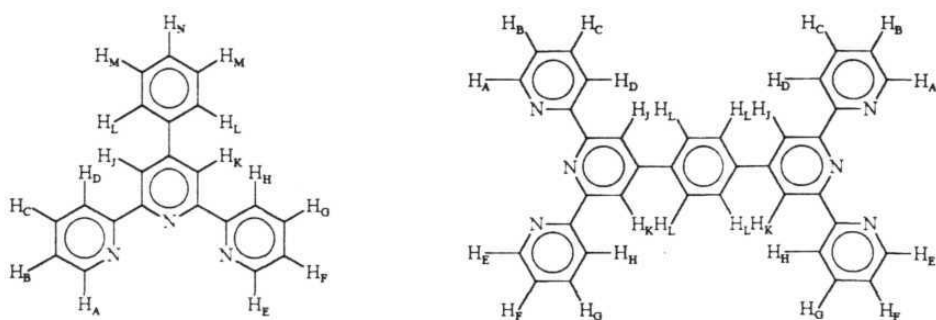
#### 4.1. Abstract

Reaction of  $[\text{Cp}^*\text{M}(\mu\text{-Cl})\text{Cl}]_2$  ( $\text{M} = \text{Rh}, \text{Ir}$ ) with 4'-phenyl-2,2':6',2''-terpyridine, **L**<sup>19</sup> and 1,4-bis(2,2':6',2''-terpyridin-4'-yl)benzene, **L**<sup>20</sup> results in the formation of cationic complexes by the cleavage of halide bridge. These complexes,  $[\text{Cp}^*\text{RhL}^{19}\text{Cl}]\text{BF}_4$ , **23**,  $[(\text{Cp}^*\text{RhCl})_2\text{-L}^{20}](\text{BF}_4)_2$ , **24**,  $[\text{Cp}^*\text{IrL}^{19}\text{Cl}]\text{BF}_4$ , **25** and  $[(\text{Cp}^*\text{IrCl})_2\text{-L}^{20}](\text{BF}_4)_2$ , **26** are characterized by various spectral methods. Ph-terpy coordinates the metal ion in a bidentate fashion to form mononuclear complexes while diterpy bridges two metal ions to form dinuclear complexes. Complex **23** is crystallographically characterized. It crystallizes in triclinic space group  $P\bar{1}$  with  $a = 8.002$  (11) Å,  $b = 12.3028$  (14) Å,  $c = 14.6327$  (20) Å,  $\alpha = 96.994$  (12)°,  $\beta = 90.435$  (12)°,  $\gamma = 92.665$  (11)° and  $Z = 2$ . In solution, the complexes **23** and **24** show fluxional behavior where the coordination sites oscillate between the two equivalent bonding modes of ligands.

## 4.2. Introduction

The transition metal complexes containing polypyridyl ligands are associated with interesting photochemical and electrochemical properties.<sup>1-5</sup> Complexes with these ligands are also DNA intercalators with an ability to inhibit nucleic acid synthesis.<sup>6</sup> The pentamethylcyclopentadienyl complexes of the type  $[\text{Cp}^*\text{M}(\text{N},\text{N}')\text{X}]^+$  ( $\text{N},\text{N}'$  = polypyridyl ligands) exhibit properties like proton reduction *via* hydride intermediate,<sup>7,8</sup> electrochemical reduction<sup>9</sup> of  $\text{NADP}^+$  and several other catalytic properties.<sup>10,11</sup>

Terpyridine, the  $\text{N}_3$  nitrogen donor is known to act as monodentate, bidentate, tridentate or bridging ligand. Although many terpy complexes involve tridentate bonding, some complexes where terpy acts as a bidentate chelate ligand are reported.<sup>12-14</sup> A Rh(II) complex with terpy coordinating the metal ion in the monodentate fashion has been structurally characterized.<sup>15</sup>



4'-phenyl-2,2':6',2''-terpyridine,  $\text{L}^1$ <sup>19</sup>    1,4-bis(2,2':6',2''-terpyridin-4'-yl)benzene,  $\text{L}^2$

**Figure 4.1.** Structure of ligands.

Therefore reactions of  $[\text{Cp}^*\text{M}(\mu\text{-Cl})\text{Cl}]_2$  with 4'-phenyl-2,2': 6', 2''-terpyridine (Ph-terpy),  $\text{L}^{19}$  and 1,4-bis(2,2': 6', 2''-terpyridin-4'-yl)benzene (diterpy),  $\text{L}^{20}$  are investigated to study the structural characteristics of the complexes formed. The structure of the ligands along with proton labeling is shown in Figure 4.1.

### 4.3. Experimental

$\text{RhCl}_3 \cdot 3\text{H}_2\text{O}$  and  $\text{IrCl}_3 \cdot 3\text{H}_2\text{O}$  were obtained from Sisco Chem. They were activated by heating with concentrated hydrochloric acid and evaporating to dryness two to three times. Pentamethylcyclopentadiene was obtained from Lancaster and was used without further purifications.  $[\text{Cp}^*\text{M}(\mu\text{-Cl})\text{Cl}]_2$  ( $\text{M} = \text{Rh}, \text{Ir}$ ) were synthesized as reported in the literature.<sup>16,17</sup> The ligands  $\text{L}^{19}$ ,  $\text{L}^{20}$  and  $[\text{Cp}^*\text{M}(\text{DBT})\text{Cl}_2]$  ( $\text{M} = \text{Rh}, \text{Ir}$ ) were also synthesized by reported procedures.<sup>18,19,20</sup> All the solvents were distilled and dried prior to use by standard procedures.<sup>21,22</sup>

#### 4.3.1. Synthesis of complexes

Complex **23** was synthesized by the procedure given below. To the solution of  $[\text{Cp}^*\text{Rh}(\mu\text{-Cl})\text{Cl}]_2$  (0.155 g, 0.25 mmol) in 20 mL of dry methanol was added Ph-terpy (0.155 g, 0.5 mmol) and  $\text{NaBF}_4$  (0.055 g, 0.5 mmol). The reaction mixture was stirred for 3 h at room-temperature. The solvent

was removed and the solid mass was dissolved in dichloromethane. The complex was precipitated by hexane and was recrystallized by slow diffusion of ether into the methanol solution. Yield: 70-75%.

The analogous iridium complex, **25** was also synthesized by the above procedure using  $[\text{Cp}^*\text{Ir}(\mu\text{-Cl})\text{Cl}]_2$  as starting material. Yield: 65-70%.

Complexes **23** and **25** can also be synthesized by the procedure given below.

To a solution of  $[\text{Cp}^*\text{M}(\text{DBT})\text{Cl}_2]$  (0.25 mmol) in 20 mL of dry methanol, was added ph-terpy (0.25 mmol) and  $\text{NaBF}_4$  (0.5 mmol). The reaction mixture was stirred for 2 h at room-temperature. The solvent was removed and the solid was dissolved in dichloromethane. The complex was precipitated by hexane.

Complex **24** was synthesized by the following procedure.

To a solution of  $[\text{Cp}^*\text{Rh}(\mu\text{-Cl})\text{Cl}]_2$  (0.155 g, 0.25 mmol) in 25 mL of dry methanol was added diterpy (0.135 g, 0.25 mmol) and  $\text{NaBF}_4$  (0.55 g, 0.5 mmol) and the reaction mixture was stirred for 4 h. The solvent was removed and the solid was dissolved in dichloromethane. Addition of hexane gave orange red complex in quantitative yield.

Complex **26** was synthesized by the above procedure using  $[\text{Cp}^*\text{Ir}(\mu\text{-Cl})\text{Cl}]_2$  as the starting material.

Complexes **24** and **26** can also be synthesized by the procedure given below.

To a solution of  $[\text{Cp}^*\text{M}(\text{DBT})\text{Cl}_2]$  (0.50 mmol) in 30 mL of dry methanol was added diterpy (0.25 mmol) and  $\text{NaBF}_4$  (1 mmol). The reaction mixture was stirred for 2 h. The solvent was removed and the solid was dissolved in dichloromethane. The complex was precipitated by hexane.

Mass spectral data (positive FAB):

- 23:**  $m/z$  582  $[\text{Cp}^*\text{RhL}^{19}\text{Cl}]$ ; 547  $[\text{Cp}^*\text{RhL}^{19}]$ ; 448  $[\text{RhL}^{19}\text{Cl}]$ ; 412  $[\text{RhL}^{19}]$ ; 274  $[\text{Cp}^*\text{RhCl}]$  and 238  $[\text{Cp}^*\text{Rh}]$
- 24:**  $m/z$  1174  $[(\text{Cp}^*\text{RhCl})_2\text{L}^{20}(\text{BF}_4)]$ ; 1087  $[(\text{Cp}^*\text{RhCl})_2\text{L}^{20}]$ ; 951  $[\text{Cp}^*\text{Rh}_2\text{Cl}_2\text{L}^{20}]$ ; 916  $[\text{Cp}^*\text{RhClL}^{20}]$ ; 813  $[\text{Cp}^*\text{RhClL}^{20}]$ ; 778  $[\text{CpRhL}^{20}]$  and 643  $[\text{RhL}^{20}]$
- 25:**  $m/z$  672  $[\text{Cp}^*\text{IrL}^{19}\text{Cl}]$ ; 637  $[\text{Cp}^*\text{IrL}^{19}]$ ; 537  $[\text{IrL}^{19}\text{Cl}]$ ; 502  $[\text{IrL}^{19}]$ ; 363  $[\text{Cp}^*\text{IrCl}]$  and 328  $[\text{Cp}^*\text{Ir}]$
- 26:**  $m/z$  1354  $[(\text{Cp}^*\text{IrCl})_2\text{L}^{20}(\text{BF}_4)]$ ; 1267  $[(\text{Cp}^*\text{IrCl})_2\text{L}^{20}]$ ; 1132  $[\text{Cp}^*\text{Ir}_2\text{Cl}_2\text{L}^{20}]$ ; 904  $[\text{Cp}^*\text{IrClL}^{20}]$ ; 868  $[\text{Cp}^*\text{IrL}^{20}]$  and 733  $[\text{IrL}^{20}]$

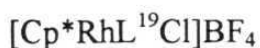
Anal. Calcd for  $\text{IrC}_{31}\text{H}_{30}\text{N}_3\text{ClBF}_4$ , **25**: C, 48.9; H, 3.9; N, 5.5. Found : C, 47.5; H, 3.8; N, 5.2.

Anal. Calcd for  $\text{Ir}_2\text{C}_{56}\text{H}_{54}\text{N}_6\text{Cl}_2\text{B}_2\text{F}_8$ , **26**: C, 46.6; H, 3.7; N, 5.8. Found : C, 45.9; H, 3.2; N, 5.3.

#### 4.4. Physical measurements

The elemental analysis were carried out on Perkin-Elmer 240C elemental analyzer. IR spectra were recorded on JASCO FT/IR-5300 spectrophotometer in KBr pellets.  $^1\text{H}$  NMR spectra were recorded on Bruker ACF-200 spectrometer at 200 MHz. Electronic absorption spectra were recorded on JASCO model 7800 UV-vis spectrophotometer. Fast atom bombardment (FAB) mass spectra were recorded on JEOL SX 102/DA-6000 mass spectrometer/data system using Xenon (6KV, 10 mA) as the FAB gas and *m*-nitrobenzyl alcohol was used as matrix. Cyclic voltammograms were recorded on Cypress systems model CS-1090/CS-1087 computer controlled electroanalytical system. All the experiments were performed under dry nitrogen in acetonitrile and dichloromethane solvents.  $1 \times 10^{-3}$  M solutions were used with 0.1 M  $\text{NBu}_4\text{ClO}_4$  as supporting electrolyte using glassy carbon working electrode, Ag-AgCl electrode as reference and platinum wire as auxiliary electrode. Ferrocene-ferrocenium couple was used as the redox standard.

##### 4.4.1. X-ray crystal structure determination



A crystal of dimensions  $0.22 \times 0.40 \times 0.40$  mm, obtained by diffusion of ether into methanol solution was sealed in a glass capillary. Preliminary examination and intensity data collection were carried out with an Enraf-Nonius CAD-4 automatic diffractometer using graphite monochromated

Mo K $\alpha$  radiation ( $\lambda = 0.71073$  Å). Intensity data were collected using the  $\theta$ - $2\theta$  scan mode for  $2\theta \leq 45^\circ$  and then corrected for absorption and decay. The structure was solved by MULTAN<sup>23</sup> in triclinic space group  $P\bar{1}$  and was refined with full-matrix least-squares on F with  $w = 1.0/[\sigma^2(F_o) + 0.0001F_o^2]$ . In the final cycles all the non-hydrogen atoms were refined anisotropically and the hydrogen atoms were fixed at idealized positions ( $d_{C-H} = 1.00$  Å) calculated during anisotropic convergence stage. Scattering factors for neutral atoms and anomalous scattering coefficients for non-hydrogen atoms were taken from ref 24. All calculations were carried out with a Micro VAX 3600 computer using NRC VAX program package.<sup>25</sup> There were 5018 unique reflections of which 4477 with  $F > 6\sigma F$  were used for the structure solution. Refinement converged at a final  $R = 3.3$  % and  $R_w = 3.6$  %.

#### 4.5. Results and Discussion

Reactions of  $[\text{Cp}^*\text{Rh}(\mu\text{-Cl})\text{Cl}]_2$  with  $L^{19}$  (Ph-terpy) and  $L^{20}$  (diterpy) in methanol in presence of  $\text{NaBF}_4$  gave orange red microcrystalline products **23** and **24**. Similarly reaction of these ligands with  $[\text{Cp}^*\text{Ir}(\mu\text{-Cl})\text{Cl}]_2$  gave complexes **25** and **26**. Synthetic details are given in the experimental section 4.3.1. The IR spectra of the complexes exhibit sharp bands with medium intensities in the range  $1600 - 1400$   $\text{cm}^{-1}$  originating from the polypyridyl ligands. In addition, complexes gave broad band at  $1050$   $\text{cm}^{-1}$  due to  $\text{BF}_4^-$ . The C, H, N analytical data agree with mononuclear structure for Ph-terpy



complexes **23** and **25** and dinuclear structure for diterpy complexes **24** and **26**.

The FAB-mass spectra of the mononuclear complexes, **23** and **25** exhibit peaks corresponding to  $[\text{Cp}^*\text{ML}^{19}\text{Cl}]$  and the dinuclear complexes, **24** and **26** to  $[(\text{Cp}^*\text{MCl})_2\text{L}^{20}(\text{BF}_4)]$ . In addition, fragments due to  $[\text{Cp}^*\text{ML}^{19}]$ ,  $[\text{ML}^{19}]$  and  $[\text{Cp}^*\text{M}]$  for mononuclear complexes and  $[(\text{Cp}^*\text{M})_2\text{L}^{20}\text{Cl}]$ ,  $[(\text{Cp}^*\text{M})_2\text{L}^{20}]$ ,  $[\text{ML}^{20}]$  and  $[\text{Cp}^*\text{M}]$  for dinuclear complexes are observed. The data is given in experimental section 4.3.1.

Based on these data, the complexes, **23** and **25** are assigned mononuclear structure where the metal ion is coordinated by  $\text{Cp}^*$ , chloride and the ligand in a bidentate fashion. The complexes, **24** and **26** are assigned dinuclear structure where the ligand diterpy acts as a bridge coordinating two metal ions at two ends in a bidentate bonding mode. Each metal ion is also coordinated by  $\text{Cp}^*$  and chloride. The proposed structures of the complexes are given in Figure 4.2.

The room temperature  $^1\text{H}$  NMR spectrum of the complex **23**,  $[\text{Cp}^*\text{RhL}^{19}\text{Cl}]\text{BF}_4$  consists of six set of overlapping signals in the aromatic region arising from the Ph-terpy ligand. The signal due to  $\text{Cp}^*$  is observed at 1.19 ppm. The  $^1\text{H}$  NMR spectrum of compound **23** is shown in Figure 4.3. The peaks are fully assigned by the two dimensional correlation spectroscopy (COSY) to eight non-equivalent protons labeled A to N in Figure 4.1. The COSY spectrum of **23** is given in Figure 4.4. The  $^1\text{H}$  NMR data are presented in Table 4.1. On cooling the solution, dramatic changes occur in the NMR spectrum as shown in Figure 4.5. At 213 K, the spectrum consisted of multiplets arising from thirteen non-equivalent protons of the Ph-terpy ligand

indicating bidentate coordination of the ligand to the metal center. At room-temperature there is a rapid exchange between the analogous pairs of protons

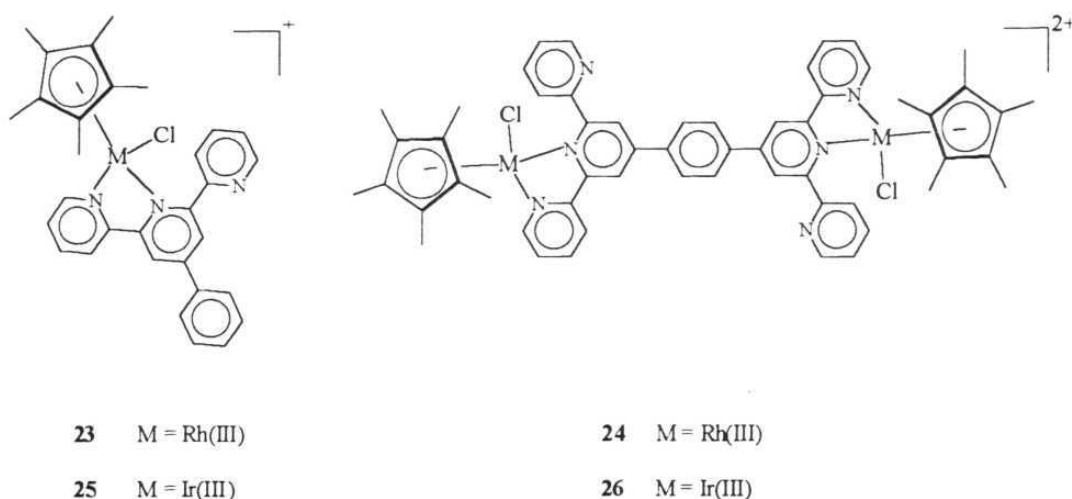


**Figure 4.2.** Generalized structures of Rh(III) and Ir(III) complexes.

in the pyridyl ring namely  $H_{A/E}$ ,  $H_{B/F}$ ,  $H_{C/G}$ ,  $H_{D/H}$  and  $H_{J/K}$  according to spin problem  $ABCDJ \rightleftharpoons EFGHK$  and an average spectrum consisting of six set of multiplets corresponding to eight different protons is obtained. Hydrogens  $H_A$  and  $H_E$   $\alpha$  to nitrogen atoms give rise to the signals at highest frequency. On cooling, these protons appear separately with proton  $\alpha$  to N, coordinated to the metal ion experiencing an additional coordination induced shift. The coupling constants  $J_{AB}$  and  $J_{EF}$  are 8.3 Hz. This indicates that at room-

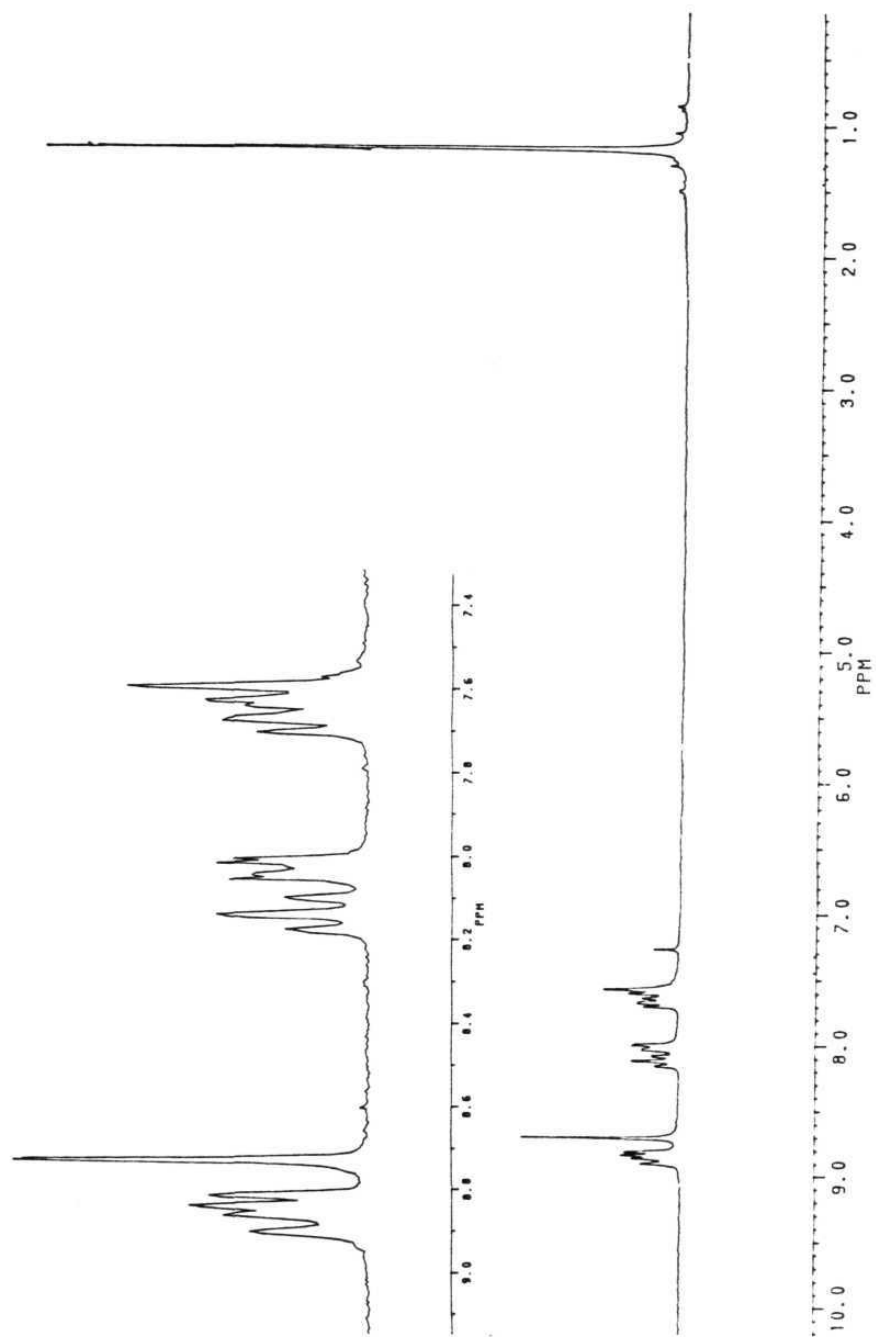


**Figure 4.3.** Room-temperature  $^1\text{H}$  NMR spectrum of complex **23**,  $[\text{Cp}^*\text{RhL}^{19}\text{C}]\text{BF}_4$

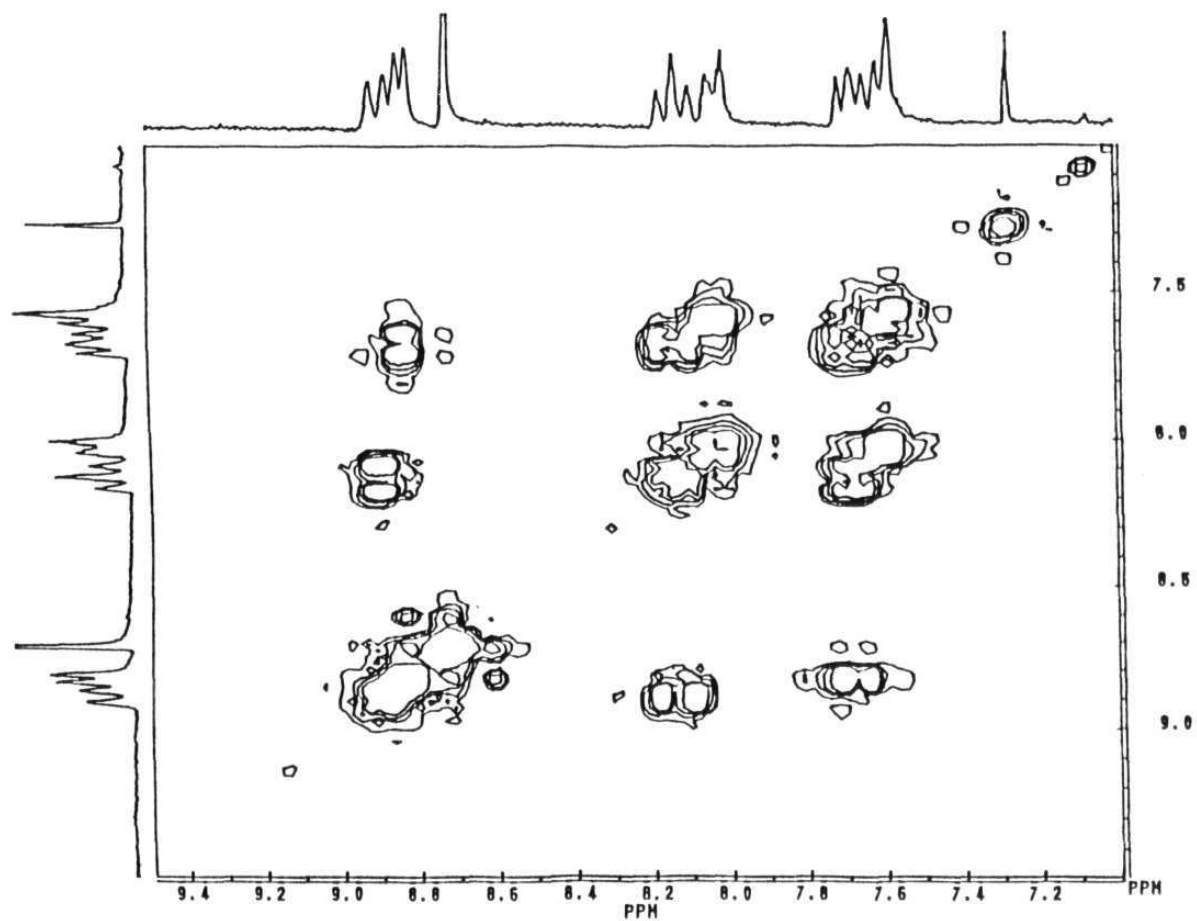


**Figure 4.4.** Room-temperature <sup>1</sup>H NMR COSY spectrum of complex **23**, [Cp\*RhL<sup>19</sup>Cl]BF<sub>4</sub>

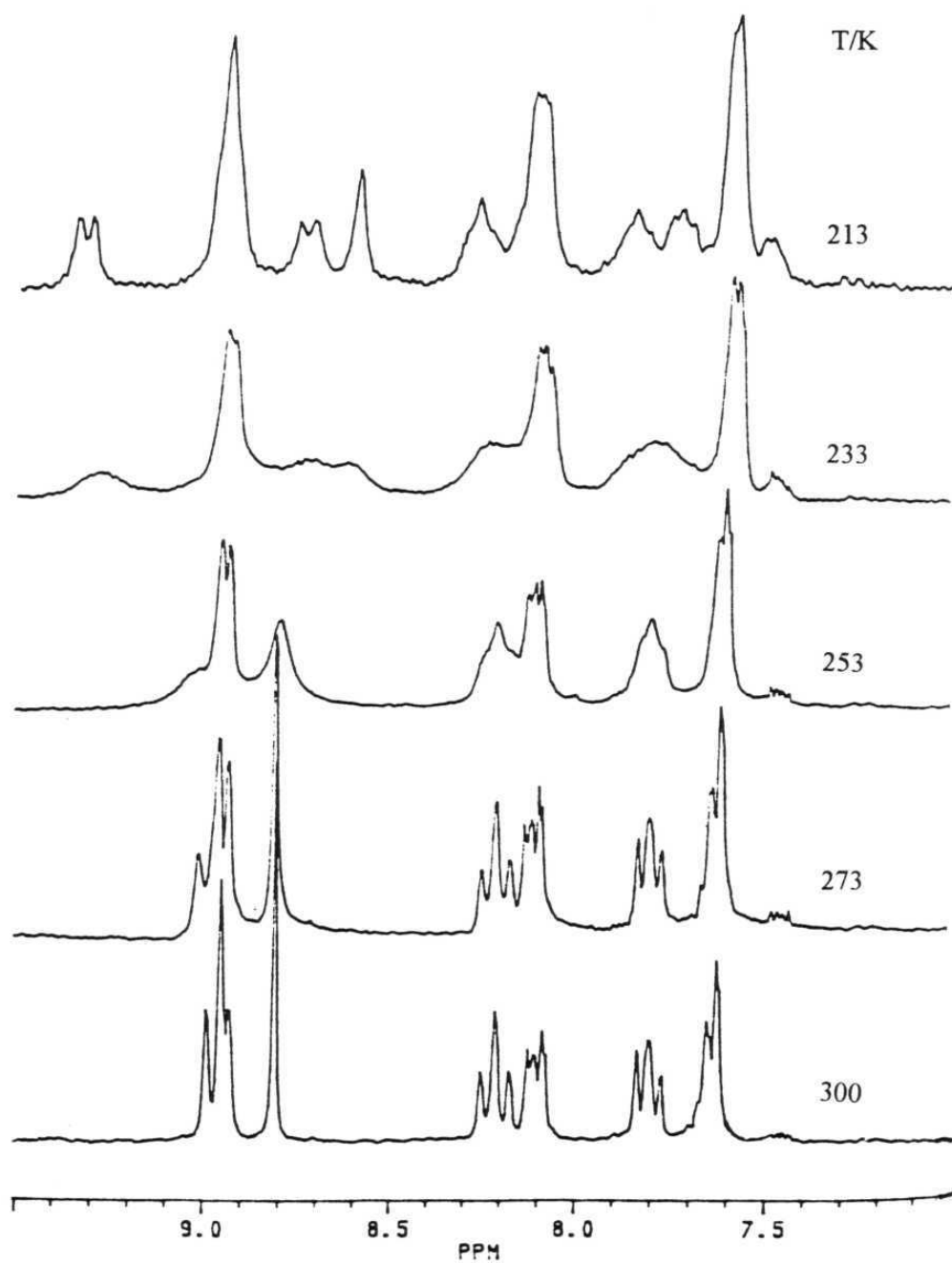


**Figure 4.5.** Variable-temperature  $^1\text{H}$  NMR spectra of complex **23**,  $[\text{Cp}^*\text{RhL}^{19}\text{Cl}]\text{BF}_4$

temperature the ligand is involved in a fluxional process in which the coordination sites oscillates between the two equivalent forms involving bidentate chelate bonding as shown in Figure 4.6.

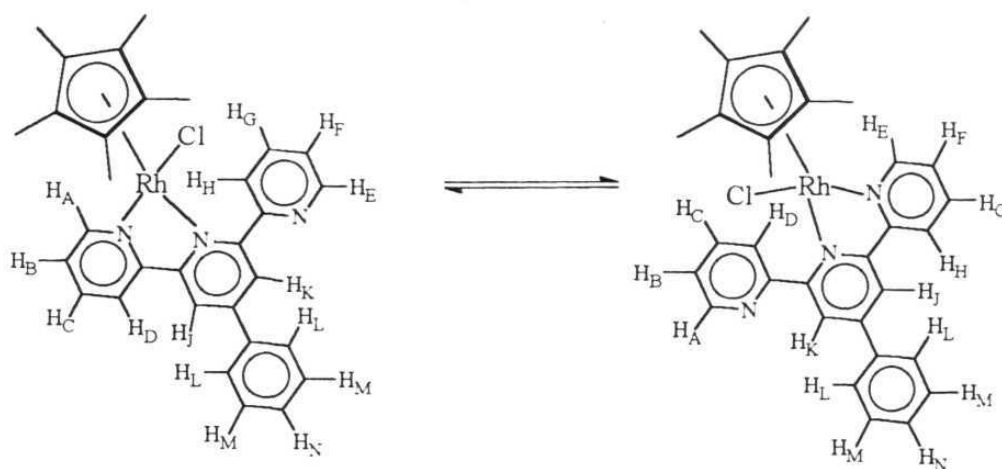


**Figure 4.6.** Interconverting structures of  $[\text{Cp}^*\text{RhL}^{19}\text{Cl}]\text{BF}_4$  complex showing the hydrogen labeling.

The room temperature  $^1\text{H}$  NMR spectrum of complex **24**,  $[(\text{Cp}^*\text{RhCl})_2\text{L}^{20}](\text{BF}_4)_2$  consisted of five set of signals corresponding to six non-equivalent protons of the diterpy ligand. All the peaks were assigned by the two dimensional correlation spectroscopy. The COSY spectrum is shown in Figure 4.7. At low temperatures, extensive spectral changes take place and exchange broadening occurs between the analogous pairs of protons. On cooling to 213 K, spectral lines sharpened considerably and a spectrum corresponding to eleven non-equivalent protons of ligand coordinating the

metal ions in the bidentate chelate mode is obtained. The proton,  $H_A$   $\alpha$  to N, coordinating the metal ion is seen at highest frequency. The coupling constants  $J_{AB}$  and  $J_{EF}$  are 8.3 Hz. The variable-temperature  $^1H$  NMR spectra is given in Figure 4.8. The dinuclear complex like mononuclear complex exhibits fluxional behavior in which the coordination complex oscillates between the two forms both of which involve diterpy functioning as bidentate chelate ligand at two ends.

The ambient temperature  $^1H$  NMR spectrum of complex **25**,  $[Cp^*IrL^{19}Cl]BF_4$  consists of complex pattern of overlapping signals which is clearly associated with an unsymmetrically coordinated and nonfluxional Ph-terpy ligand. The spectrum is shown in Figure 4.9. It was fully assigned by the two dimensional correlation spectroscopy to thirteen non-equivalent protons labeled A - N and was consistent with bidentate terpyridyl ligand. The coupling constants  $J_{AB}$  and  $J_{EF}$  are 8.1 Hz. The COSY spectrum is given in Figure 4.10.

At ambient temperature, the  $^1H$  NMR spectrum of complex **26**,  $[(Cp^*IrCl)_2L^{20}](BF_4)_2$  exhibits line broadening of all the signals. On cooling the solution, the spectral lines sharpened and well resolved spectra were obtained. The variable-temperature proton NMR spectra of complex **26** are given in Figure 4.11. All the chemical shifts are given in Table 4.1. The spectrum consisted of multiplets arising from eleven non-equivalent protons of diterpy labeled A-L in Figure 4.1 and was clearly associated with diterpy acting in a bidentate chelate mode of bonding to iridium. All the peaks were assigned by two dimensional COSY and the spectrum is shown in Figure 4.12.

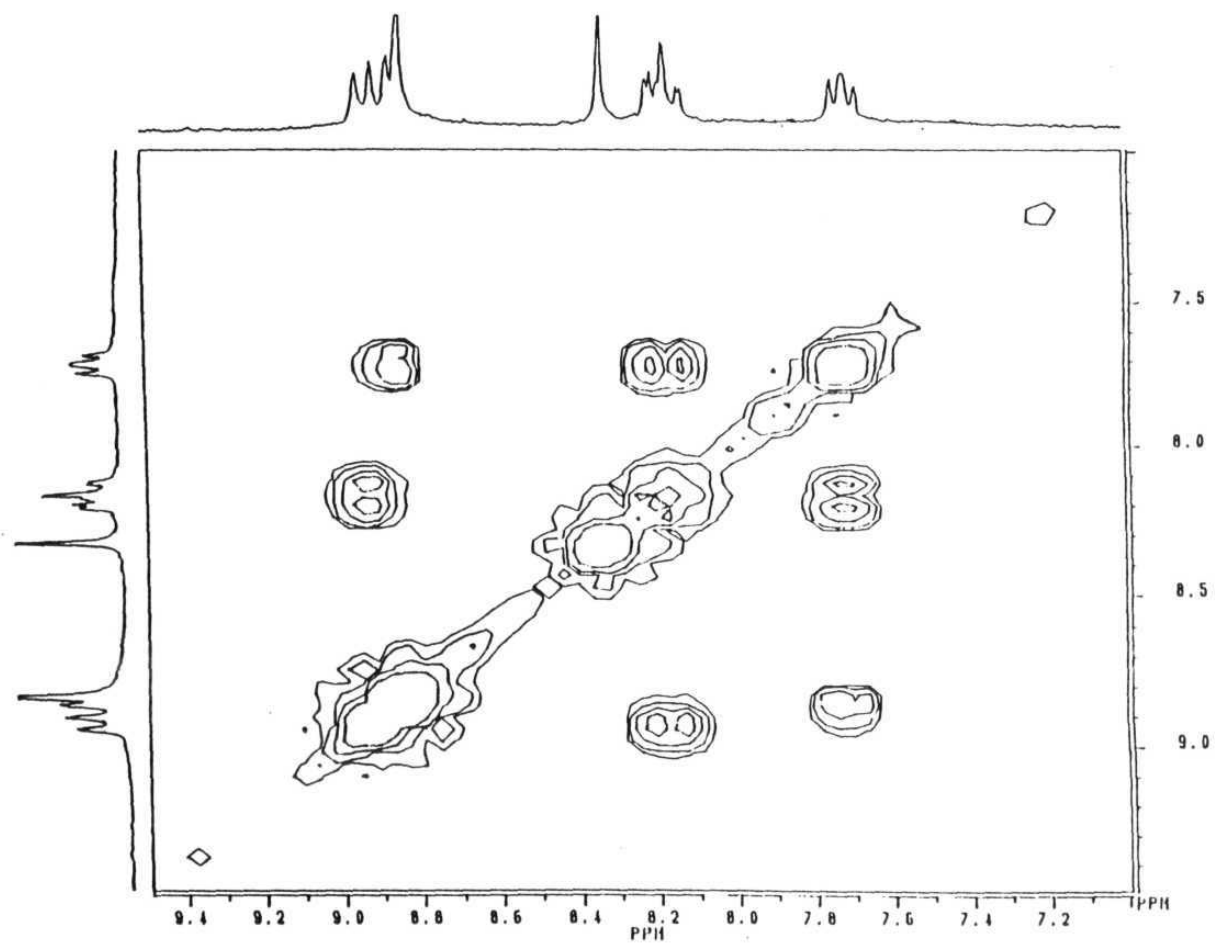


**Figure 4.7.**  $^1\text{H}$  NMR COSY spectrum of complex **24**,  $[(\text{Cp}^*\text{RhCl})_2\text{L}^{20}](\text{BF}_4)_2$



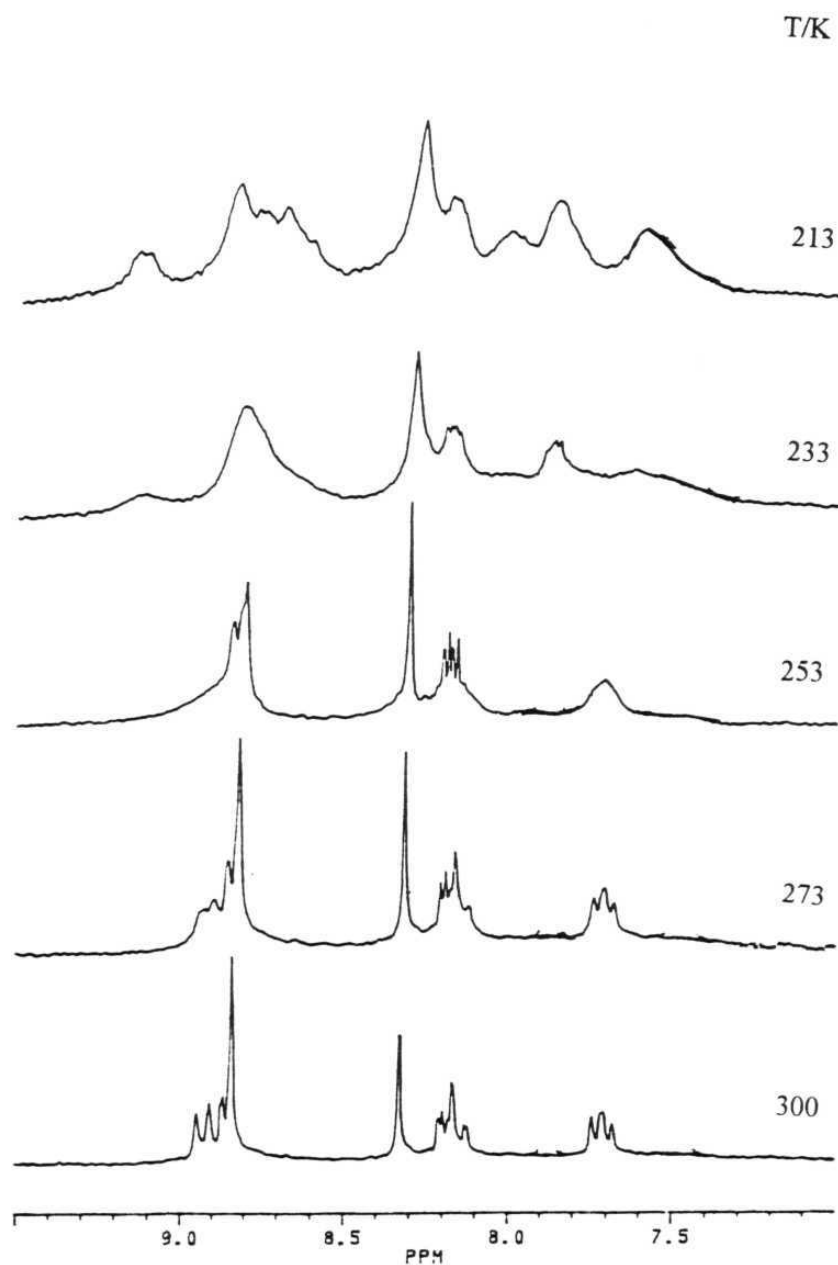


**Figure 4.8.** Variable-temperature  $^1\text{H}$  NMR spectra of complex **24**,  $[(\text{Cp}^*\text{RhCl})_2\text{L}^{20}](\text{BF}_4)_2$

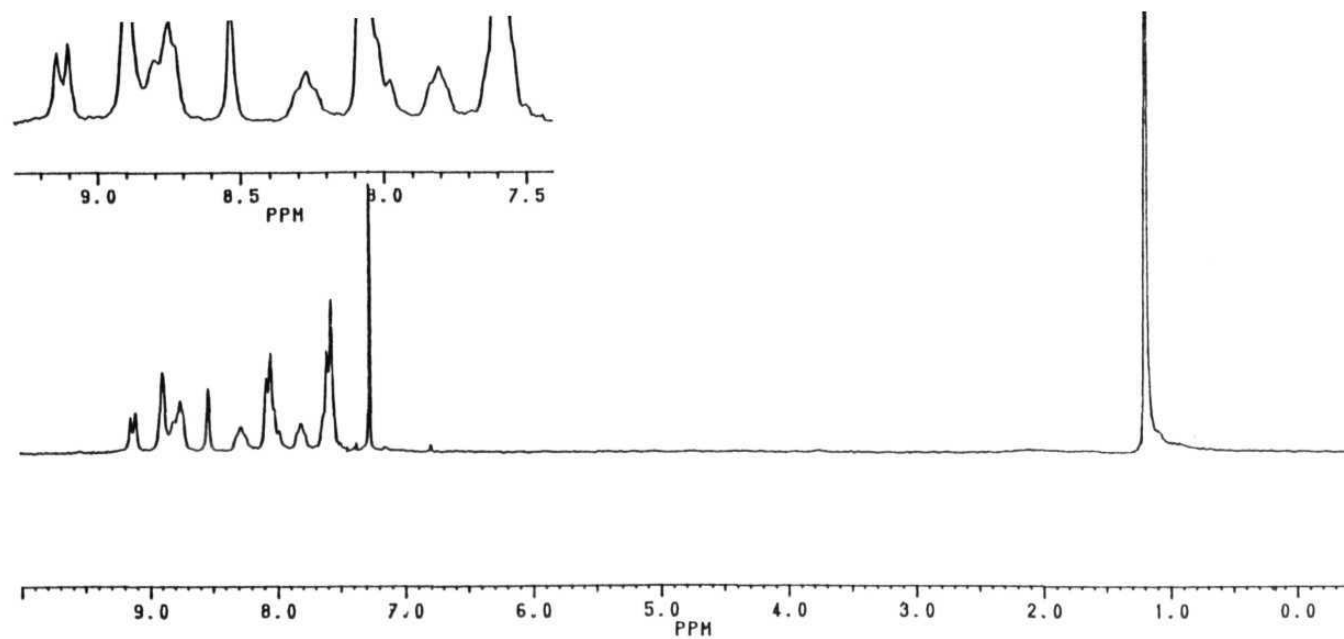


**Figure 4.9.** Room-temperature  $^1\text{H}$  NMR spectrum of complex **25**,  $[\text{Cp}^*\text{IrL}^{19}\text{Cl}]\text{BF}_4$

**Figure 4.10.** Room-temperature  $^1\text{H}$  NMR COSY spectrum of complex **25**,  $[\text{Cp}^*\text{IrL}^{19}\text{C}]\text{BF}_4$

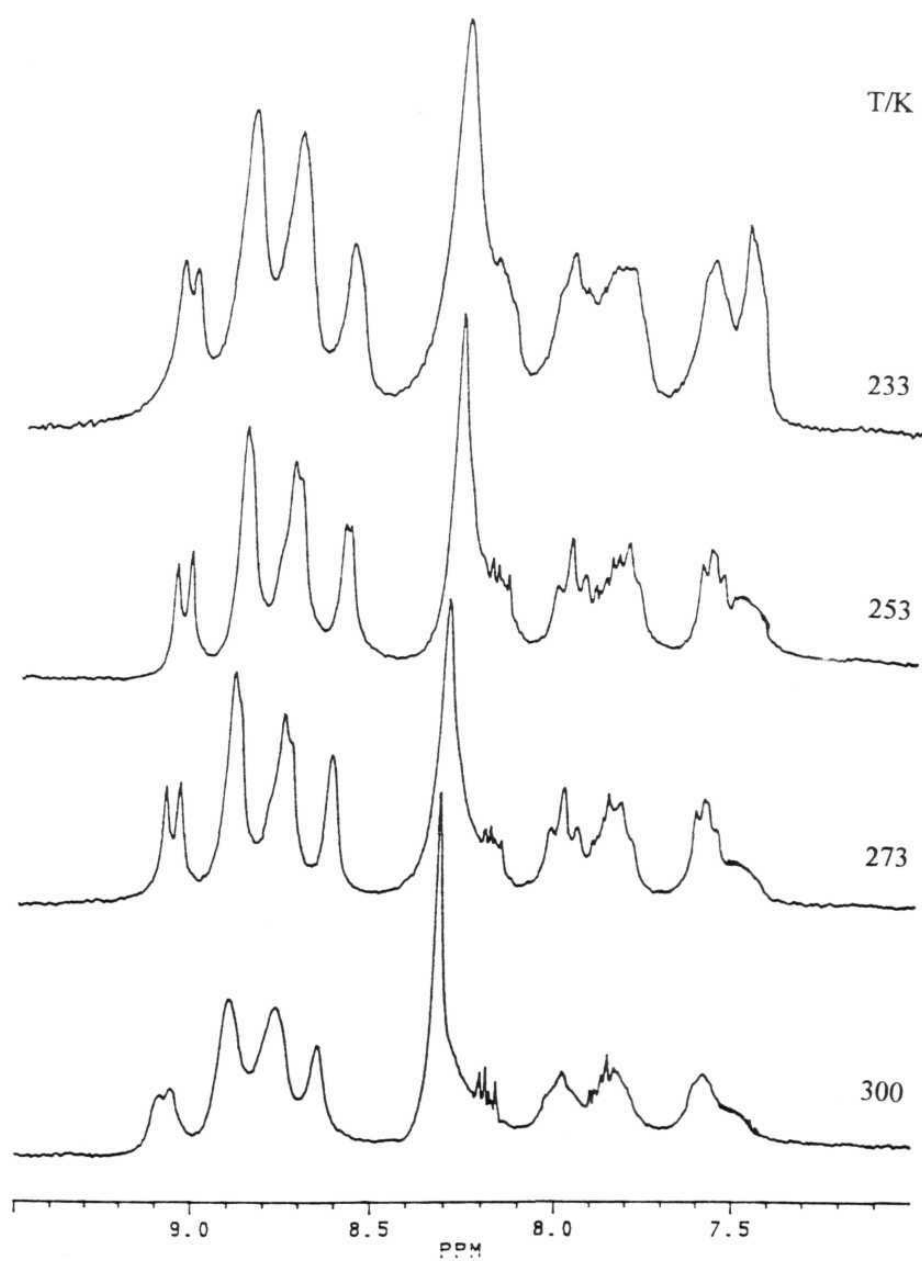


**Figure 4.11.** Variable-temperature  $^1\text{H}$  NMR spectra of complex **26**,  $[(\text{Cp}^*\text{IrCl})_2\text{L}^{20}](\text{BF}_4)_2$

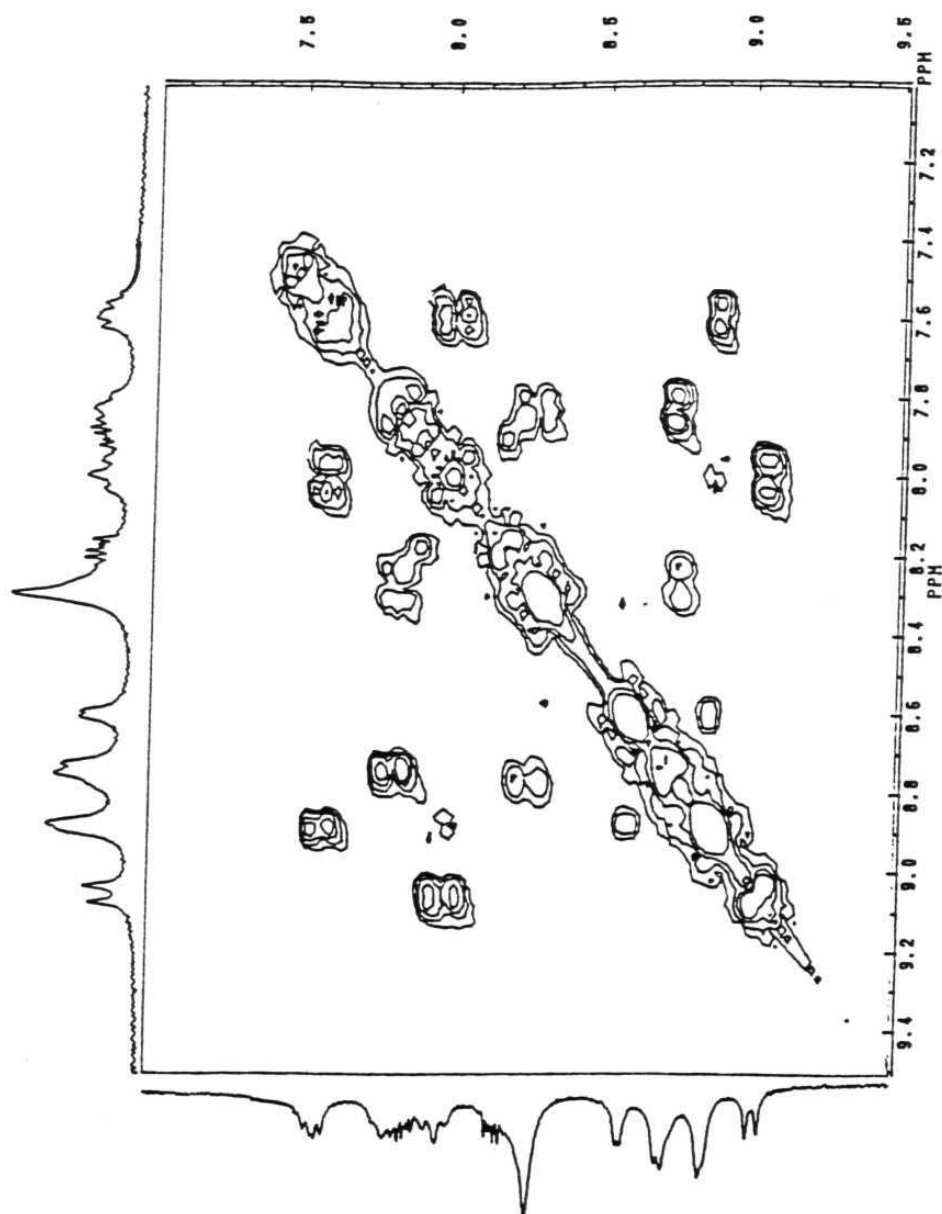


**Figure 4.12.**  $^1\text{H}$  NMR COSY spectrum of complex **26**,  $[(\text{Cp}^*\text{IrCl})_2\text{L}^{20}](\text{BF}_4)_2$  at 253 K

**Table 4.1.** <sup>1</sup>H NMR data for complexes 23-26

Complex	Solvent	T / K	AE	BF	CG	DH	JK	L	MN	Cp*
23	CDCl <sub>3</sub>	300	8.88	8.14	7.68	8.83	8.73	8.03	7.60	1.19
23	CD <sub>3</sub> OD	213	9.25(A)	7.84(B)	7.56(C)	8.92(D)	8.92(J)	8.11	7.56	1.16
24	CD <sub>2</sub> Cl <sub>2</sub>	300	8.72(E)	8.26(F)	7.72(G)	8.92(H)	8.58(K)			
24	CD <sub>2</sub> Cl <sub>2</sub>	213	8.92	8.12	7.71	8.86	8.84	8.33		1.18
24	CD <sub>2</sub> Cl <sub>2</sub>	213	9.14(A)	8.05(B)	7.60(C)	8.83(D)	8.83(J)	8.27		1.15
25	CDCl <sub>3</sub>	300	8.84(E)	8.19(F)	7.86(G)	8.76(H)	8.68(K)			
25	CDCl <sub>3</sub>	300	9.06(A)	7.95(B)	7.62(C)	8.88(D)	8.88(J)	8.04	7.58	1.19
25	CDCl <sub>3</sub>	300	8.77(E)	8.25(F)	7.71(G)	8.73(H)	8.51(K)			
26	CD <sub>2</sub> Cl <sub>2</sub>	253	9.06(A)	7.98(B)	7.58(C)	8.89(D)	8.89(J)	8.25		1.15
26	CD <sub>2</sub> Cl <sub>2</sub>	253	8.76(E)	8.20(F)	7.86(G)	8.70(H)	8.62(K)			

Electronic spectra of the complexes show high intensity charge-transfer transitions at  $\sim 425$  nm in addition to the intra ligand transitions of the polypyridyl ligands at  $\sim 290$  and  $\sim 230$  nm.

Electron transfer properties of all the complexes have been studied in dichloromethane and acetonitrile solvents by cyclic voltammetry and the data is given in Table 4.2. In dichloromethane, the complex **23**, shows an irreversible reduction peak at 0.89 V. For the analogous dinuclear complex **24**, a reduction peak is observed at 0.91 V indicating that both the metal ions are in the identical environment with no interaction between them. In acetonitrile, the mononuclear complex **23**, shows an irreversible reduction peak at 0.85 V but the dinuclear complex **24**, exhibits a quasi-reversible reduction couple at 0.78 V. The peak to peak separation,  $\Delta E_p$  value is in the range of 50 to 60 mV at a scan rate of 100 mV/sec. On increasing the scan rate the  $\Delta E_p$  value increases and at a scan rate of 500 mV/sec., it is in the range of 100 to 110 mV. The mono and dinuclear complexes of iridium, **25** and **26** show double reduction peaks in the range of 1 V to 1.2 V in dichloromethane solvent. Both the peaks are quasi-reversible to irreversible. In the acetonitrile solvent, the complex **25**, shows quasi-reversible reduction peak at 0.9 V and the  $\Delta E_p$  value is 125 mV at a scan rate of 100 mV/sec. The dinuclear complex **26**, exhibits quasi-reversible double reduction peaks in the range of 0.72 V and 0.81 V. For the  $[\text{Cp}^*\text{Rh}(\text{bpy})\text{Cl}]^+$  complex and series of analogous complexes, a quasi-reversible reduction peak was reported at  $\sim 0.75$  to 0.95 V and the separation of the cathodic and anodic peak was 150 to 300 mV.<sup>26,7</sup> This behavior was explained to two-electron reduction of

Rh(III) to Rh(I) with concomitant loss of chloride. This electrochemical behavior was explained by equations 1 and 2.



The redox behavior of the present set of complexes can be similarly explained by the equations 1 and 2 to reduction of M(III) to M(I) state. The cyclic voltammograms of the complexes are shown in the Figure 4.13 and Figure 4.14.

**Table 4.2.** Electronic spectral and cyclic voltammetric data.

Complex	UV-vis data <sup>a</sup> $\lambda$ , nm ( $\epsilon$ , $\text{M}^{-1} \text{cm}^{-1}$ )	CV data <sup>b</sup> M(III) $\rightarrow$ M(I) $E_{1/2}$ , V ( $\Delta E_p$ mV)
$[\text{Cp}^*\text{RhL}^{19}\text{Cl}]\text{BF}_4$	385 (3605) 288 (37585)	0.85
$[(\text{Cp}^*\text{RhCl})_2\text{L}^{20}](\text{BF}_4)_2$	420 (5445)	0.78 (50)
$[\text{Cp}^*\text{IrL}^{19}\text{Cl}]\text{BF}_4$	425 (1250) 365 (4935)	0.91 (125)
$[(\text{Cp}^*\text{IrCl})_2\text{L}^{20}](\text{BF}_4)_2$	436 (4625)	0.73 (310) 0.81 (300)

<sup>a</sup> in dichloromethane.

<sup>b</sup> potential measured at glassy carbon electrode in acetonitrile solvent (0.1 M TBAP) with Ag-AgCl as reference electrode.



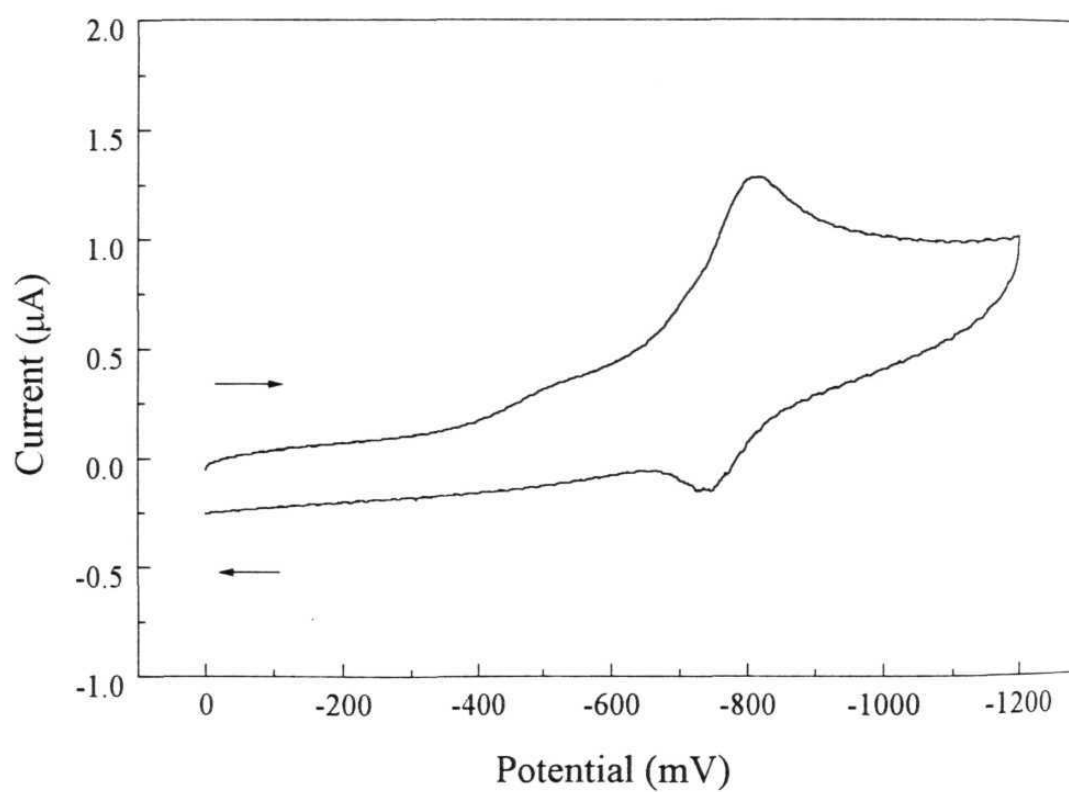


**Figure 4.13.** Cyclic voltammogram of complex **24**,  $[(\text{Cp}^*\text{RhCl})_2\text{L}^{20}](\text{BF}_4)_2$  in  $\text{CH}_3\text{CN}$  (0.1 M TBAP) at glassy carbon electrode at a scan rate of  $100 \text{ mV s}^{-1}$

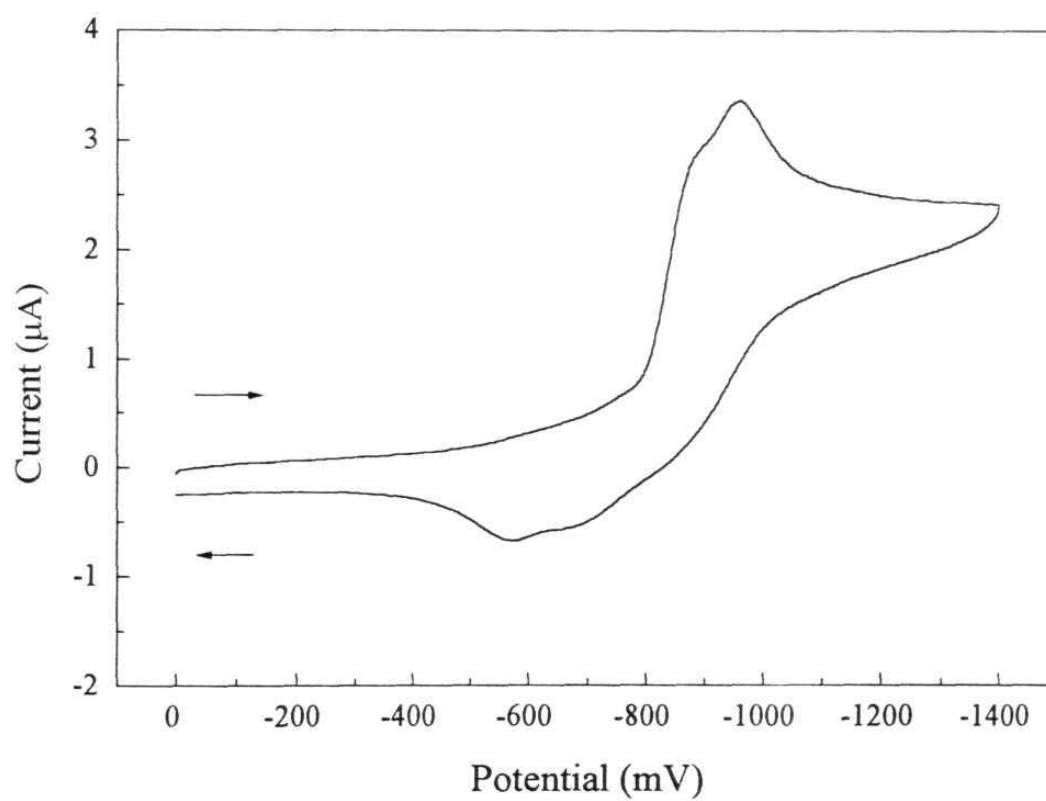


**Figure 4.14.** Cyclic voltammogram of complex **26**,  $[(\text{Cp}^*\text{IrCl})_2\text{L}^{20}](\text{BF}_4)_2$  in  $\text{CH}_3\text{CN}$  (0.1 M TBAP) at glassy carbon electrode electrode at a scan rate of  $100 \text{ mV s}^{-1}$

### Crystal and molecular structure of $[\text{Cp}^*\text{RhL}^{19}\text{Cl}]\text{BF}_4$ , **23** complex

To confirm the proposed structures of the complexes, crystal structure of complex  $[\text{Cp}^*\text{RhL}^{19}\text{Cl}]\text{BF}_4$ , **23** was solved.

The complex crystallizes in triclinic  $P\bar{1}$  space group with two molecules per unit cell. The crystallographic parameters are given in Table 4.3. The positional parameters are presented in Table 4.4. The anisotropic thermal parameters, hydrogen atom coordinates, bond lengths and bond angles are given in Appendix Tables A9-A12. The ORTEP drawing of the molecule **23** along with the atom-numbering scheme is shown in Figure 4.15. Selected bond parameters are listed in Table 4.5. The asymmetric unit consists of a rhodium atom displaying the characteristic three-legged "piano stool" geometry. It is coordinated to one  $\eta^5\text{-C}_5(\text{CH}_3)_5$  group, one chloride and two nitrogens of Ph-terpy in a bidentate bonding mode, as postulated from experimental data.

The pentamethylcyclopentadienyl ligand is symmetrically bound to the metal ion. All the  $\text{Cp}^*$  atoms fall in a fairly good plane, the root mean square deviation of the  $\text{Cp}^*$  from a least-square plane being 0.015 Å. The distance between Rh and the least-square plane of the  $\text{Cp}^*$  ring is 1.783 Å. The Rh-Cl bond length is 2.398 (1) Å. These bond distances are close to the Rh- $\text{Cp}^*$ , 1.782 and Rh-Cl, 2.386 bond lengths in  $[\text{Cp}^*\text{Rh}(\text{phen})\text{Cl}]^+$  complex.<sup>27</sup>

**Table 4.3.** Crystallographic data for [Cp\*RhL<sup>19</sup>Cl]BF<sub>4</sub>

chemical formula	C <sub>31</sub> H <sub>30</sub> N <sub>3</sub> BF <sub>4</sub> ClRh
fw	669.75
space group	P $\bar{1}$
a, Å	8.0022 (11)
b, Å	12.3028 (14)
c, Å	14.6327 (20)
$\alpha$ , deg	96.994(12)
$\beta$ , deg	90.435(12)
$\gamma$ , deg	92.665 (11)
V, Å <sup>3</sup>	1428.2 (3)
Z	2
D calcd, g cm <sup>-3</sup>	1.557
T, °C	25
$\lambda$ (Mo K $\alpha$ ), Å	0.71073
$\mu$ (Mo K $\alpha$ ), cm <sup>-1</sup>	12.88
F(000)	678
transm. coeff.	0.918-1.000
R	0.033
R <sub>w</sub>	0.036

$$R = \sum(F_o - F_c) / \sum(F_o)$$

$$R_w = [\sum(W(F_o - F_c)^2 / \sum(WF_o^2))]^{1/2}$$

**Table 4.4.** Atomic coordinates ( $\times 10^5$  for Rh and Cl and  $\times 10^4$  for others) and equivalent isotropic displacement coefficients with estimated standard deviations in parentheses for  $[\text{Cp}^*\text{RhL}^{19}\text{Cl}]\text{BF}_4$

Atom	x	y	z	$B_{\text{eq}}$
Rh	78281(3)	34906(2)	23268(2)	2.57(1)
Cl	104581(11)	30783(9)	16229(7)	4.30(5)
N(1)	84150(4)	24587(24)	33016(19)	3.16(13)
N(2)	63290(3)	19718(23)	18924(19)	2.84(12)
N(3)	44760(4)	22030(3)	-3343(21)	4.28(16)
C(1)	9766(5)	2586(3)	3862(3)	4.11(18)
C(2)	9960(5)	1949(4)	4558(3)	4.87(21)
C(3)	8741(6)	1153(4)	4677(3)	4.88(21)
C(4)	7373(5)	993(3)	4090(3)	4.00(19)
C(5)	7255(4)	1654(3)	3391(2)	3.13(16)
C(6)	5950(4)	1486(3)	2662(2)	3.00(15)
C(7)	4492(5)	868(3)	2736(2)	3.36(16)
C(8)	3345(4)	684(3)	2008(3)	3.21(16)
C(9)	1710(5)	94(3)	2093(3)	3.48(17)
C(10)	1438(5)	-573(3)	2782(3)	4.39(19)
C(11)	-111(6)	-1094(4)	2870(3)	5.49(23)
C(12)	-1390(6)	-966(4)	2270(4)	5.78(24)
C(13)	-1150(5)	-328(4)	1574(4)	5.34(23)
C(14)	391(5)	202(3)	1488(3)	4.58(21)

....Cont.

....cont. Table 4.4

C(15)	3828(5)	1086(3)	1200(2)	3.53(16)
C(16)	5302(4)	1712(3)	1154(2)	3.03(15)
C(17)	5829(5)	2055(3)	250(2)	3.45(16)
C(18)	7498(5)	2148(3)	29(3)	3.80(18)
C(19)	7908(6)	2434(4)	-834(3)	4.67(20)
C(20)	6665(7)	2605(4)	-1430(3)	4.85(23)
C(21)	5040(6)	2485(4)	-1159(3)	4.95(22)
C(22)	8488(4)	5189(3)	2683(3)	3.49(17)
C(23)	7644(5)	5043(3)	1789(3)	3.31(17)
C(24)	6007(4)	4625(3)	1916(2)	2.85(14)
C(25)	5814(4)	4466(3)	2870(2)	2.89(14)
C(26)	7333(5)	4857(3)	3336(2)	3.28(15)
C(27)	10206(5)	5697(4)	2876(4)	5.78(24)
C(28)	8382(6)	5338(4)	910(3)	5.27(22)
C(29)	4652(5)	4427(3)	1205(3)	4.16(18)
C(30)	4248(5)	4081(4)	3302(3)	4.39(19)
C(31)	7615(6)	4914(4)	4354(3)	5.23(22)
B	5324(8)	7639(5)	4064(4)	5.2(3)
F(1)	4866(5)	8614(3)	3923(3)	10.4(2)
F(2)	6575(6)	7300(3)	3525(3)	12.3(3)
F(3)	5713(6)	7568(5)	4909(3)	15.8(4)
F(4)	3999(6)	6963(4)	3921(4)	16.7(4)

---

$B_{eq}$  is the mean of the principle axes of the thermal ellipsoid

**Table 4.5.** Selected bond distances (Å) and bond angles (°) in  $[\text{Cp}^*\text{RhL}^{19}\text{Cl}]\text{BF}_4$

Bond lengths

Rh-Cl	2.3984(10)	Rh-C(23)	2.163(4)
Rh-N(1)	2.086(3)	Rh-C(24)	2.194(3)
Rh-N(2)	2.197(3)	Rh-C(25)	2.153(3)
Rh-C(22)	2.132(4)	Rh-C(26)	2.151(3)

Bond angles

Cl-Rh-N(1)	87.61(8)	Rh-C(22)-C(23)	71.34(20)
Cl-Rh-N(2)	101.39(8)	Rh-C(22)-C(26)	71.42(20)
Cl-Rh-C(22)	94.34(10)	Rh-C(22)-C(27)	126.9(3)
Cl-Rh-C(23)	95.04(10)	Rh-C(23)-C(22)	69.04(20)
Cl-Rh-C(24)	127.32(9)	Rh-C(23)-C(24)	72.36(20)
Cl-Rh-C(25)	158.37(10)	Rh-C(23)-C(28)	126.1(3)
Cl-Rh-C(26)	127.0(10)	Rh-C(24)-C(23)	69.97(20)
N(1)-Rh-N(2)	75.94(11)	Rh-C(24)-C(25)	69.11(18)

....cont.

...cont. Table 4.5

N(1)-Rh-C(22)	116.22(13)	Rh-C(24)-C(29)	129.2(3)
N(1)-Rh-C(23)	155.78(13)	Rh-C(25)-C(24)	72.17(19)
N(1)-Rh-C(24)	144.96(12)	Rh-C(25)-C(26)	70.60(19)
N(1)-Rh-C(25)	107.34(12)	Rh-C(25)-C(30)	127.6(3)
N(1)-Rh-C(26)	94.32(13)	Rh-C(26)-C(22)	69.95(20)
N(2)-Rh-C(22)	160.68(12)	Rh-C(26)-C(25)	70.76(19)
N(2)-Rh-C(23)	126.65(12)	Rh-C(26)-C(31)	126.1(3)
N(2)-Rh-C(24)	96.76(12)	C(24)-Rh-C(25)	38.72(13)
N(2)-Rh-C(25)	97.45(12)	C(24)-Rh-C(26)	64.10(13)
N(2)-Rh-C(26)	130.46(12)	C(25)-Rh-C(26)	38.64(13)
C(22)-Rh-C(23)	39.61(15)	Rh-N(1)-C(1)	125.4(3)
C(22)-Rh-C(24)	64.51(13)	Rh-N(1)-C(5)	114.75(22)
C(22)-Rh-C(25)	65.26(14)	Rh-N(2)-C(6)	107.91(21)
C(22)-Rh-C(26)	38.63(15)	Rh-N(2)-C(16)	129.76(23)
C(23)-Rh-C(24)	37.67(13)	C(23)-Rh-C(26)	64.97(14)
C(23)-Rh-C(25)	64.90(13)		

---



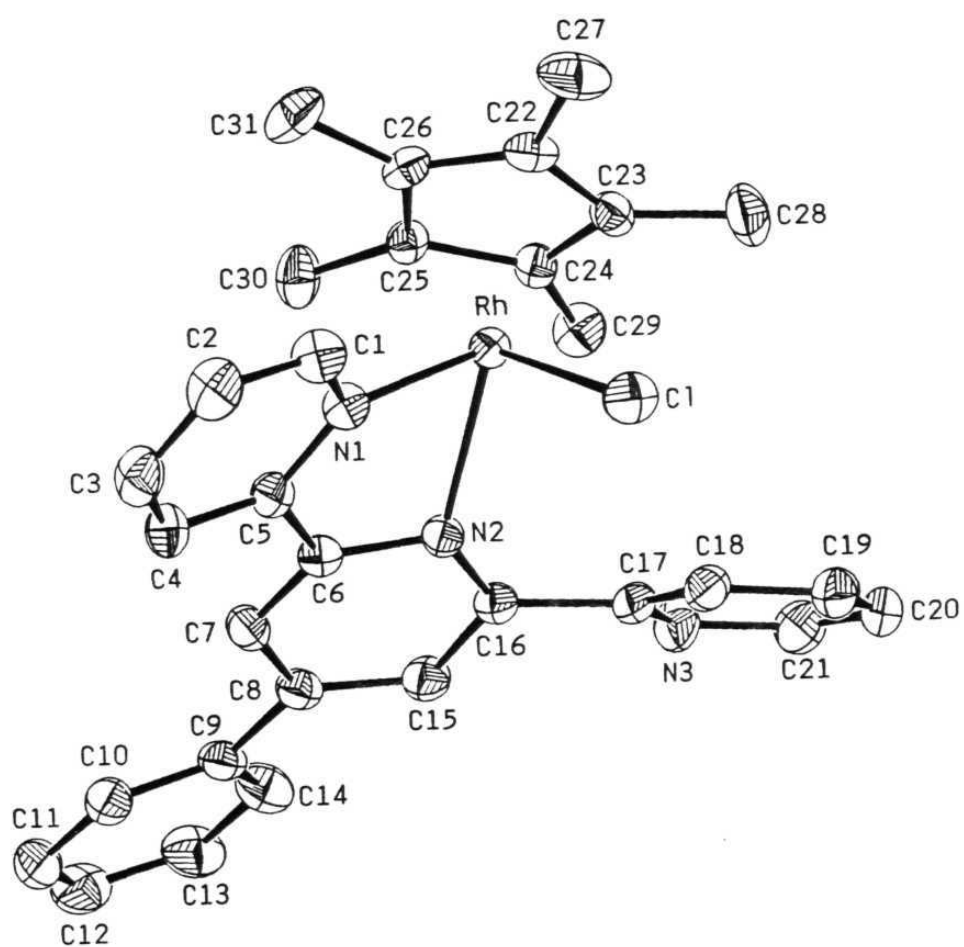


**Figure 4.15.** ORTEP drawing of the molecular structure of [Cp\*RhL<sup>19</sup>Cl]BF<sub>4</sub> showing the thermal ellipsoids at the 50% probability level with atom-labeling scheme.

The angle between the Cp\* plane normal and Rh-Cl, Rh-N(1) and Rh-N(2) are 84.3°, 115.1° and 168.0° respectively. The Rh-N distances are unequal with Rh-N(1), 2.086 (3) Å and Rh-N(2), 2.197 (3) Å. This has been observed in other complexes involving bidentate terpy.<sup>12</sup> The presence of uncoordinated pyridine ring gives rise to steric interactions, resulting in significantly longer Rh-N(2) bond compared to the Rh-N(1).

The metallacyclic moiety containing Rh, N(1), C(5), C(6) and N(2) shows considerable deviation from planarity (the root mean square deviation of these atoms from a least-square plane is 0.30 Å). The structure is stabilized by hydrogen bonding between chloride and H(18) of the uncoordinated pyridine ring, the distance between them being 2.56 Å which is less than the sum of their respective Vanderwaals radii.

#### 4.6. Conclusions

Reaction of  $[\text{Cp}^*\text{M}(\mu\text{-Cl})\text{Cl}]_2$  ( $\text{M} = \text{Rh}, \text{Ir}$ ) with polypyridyl ligands results in formation of cationic complexes by cleavage of halide bridge. At room-temperature, Ph-terpy and diterpy behave as fluxional ligands in  $[\text{Cp}^*\text{RhL}^{19}\text{Cl}]\text{BF}_4$  and  $[(\text{Cp}^*\text{RhCl})_2\text{L}^{20}](\text{BF}_4)_2$  complex. In the analogous iridium complex no fluxional behavior is observed. All the complexes are proposed to have the characteristic three legged "piano stool" geometry at the metal center. Crystal structure of complex  $[\text{Cp}^*\text{RhL}^{19}\text{Cl}]\text{BF}_4$  shows hydrogen bonding interactions between the chloride and H(18).

#### 4.7. References

1. Thompson, A. M. W. *Coord. Chem. Rev.* 1997, **160**, 1. Sauvage, J. P.; Collin, J. P.; Chambron, J. C.; Guillerez, S.; Coudret, C.; Balzani, V.; Barigelletti, F.; De Cola, L.; Flamigni, L. *Chem. Rev.* 1994, **94**, 993.
2. Constable, E. C. *Adv. Inorg. Chem.* 1989, **34**, 1. Constable, E. C. *Adv. Inorg. Chem. Radiochem.* 1986, **30**, 69. Constable, E. C. *Prog. Inorg. Chem.* 1994, **42**, 67.
3. Fagalde, F.; Katz, N. E. *J. Chem. Soc., Dalton Trans.* 1993, 571.
4. Bailey, J. A.; Miskowski, V. M.; Gray, H. B. *Inorg. Chem.* 1993, **32**, 369.
5. Yip, H.-K.; Cheng, L.-K.; Cheung, K.-K.; Che C.-M. *J. Chem. Soc., Dalton Trans.* 1993, 2933.
6. Sundquist, W. I.; Lippard, S. J. *Coord. Chem. Rev.* 1990, **100**, 293.
7. Koelle, U.; Graetzel, M. *Angew. Chem. Int. Ed. Engl.* 1987, **26**, 567.
8. Ladwig, M.; Kaim, W. *J. Organomet. Chem.* 1992, **439**, 79.
9. Steckhan, E.; Herrmann, S.; Ruppert, R.; Dietz, E.; Frede, M.; Spika, E. *Organometallics* 1991, **10**, 1568. Steckhan, E.; Herrmann, S.; Thoemmes, J.; Wandray, C.; Ruppert, R. *Angew. Chem. Int. Ed. Engl.* 1990, **29**, 388.
10. Cosnier, S.; Deronzier, A.; Vlachopoulos, N.; *J. Chem. Soc., Chem. Commun.* 1989, 1229.
11. Zeissel, R. *J. Chem. Soc., Chem. Commun.* 1988, 16.

12. Abel, E. W.; Orrell, K. G.; Osborne, A. G.; Pain, H. M.; Sik, V. *J. Chem. Soc., Dalton Trans.* 1994, 111. Abel, E. W.; Dimitrov, V. S.; Long, N. S.; Orrell, K. G.; Osborne, A. G.; Pain, H. M.; Sik, V.; Hursthouse, M. B.; Mazid, M. A. *J. Chem. Soc., Dalton Trans.* 1993, 597. Abel, E. W.; Dimitrov, V. S.; Long, N. S.; Orrell, K. G.; Osborne, A. G.; Sik, V.; Hursthouse, M. B.; Mazid, M. A. *J. Chem. Soc., Dalton Trans.* 1993, 291.
13. Mohan Rao, K.; Rao, Ch. R. K.; Zacharias, P. S. *Polyhedron* 1997, 16, 2369.
14. Chotalia, R.; Constable, E. C.; Hannon, M. J.; Tocher, D. A. *J. Chem. Soc., Dalton Trans.* 1995, 3571.
15. Pruchnik, F. P.; Robert, F.; Jeannin, Y.; Jeannin S. *Inorg. Chem.* 1996, **35**, 4261.
16. Kang, J. W.; Moseley, K.; Maitlis, P. M. *J. Am. Chem. Soc.* 1969, **91**, 5970.
17. White, C.; Yates, A.; Maitlis, P. M. *Inorganic Synthesis* 1992, **29**, 228.
18. Constable, E. C.; Lewis, J.; Liptrot, M. C.; Raithby, P. R. *Inorg. Chim. Acta.* 1990, **178**, 47.
19. Constable, E. C.; Thompson, A. M. W. *J. Chem. Soc., Dalton Trans.* 1992, 3467.
20. Mohan Rao, K.; Day, C.; Jacobson, R. A. Angelici, R. J. *Inorg. Chem.* 1992, 30, 5046.

21. Vogel, A. I. *Text Book of Practical Organic Chemistry* ELBS and Longman, 4th Ed. 1978.
22. Perrin, D. D.; Armarego, W. L. F.; Perrin, D. R. *Purification of Laboratory Chemicals* Pergamon Press, London, 1966.
23. Main, P.; Fiske, S. J.; Hill, S. E.; Lessinger, L.; Germain, G.; Declercq, J.-P.; Woolfson, M. M. MULTAN 80, A system of computer programs for the automatic solution of crystal structures from X-ray diffraction data, Universities of York and Louvain.
24. Ibers, J. A.; Hamilton, W. C. *International Tables for X-Ray Crystallography*, Kynoch Press, Birmingham, 1974, **4**, Tables 2.2 B and 2.3.1.
25. Gabe, E. J.; Lee, F. L.; Le Page, Y. in *Crystallographic Computing 3: Data Collection, Structure Determination, Proteins and Databases*, Eds., Sheldrick, G. M.; Krueger, C.; Goddard, Clarendon Press, Oxford, 1985, p 167.
26. Kolle, U.; Kang, B.-S.; Infelta, P.; Comte, P.; Gratzel, M. *Chem. Ber.* 1989, **122**, 1869.
27. Youinou, M.-T.; Zeissel, R. *J. Organomet. Chem.* 1989, **363**, 197.

## APPENDIX

**Table A1.** Anisotropic displacement coefficients for  $[\text{Ru}_2\text{L}^2(\text{dmsO})_4\text{Cl}_4]\cdot\text{CH}_2\text{Cl}_2$  complex ( $\text{\AA}^2 \times 10^4$  for Ru and  $\text{\AA}^2 \times 10^3$  for others).

Atom	U11	U22	U33	U12	U13	U23
Ru(1)	553(3)	483(3)	609(3)	27(2)	-76(2)	18(2)
Ru(2)	456(2)	494(3)	599(3)	23(2)	-77(2)	-32(2)
Cl(1)	98(1)	61(1)	101(1)	-7(1)	-1(1)	17(1)
Cl(2)	97(1)	89(1)	102(1)	-14(1)	1(1)	33(1)
Cl(3)	69(1)	78(1)	71(1)	1(1)	-1(1)	16(1)
Cl(4)	80(1)	70(1)	94(1)	-13(1)	-4(1)	15(1)
S(1)	71(1)	62(1)	74(1)	9(1)	-14(1)	-10(1)
S(2)	65(1)	66(1)	82(1)	11(1)	-13(1)	-4(1)
S(3)	55(1)	70(1)	65(1)	0(1)	-10(1)	-10(1)
S(4)	52(1)	62(1)	99(1)	10(1)	-13(1)	-12(1)
O(1)	59(2)	68(2)	70(2)	8(2)	-19(2)	-12(2)
O(2)	66(2)	74(2)	68(2)	18(2)	-10(2)	-8(2)
O(3)	56(2)	64(2)	61(2)	4(2)	-7(2)	-13(2)
O(4)	53(2)	64(2)	79(2)	12(2)	-13(2)	-18(2)
O(5)	85(2)	82(2)	96(2)	16(2)	-37(2)	-25(2)
O(6)	90(2)	96(2)	131(2)	36(2)	-15(2)	-50(2)
O(7)	67(2)	104(2)	92(2)	14(2)	-12(2)	-45(2)
O(8)	50(2)	100(2)	112(2)	4(2)	-18(2)	-30(2)
N(1)	65(2)	50(2)	67(2)	-10(2)	-9(2)	3(2)

....cont.

....cont. Table A1

N(2)	74(2)	43(2)	58(2)	-6(2)	4(2)	3(2)
C(1)	54(2)	49(2)	65(2)	-3(2)	2(2)	4(2)
C(2)	46(2)	60(2)	66(2)	-5(2)	-2(2)	7(2)
C(3)	46(2)	69(2)	89(2)	6(2)	11(2)	12(2)
C(4)	56(2)	74(2)	84(2)	8(2)	3(2)	-11(2)
C(5)	64(2)	78(3)	70(2)	-1(2)	2(2)	-7(2)
C(6)	49(2)	61(2)	61(2)	0(2)	-3(2)	-4(2)
C(7)	66(2)	69(2)	59(2)	2(2)	-6(2)	-7(2)
C(8)	70(2)	138(3)	126(3)	33(3)	6(3)	-33(3)
C(9)	51(2)	63(2)	86(2)	-10(2)	-8(2)	25(2)
C(10)	46(2)	47(2)	54(2)	-2(2)	-1(2)	4(2)
C(11)	47(2)	56(2)	62(2)	0(2)	-9(2)	-5(2)
C(12)	62(2)	80(2)	67(2)	-2(2)	-10(2)	-14(2)
C(13)	52(2)	84(3)	88(2)	7(2)	-20(2)	-11(2)
C(14)	52(2)	69(2)	82(2)	8(2)	0(2)	10(2)
C(15)	44(2)	51(2)	65(2)	2(2)	1(2)	7(2)
C(16)	65(2)	64(2)	64(2)	1(2)	-11(2)	-13(2)
C(17)	59(2)	152(3)	130(3)	21(3)	-35(2)	-35(3)
C(18)	60(2)	44(2)	68(2)	2(2)	11(2)	6(2)
C(19)	77(2)	55(2)	87(2)	-21(2)	-23(2)	9(2)
C(20)	80(2)	55(2)	74(2)	4(2)	-11(2)	-9(2)
C(21)	74(2)	59(2)	62(2)	5(2)	-1(2)	-6(2)
C(22)	109(3)	109(3)	67(2)	21(3)	6(2)	-9(2)
C(23)	109(3)	67(2)	120(3)	5(2)	-30(3)	-27(2)
C(24)	85(3)	153(3)	51(3)	57(3)	-12(3)	-4(3)

....cont.

....cont. Table A1

C(25)	56(3)	81(3)	132(3)	29(3)	-24(3)	4(3)
C(24')	43(3)	74(3)	275(3)	36(3)	-64(3)	-58(3)
C(25')	95(3)	303(3)	207(3)	141(3)	46(3)	132(3)
C(26)	70(2)	67(2)	94(2)	-13(2)	-18(2)	-11(2)
C(27)	87(3)	117(3)	68(2)	-8(3)	-21(2)	5(2)
C(28)	65(3)	116(3)	259(3)	26(3)	12(3)	-81(3)
C(29)	66(3)	60(3)	167(3)	4(3)	-19(3)	-18(3)
C(28')	67(3)	230(3)	149(3)	55(3)	-59(3)	-143(3)
C(29')	76(3)	77(3)	239(3)	14(3)	-37(3)	-45(3)
C(30)	295(3)	45(3)	402(3)	12(3)	-196(3)	0(3)
Cl(5)	310(3)	155(2)	249(2)	-42(2)	-65(2)	14(2)
Cl(6)	331(3)	279(3)	178(2)	-48(3)	-48(2)	88(2)

The anisotropic displacement factor exponent =  $-2\pi^2(U_{11}h^2a^{*2} + U_{22}K^2b^{*2} + U_{33}l^2c^{*2} + 2U_{12}hka^*b^*\cos\gamma + 2U_{13}hla^*c^*\cos\beta + 2U_{23}klb^*c^*\cos\alpha)$



**Table A2.** Hydrogen atom coordinates ( $\times 10^4$ ) and isotropic displacement coefficients ( $\text{\AA}^2 \times 10^3$ ) for  $[\text{Ru}_2\text{L}^2(\text{dmso})_4\text{Cl}_4] \cdot \text{CH}_2\text{Cl}_2$  complex

Atom	x	y	z	U
H(1A)	4711	1970	3572	80
H(3B)	6268	176	4481	80
H(3A)	6475	624	2944	80
H(5B)	4449	711	1926	80
H(7B)	3270	1288	2031	80
H(8B)	5616	99	1707	80
H(8C)	6549	313	1900	80
H(8D)	6066	-190	2201	80
H(9A)	6513	1155	3739	80
H(12A)	4787	-865	2933	80
H(14A)	3555	311	3850	80
H(16A)	6202	-1151	3049	80
H(17A)	3307	-609	2727	80
H(17B)	2729	-450	3223	80
H(17C)	3086	40	2849	80
H(18A)	4266	769	4571	80
H(19A)	6355	2209	4521	80
H(19B)	6574	1552	4557	80
H(20A)	4882	1824	4841	80
H(20B)	5592	2026	5246	80
H(21A)	5958	1112	5441	80
H(21B)	4928	1099	5426	80

....cont.

....cont. Table A2

H(22A)	2893	2773	4836	80
H(22B)	2134	2671	4421	80
H(22C)	2742	2155	4596	80
H(23A)	3469	3646	4309	80
H(23B)	3719	3633	3706	80
H(23C)	2725	3569	3881	80
H(24A)	551	2175	3035	80
H(24B)	1267	1767	2783	80
H(24C)	1177	1808	3401	80
H(25A)	1256	3080	2465	80
H(25B)	2275	3208	2418	80
H(25C)	1901	2603	2249	80
H(24D)	421	2360	2977	80
H(24E)	1110	1954	2696	80
H(24F)	961	1908	3309	80
H(25D)	1001	3174	2605	80
H(25E)	2007	3345	2616	80
H(25F)	1699	2794	2304	80
H(26A)	9023	779	5028	80
H(26B)	9380	331	4613	80
H(26C)	8711	813	4436	80
H(27A)	8598	-24	5670	80
H(27B)	8005	-560	5532	80
H(27C)	8956	-502	5285	80
H(28A)	9770	-1025	3355	80

....cont.

....cont. Table A2

H(28B)	8758	-1051	3214	80
H(28C)	9224	-451	3294	80
H(29A)	9437	-1782	4083	80
H(29B)	8624	-1742	4469	80
H(29C)	8468	-1795	3857	80
H(28D)	9603	-1302	3441	80
H(28E)	8580	-1394	3364	80
H(28F)	9009	-791	3238	80
H(29D)	9542	-1661	4433	80
H(29E)	8898	-1380	4847	80
H(29F)	8518	-1772	4394	80
H(30A)	3940	2957	913	80
H(30B)	4275	2681	1443	80

---

Hydrogen atoms are labelled according to the carbon atom to which they are attached.

**Table A3.** Bond distances (Å) in [Ru<sub>2</sub>L<sup>2</sup>(dmso)<sub>4</sub>Cl<sub>4</sub>].CH<sub>2</sub>Cl<sub>2</sub> complex

---

Ru(1)-Cl(1)	2.386(2)	Ru(1)-Cl(2)	2.418(2)
Ru(1)-S(1)	2.211(2)	Ru(1)-S(2)	2.228(2)
Ru(1)-O(1)	2.076(4)	Ru(1)-O(2)	2.081(4)
Ru(2)-Cl(3)	2.389(2)	Ru(2)-Cl(4)	2.389(2)
Ru(2)-S(3)	2.225(2)	Ru(2)-S(4)	2.221(2)
Ru(2)-O(3)	2.066(4)	Ru(2)-O(4)	2.095(4)
S(1)-O(5)	1.487(5)	S(1)-C(22)	1.751(7)
S(1)-C(23)	1.780(7)	S(2)-O(6)	1.470(6)
S(2)-C(24)	1.774(17)	S(2)-C(25)	1.791(16)
S(2)-C(24')	1.703(11)	S(2)-C(25')	1.673(16)
S(3)-O(7)	1.487(5)	S(3)-C(26)	1.762(7)
S(3)-C(27)	1.767(7)	S(4)-O(8)	1.457(5)
S(4)-C(28)	1.780(17)	S(4)-C(29)	1.762(14)
S(4)-C(28')	1.685(13)	S(4)-C(29')	1.748(13)
O(1)-C(1)	1.274(7)	O(2)-C(7)	1.232(8)
O(3)-C(10)	1.280(7)	O(4)-C(16)	1.245(7)
N(1)-C(9)	1.290(8)	N(1)-C(19)	1.468(8)
N(2)-C(18)	1.294(8)	N(2)-C(21)	1.474(7)
C(1)-C(2)	1.440(8)	C(1)-C(6)	1.412(8)
C(2)-C(3)	1.385(9)	C(2)-C(9)	1.441(9)
C(3)-C(4)	1.384(9)	C(4)-C(5)	1.367(9)
			....cont.

---

....cont. Table A3

C(4)-C(8)	1.517(11)	C(5)-C(6)	1.408(9)
C(6)-C(7)	1.435(8)	C(10)-C(11)	1.421(8)
C(10)-C(15)	1.432(8)	C(11)-C(12)	1.414(8)
C(11)-C(16)	1.438(8)	C(12)-C(13)	1.380(9)
C(13)-C(14)	1.383(9)	C(13)-C(17)	1.513(10)
C(14)-C(15)	1.409(8)	C(15)-C(18)	1.434(8)
C(19)-C(20)	1.524(9)	C(20)-C(21)	1.505(9)
C(30)-Cl(5)	1.832(13)	C(30)-Cl(6)	1.718(15)

---

**Table A4.** Bond angles (°) in [Ru<sub>2</sub>L<sup>2</sup>(dmsO)<sub>4</sub>Cl<sub>4</sub>].CH<sub>2</sub>Cl<sub>2</sub> complex

Cl(1)-Ru(1)-Cl(2)	170.6(1)	Cl(1)-Ru(1)-S(1)	93.0(1)
Cl(2)-Ru(1)-S(1)	91.3(1)	Cl(1)-Ru(1)-S(2)	92.7(1)
Cl(2)-Ru(1)-S(2)	95.3(1)	S(1)-Ru(1)-S(2)	95.0(1)
Cl(1)-Ru(1)-O(1)	85.4(1)	Cl(2)-Ru(1)-O(1)	86.4(1)
S(1)-Ru(1)-O(1)	87.9(1)	S(2)-Ru(1)-O(1)	176.7(1)
Cl(1)-Ru(1)-O(2)	87.1(1)	Cl(2)-Ru(1)-O(2)	88.2(1)
S(1)-Ru(1)-O(2)	177.2(1)	S(2)-Ru(1)-O(2)	87.8(1)
O(1)-Ru(1)-O(2)	89.4(2)	Cl(3)-Ru(2)-Cl(4)	171.0(1)
Cl(3)-Ru(2)-S(3)	92.0(1)	Cl(4)-Ru(2)-S(3)	93.1(1)
Cl(3)-Ru(2)-S(4)	92.2(1)	Cl(4)-Ru(2)-S(4)	94.8(1)
S(3)-Ru(2)-S(4)	94.3(1)	Cl(3)-Ru(2)-O(3)	87.2(1)
Cl(4)-Ru(2)-O(3)	85.6(1)	S(3)-Ru(2)-O(3)	87.6(1)
S(4)-Ru(2)-O(3)	178.1(1)	Cl(3)-Ru(2)-O(4)	87.3(1)
Cl(4)-Ru(2)-O(4)	87.1(1)	S(3)-Ru(2)-O(4)	175.9(1)
S(4)-Ru(2)-O(4)	89.8(1)	O(3)-Ru(2)-O(4)	88.3(2)
Ru(1)-S(1)-O(5)	114.7(2)	Ru(1)-S(1)-C(22)	114.9(3)
O(5)-S(1)-C(22)	105.9(3)	Ru(1)-S(1)-C(23)	114.3(3)
O(5)-S(1)-C(23)	106.2(3)	C(22)-S(1)-C(23)	99.4(4)
Ru(1)-S(2)-O(6)	121.7(2)	Ru(1)-S(2)-C(24)	102.0(5)
O(6)-S(2)-C(24)	111.1(6)	Ru(1)-S(2)-C(25)	102.4(5)
O(6)-S(2)-C(25)	116.0(6)	C(24)-S(2)-C(25)	100.8(8)
Ru(1)-S(2)-C(24')	115.6(4)	O(6)-S(2)-C(24')	105.1(5)
Ru(1)-S(2)-C(25')	118.2(5)	O(6)-S(2)-C(25')	99.8(6)
C(24')-S(2)-C(25')	91.3(8)	Ru(2)-S(3)-O(7)	114.5(2)
Ru(2)-S(3)-C(26)	114.1(2)	O(7)-S(3)-C(26)	106.2(3)

....cont.

....cont. Table A4

Ru(2)-S(3)-C(27)	114.7(3)	O(7)-S(3)-C(27)	106.7(3)
C(26)-S(3)-C(27)	99.2(3)	Ru(2)-S(4)-O(8)	121.4(2)
Ru(2)-S(4)-C(28)	109.1(6)	O(8)-S(4)-C(28)	94.7(7)
Ru(2)-S(4)-C(29)	114.0(6)	O(8)-S(4)-C(29)	116.0(6)
C(28)-S(4)-C(29)	95.5(9)	Ru(2)-S(4)-C(28')	111.4(4)
O(8)-S(4)-C(28')	110.5(5)	Ru(2)-S(4)-C(29')	111.6(4)
O(8)-S(4)-C(29')	95.6(5)	C(28')-S(4)-C(29')	104.0(7)
Ru(1)-O(1)-C(1)	127.7(4)	Ru(1)-O(2)-C(7)	124.0(4)
Ru(2)-O(3)-C(10)	129.5(3)	Ru(2)-O(4)-C(16)	125.6(4)
C(9)-N(1)-C(19)	123.6(5)	C(18)-N(2)-C(21)	122.3(5)
O(1)-C(1)-C(2)	118.5(5)	O(1)-C(1)-C(6)	124.5(5)
C(2)-C(1)-C(6)	117.0(5)	C(1)-C(2)-C(3)	119.7(5)
C(1)-C(2)-C(9)	121.1(5)	C(3)-C(2)-C(9)	119.1(5)
C(2)-C(3)-C(4)	123.5(6)	C(3)-C(4)-C(5)	116.4(6)
C(3)-C(4)-C(8)	122.5(6)	C(5)-C(4)-C(8)	121.1(6)
C(4)-C(5)-C(6)	124.0(6)	C(1)-C(6)-C(5)	119.3(5)
C(1)-C(6)-C(7)	124.2(5)	C(5)-C(6)-C(7)	116.5(5)
O(2)-C(7)-C(6)	130.1(6)	N(1)-C(9)-C(2)	125.2(6)
O(3)-C(10)-C(11)	123.6(5)	O(3)-C(10)-C(15)	118.7(5)
C(11)-C(10)-C(15)	117.7(5)	C(10)-C(11)-C(12)	119.4(5)
C(10)-C(11)-C(16)	124.8(5)	C(12)-C(11)-C(16)	115.7(5)
C(11)-C(12)-C(13)	122.9(6)	C(12)-C(13)-C(14)	117.8(6)
C(12)-C(13)-C(17)	122.0(6)	C(14)-C(13)-C(17)	120.3(6)
C(13)-C(14)-C(15)	122.5(6)	C(10)-C(15)-C(14)	119.7(5)
C(10)-C(15)-C(18)	121.7(5)	C(14)-C(15)-C(18)	118.6(5)
O(4)-C(16)-C(11)	128.3(6)	N(2)-C(18)-C(15)	124.2(5)
N(1)-C(19)-C(20)	112.2(5)	C(19)-C(20)-C(21)	115.4(5)
N(2)-C(21)-C(20)	113.1(5)	Cl(5)-C(30)-Cl(6)	104.6(6)

---

**Table A5.** Anisotropic displacement parameters for [RuL<sup>5'</sup>(PPh<sub>3</sub>)<sub>2</sub>COCl] ( $\text{\AA}^2 \times 10^4$  for Ru, Cl, P, O, N;  $\text{\AA}^2 \times 10^3$  for C)

Atom	U11	U22	U33	U12	U13	U23
Ru	279(2)	230(3)	367(3)	0(2)	76(2)	2(2)
Cl	485(9)	343(9)	510(10)	126(7)	74(7)	93(8)
P(1)	330(8)	324(9)	371(9)	58(7)	95(7)	10(7)
P(2)	357(8)	332(9)	409(9)	-32(7)	118(7)	-20(8)
O(1)	300(2)	280(2)	430(2)	-10(2)	50(2)	30(2)
O(2)	460(3)	480(3)	830(4)	-110(2)	-70(2)	-120(3)
N(1)	300(3)	340(3)	460(3)	-30(2)	40(2)	-40(2)
C(1)	31(3)	29(3)	34(3)	3(3)	12(3)	-1(3)
C(2)	29(3)	26(3)	38(3)	-2(3)	8(3)	-1(3)
C(3)	34(3)	33(4)	52(4)	3(3)	6(3)	-6(3)
C(4)	36(3)	33(4)	53(4)	10(3)	4(3)	3(3)
C(5)	41(3)	23(3)	57(4)	1(3)	9(3)	-3(3)
C(6)	32(3)	28(3)	47(4)	-1(3)	9(3)	-5(3)
C(7)	41(4)	24(3)	66(4)	-6(3)	14(3)	-5(3)
C(8)	32(3)	42(4)	46(4)	-5(3)	9(3)	-6(3)
C(9)	40(4)	48(4)	74(5)	-14(3)	7(3)	2(4)
C(10)	58(5)	65(5)	88(6)	-24(4)	20(4)	-5(5)
C(11)	42(4)	96(7)	74(6)	-25(4)	-1(4)	-5(5)
C(12)	40(4)	87(6)	58(5)	-3(4)	2(3)	4(4)
C(13)	39(4)	57(5)	47(4)	-5(3)	9(3)	0(4)
C(14)	53(4)	65(5)	69(5)	4(4)	6(4)	17(4)

....cont.



....cont Table A5

C(15)	47(4)	46(4)	85(5)	7(3)	-9(4)	8(4)
C(16)	39(3)	28(3)	45(4)	4(3)	7(3)	-5(3)
C(17)	39(3)	36(4)	37(4)	9(3)	7(3)	-6(3)
C(18)	60(4)	41(4)	69(5)	8(4)	22(4)	-9(4)
C(19)	90(6)	42(5)	86(6)	3(4)	22(5)	-15(4)
C(20)	91(6)	68(6)	73(6)	31(5)	18(5)	-21(5)
C(21)	67(5)	78(6)	69(5)	23(5)	23(4)	-14(5)
C(22)	56(4)	56(5)	60(5)	8(4)	22(4)	-6(4)
C(23)	38(3)	41(4)	43(4)	-1(3)	18(3)	0(3)
C(24)	40(4)	53(4)	50(4)	2(3)	11(3)	3(3)
C(25)	34(4)	84(6)	57(5)	-1(4)	11(3)	1(4)
C(26)	53(4)	80(6)	60(5)	-21(4)	26(4)	-13(4)
C(27)	66(5)	54(5)	78(5)	-15(4)	33(4)	-5(4)
C(28)	49(4)	46(4)	55(4)	-4(3)	18(3)	2(3)
C(29)	50(4)	34(4)	40(4)	7(3)	12(3)	4(3)
C(30)	57(4)	76(5)	48(4)	14(4)	22(3)	12(4)
C(31)	97(6)	101(7)	44(5)	22(6)	30(4)	24(5)
C(32)	81(6)	85(6)	47(5)	27(5)	-6(4)	13(4)
C(33)	57(4)	70(5)	57(5)	7(4)	-6(4)	12(4)
C(34)	40(4)	52(4)	49(4)	1(3)	0(3)	4(3)
C(35)	39(4)	55(5)	50(4)	2(3)	22(3)	-1(3)
C(36)	47(4)	60(5)	87(6)	11(4)	27(4)	10(4)

....cont.

....cont. Table A5

C(37)	78(6)	79(6)	103(7)	38(5)	42(5)	19(5)
C(38)	53(5)	15(1)	71(6)	36(6)	14(4)	5(6)
C(39)	40(5)	139(9)	100(7)	9(5)	9(4)	-24(7)
C(40)	38(4)	74(6)	89(6)	0(4)	10(4)	-16(5)
C(41)	52(4)	(40)4	43(4)	-9(3)	21(3)	-6(3)
C(42)	49(4)	53(4)	42(4)	-7(3)	14(3)	1(3)
C(43)	63(5)	87(6)	45(4)	-29(4)	7(4)	1(4)
C(44)	102(6)	80(6)	48(5)	-43(5)	20(5)	-18(4)
C(45)	98(6)	92(7)	63(5)	-16(5)	36(5)	-41(5)
C(46)	59(4)	76(6)	68(5)	-9(4)	28(4)	-26(4)

The anisotropic displacement factor exponent =  $-2\pi^2(U_{11}h^2a^{*2} + U_{22}K^2b^{*2} + U_{33}l^2c^{*2} + 2U_{12}hka^*b^*\cos\gamma + 2U_{13}hla^*c^*\cos\beta + 2U_{23}klb^*c^*\cos\alpha)$

**Table A6.** Hydrogen atom coordinates(  $\times 10^4$ ) and isotropic thermal parameters ( $\text{\AA}^2 \times 10^4$ ) for  $[\text{RuL}^{5'}(\text{PPh}_3)_2\text{COCl}]$

Atom	x	y	z	B <sub>eq</sub>
H(1)	2099	-1854	2158	38891
H(2)	1487	-5285	1644	39440
H(3)	807	-5121	1115	41402
H(4)	204	-5782	1064	51592
H(5)	-454	-6545	782	65999
H(6)	-916	-5212	229	68915
H(7)	-733	-3103	-26	60176
H(8)	244	-1655	321	60467
H(9)	-75	-1820	-187	60467
H(10)	-188	-1129	283	60467
H(11)	2093	-5111	2482	59729
H(12)	2288	-5111	2010	59729
H(13)	2388	-3963	2415	59729
H(14)	1297	3065	2247	52458
H(15)	1149	5083	2630	68646
H(16)	628	5106	3072	72977
H(17)	265	3163	3123	66474
H(18)	414	1147	2734	52207
H(19)	242	861	1630	45467
H(20)	-328	-469	1330	54758
H(21)	-334	-2746	1529	59742
H(22)	233	-3753	2028	59976
H(23)	803	-2481	2330	46027

....cont.

....cont. Table A6

H(24)	835	-950	3108	56006
H(25)	1200	-1816	3879	74200
H(26)	1895	-1802	4051	70234
H(27)	2225	-921	3463	60872
H(28)	1873	-93	2678	45750
H(29)	2032	-2241	901	59551
H(30)	2668	-3226	1224	78343
H(31)	3209	-1822	1553	85267
H(32)	3134	499	1541	90334
H(33)	2508	1482	1239	63978
H(34)	907	110	281	44837
H(35)	596	-823	-509	62756
H(36)	964	-1868	-1027	71905
H(37)	1662	-2044	-749	77321
H(38)	1976	-1142	29	62250

---

Hydrogen atoms are labelled according to the carbon atom to which they are attached.

**Table A7.** Bond distances (Å) in [RuL<sup>5'</sup>(PPh<sub>3</sub>)<sub>2</sub>COCl]

Ru-Cl(1)	2.484(2)	Ru-P(1)	2.377(2)
Ru-P(2)	2.381(2)	Ru-O(1)	2.246(4)
Ru-C(2)	2.040(5)	Ru-C(16)	1.805(6)
C(1)-O(1)	1.316(6)	C(16)-O(2)	1.158(6)
P(1)-C(17)	1.842(6)	P(1)-C(23)	1.817(6)
P(1)-C(29)	1.832(6)	P(2)-C(35)	1.831(6)
P(2)-C(41)	1.819(6)	P(2)-C(47)	1.847(7)
N(1)-C(7)	1.317(7)	N(1)-C(8)	1.427(7)
O(1)-C(1)	1.316(6)	O(2)-C(16)	1.158(6)
N(1)-C(7)	1.317(7)	N(1)-C(8)	1.427(7)
C(1)-C(2)	1.418(7)	C(1)-C(6)	1.417(7)
C(2)-C(3)	1.363(7)	C(3)-C(4)	1.436(8)
C(4)-C(5)	1.363(8)	C(4)-C(15)	1.512(8)
C(5)-C(6)	1.423(8)	C(6)-C(7)	1.401(8)
C(8)-C(9)	1.382(8)	C(8)-C(13)	1.387(8)
C(9)-C(10)	1.386(9)	C(10)-C(11)	1.37(1)
C(11)-C(12)	1.38(1)	C(12)-C(13)	1.402(8)
C(13)-C(14)	1.485(9)	C(17)-C(18)	1.365(8)
C(17)-C(22)	1.381(8)	C(18)-C(19)	1.390(9)
C(19)-C(20)	1.39(1)	C(20)-C(21)	1.36(1)
C(21)-C(22)	1.397(9)	C(23)-C(24)	1.408(8)
C(23)-C(28)	1.389(8)	C(24)-C(25)	1.394(9)

....cont.

....cont. Table A7

C(25)-C(26)	1.363(10)	C(26)-C(27)	1.371(10)
C(27)-C(28)	1.375(9)	C(29)-C(30)	1.397(8)
C(29)-C(34)	1.394(8)	C(30)-C(31)	1.377(9)
C(31)-C(32)	1.378(10)	C(32)-C(33)	1.355(10)
C(33)-C(34)	1.381(8)	C(35)-C(36)	1.383(9)
C(35)-C(40)	1.390(9)	C(36)-C(37)	1.412(9)
C(37)-C(38)	1.37(1)	C(38)-C(39)	1.36(1)
C(39)-C(40)	1.39(1)	C(41)-C(42)	1.401(8)
C(41)-C(46)	1.396(8)	C(42)-C(43)	1.389(9)
C(43)-C(44)	1.367(10)	C(44)-C(45)	1.39(1)
C(45)-C(46)	1.362(10)	C(47)-C(48)	1.54(1)
C(47)-C(52)	1.30(1)	C(47)-C(53)	1.39(2)
C(47)-C(56)	1.41(2)	C(48)-C(49)	1.41(2)
C(48)-C(53)	1.34(2)	C(49)-C(50)	1.58(2)
C(49)-C(54)	1.43(2)	C(50)-C(51)	1.24(2)
C(50)-C(54)	1.36(2)	C(50)-C(55)	1.44(2)
C(51)-C(52)	1.45(2)	C(51)-C(55)	0.75(2)
C(51)-C(56)	1.67(2)	C(52)-C(55)	1.55(2)
C(52)-C(56)	0.74(2)	C(53)-C(54)	1.44(2)
C(55)-C(56)	1.40(2)		

---

**Table A8.** Bond angles (°) in  $[\text{RuL}^{5+}(\text{PPh}_3)_2\text{COCl}]$ 

Cl-Ru-P(1)	88.54(5)	Cl-Ru-P(2)	94.71(6)
Cl-Ru-O(1)	91.22(10)	Cl-Ru-C(2)	155.3(1)
Cl-Ru-C(16)	103.6(2)	P(1)-Ru-P(2)	176.75(6)
P(1)-Ru-O(1)	88.2(1)	P(1)-Ru-C(2)	87.8(2)
P(1)-Ru-C(16)	91.8(2)	P(2)-Ru-O(1)	91.79(10)
P(2)-Ru-C(2)	89.2(2)	P(2)-Ru-C(16)	87.4(2)
O(1)-Ru-C(2)	64.2(2)	O(1)-Ru-C(16)	165.2(2)
C(2)-Ru-C(16)	100.9(2)	Ru-P(1)-C(17)	118.3(2)
Ru(1)-P(1)-C(23)	110.0(2)	Ru-P(1)-C(29)	117.9(2)
C(17)-P(1)-C(23)	104.2(3)	C(17)-P(1)-C(29)	99.8(3)
C(23)-P(1)-C(29)	105.0(3)	Ru-P(2)-C(35)	112.0(2)
Ru-P(2)-C(41)	117.3(2)	Ru-P(2)-C(47)	117.1(2)
C(35)-P(2)-C(41)	104.5(3)	C(35)-P(2)-C(47)	103.1(3)
C(41)-P(2)-C(47)	101.1(3)	Ru-O(1)-C(1)	88.2(3)
C(7)-N(1)-C(8)	125.2(5)	O(1)-C(1)-C(2)	113.4(5)
O(1)-C(1)-C(6)	125.0(5)	C(2)-C(1)-C(6)	121.6(5)
Ru-C(2)-C(1)	94.2(4)	Ru-C(2)-C(3)	147.3(4)
C(1)-C(2)-C(3)	118.5(5)	C(2)-C(3)-C(4)	121.6(5)
C(3)-C(4)-C(5)	119.2(5)	C(3)-C(4)-C(15)	119.0(5)
C(5)-C(4)-C(15)	121.8(6)	C(4)-C(5)-C(6)	121.7(5)
C(1)-C(6)-C(5)	117.3(5)	C(1)-C(6)-C(7)	121.3(5)
C(5)-C(6)-C(7)	121.2(5)	N(1)-C(7)-C(6)	122.35(5)
N(1)-C(8)-C(9)	121.2(6)	N(1)-C(8)-C(13)	116.9(5)
....cont.			

....cont. Table A8

C(9)-C(8)-C(13)	121.8(5)	C(8)-C(9)-C(10)	119.8(7)
C(9)-C(10)-C(11)	119.8(7)	C(10)-C(11)-C(12)	120.1(6)
C(11)-C(12)-C(13)	121.8(7)	C(8)-C(13)-C(12)	116.7(6)
C(8)-C(13)-C(14)	122.2(6)	C(12)-C(13)-C(14)	121.1(6)
Ru-C(16)-O(2)	178.1(5)	P(1)-C(17)-C(18)	119.1(4)
P(1)-C(17)-C(22)	121.5(5)	C(18)-C(17)-C(22)	119.2(6)
C(17)-C(18)-C(19)	121.4(6)	C(18)-C(19)-C(20)	118.8(7)
C(19)-C(20)-C(21)	120.3(7)	C(20)-C(21)-C(22)	120.2(7)
C(17)-C(22)-C(21)	120.0(7)	P(1)-C(23)-C(24)	118.9(5)
P(1)-C(23)-C(28)	122.4(5)	C(24)-C(23)-C(28)	118.1(6)
C(23)-C(24)-C(25)	119.1(6)	C(24)-C(25)-C(26)	121.3(7)
C(25)-C(26)-C(27)	119.8(7)	C(26)-C(27)-C(28)	120.2(7)
C(23)-C(28)-C(27)	121.4(6)	P(1)-C(29)-C(30)	121.7(5)
P(1)-C(29)-C(34)	120.1(5)	C(30)-C(29)-C(34)	118.2(6)
C(29)-C(30)-C(31)	120.7(6)	C(30)-C(31)-C(32)	119.9(7)
C(31)-C(32)-C(33)	120.2(7)	C(32)-C(33)-C(34)	120.9(7)
C(29)-C(34)-C(35)	120.2(6)	P(2)-C(35)-C(36)	120.6(5)
P(2)-C(35)-C(40)	120.5(5)	C(36)-C(35)-C(40)	118.4(6)
C(35)-C(36)-C(37)	121.1(7)	C(36)-C(37)-C(38)	118.7(8)
C(37)-C(38)-C(39)	120.8(8)	C(38)-C(39)-C(40)	120.7(9)
C(35)-C(40)-C(39)	120.3(8)	P(2)-C(41)-C(42)	117.5(5)
P(2)-C(41)-C(46)	124.1(5)	C(42)-C(41)-C(46)	118.1(6)
C(41)-C(42)-C(43)	119.5(6)	C(42)-C(43)-C(44)	121.3(7)
C(43)-C(44)-C(45)	119.5(7)	C(44)-C(45)-C(46)	119.8(7)

....cont.



....cont. Table A8

C(41)-C(46)-C(45)	121.7(7)	P(2)-C(47)-C(48)	113.7(7)
P(2)-C(47)-C(52)	124.2(7)	P(2)-C(47)-C(53)	121.2(8)
P(2)-C(47)-C(56)	119.1(7)	C(48)-C(47)-C(52)	121.6(9)
C(48)-C(47)-C(53)	54.2(8)	C(48)-C(47)-C(56)	111.8(9)
C(52)-C(47)-C(53)	97.0(1)	C(52)-C(47)-C(56)	31.4(7)
C(53)-C(47)-C(56)	117.0(1)	C(47)-C(48)-C(49)	113.0(1)
C(47)-C(48)-C(53)	57.0(9)	C(49)-C(48)-C(53)	86.0(1)
C(48)-C(49)-C(50)	118.0(1)	C(48)-C(49)-C(54)	94.0(1)
C(50)-C(49)-C(54)	53.4(9)	C(49)-C(50)-C(51)	121.0(1)
C(49)-C(50)-C(54)	57.6(9)	C(49)-C(50)-C(55)	107.0(1)
C(51)-C(50)-C(54)	101.0(1)	C(51)-C(50)-C(55)	31.5(8)
C(54)-C(50)-C(55)	119.0(1)	C(50)-C(51)-C(52)	119.0(1)
C(50)-C(51)-C(55)	88.0(2)	C(50)-C(51)-C(56)	113.0(1)
C(52)-C(51)-C(55)	82.0(2)	C(52)-C(51)-C(56)	26.0(2)
C(55)-C(51)-C(56)	56.0(1)	C(47)-C(52)-C(51)	123.0(1)
C(47)-C(52)-C(55)	117.0(1)	C(47)-C(52)-C(56)	82.0(1)
C(51)-C(52)-C(55)	28.9(7)	C(51)-C(52)-C(56)	93.0(1)
C(55)-C(52)-C(56)	64.0(1)	C(47)-C(53)-C(48)	68.9(10)
C(47)-C(53)-C(54)	122.0(1)	C(48)-C(53)-C(54)	96.0(1)
C(49)-C(54)-C(50)	68.0(1)	C(49)-C(54)-C(53)	81.0(1)
C(50)-C(54)-C(53)	116.0(1)	C(50)-C(55)-C(51)	59.0(1)
C(50)-C(55)-C(52)	102.0(1)	C(50)-C(55)-C(56)	118.0(1)
C(51)-C(55)-C(52)	68.0(1)	C(51)-C(55)-C(56)	97.0(2)
C(52)-C(55)-C(56)	28.5(7)	C(47)-C(56)-C(51)	103.0(1)
C(47)-C(56)-C(52)	65.0(1)	C(47)-C(56)-C(55)	119.0(1)
C(51)-C(56)-C(52)	60.0(1)	C(51)-C(56)-C(55)	26.5(8)
C(52)-C(56)-C(55)	86.0(1)		

---

**Table A9.** Anisotropic thermal coordinates in [Cp\*RhL<sup>19</sup>Cl]BF<sub>4</sub> ( $\text{\AA}^2 \times 10^3$  for Rh;  $\text{\AA}^2 \times 10^2$  for others)

Atom	U11	U22	U33	U12	U13	U23
Rh	2701(15)	3634(17)	3382(16)	17(11)	32(11)	264(11)
Cl	334(5)	574(7)	696(7)	16(5)	100(5)	-48(5)
N(1)	350(17)	446(19)	405(17)	26(14)	-57(14)	52(14)
N(2)	339(16)	374(17)	358(16)	-16(13)	-8(13)	30(13)
N(3)	545(22)	670(24)	400(19)	-93(18)	-79(16)	77(17)
C(1)	412(23)	600(3)	550(3)	51(20)	-109(19)	65(21)
C(2)	550(3)	780(3)	550(3)	93(20)	-186(22)	113(24)
C(3)	710(3)	700(3)	490(3)	160(3)	-63(23)	180(23)
C(4)	540(3)	570(3)	432(23)	32(21)	-5(19)	125(20)
C(5)	394(21)	420(22)	376(21)	39(18)	5(17)	50(17)
C(6)	370(20)	368(21)	397(21)	21(16)	-10(16)	27(16)
C(7)	447(23)	390(22)	447(22)	-22(18)	20(18)	90(17)
C(8)	382(21)	347(21)	478(22)	-19(17)	21(17)	15(17)
C(9)	435(22)	335(21)	530(24)	-44(17)	43(19)	-21(18)
C(10)	580(3)	550(3)	510(3)	-149(21)	72(21)	-21(21)
C(11)	790(3)	660(3)	580(3)	-330(3)	170(3)	-31(24)
C(12)	540(3)	710(3)	850(4)	-280(3)	160(3)	-190(3)
C(13)	430(3)	630(3)	920(4)	-82(23)	-40(25)	-40(3)
C(14)	490(3)	490(3)	760(3)	-51(20)	-24(22)	81(22)
C(15)	425(22)	466(24)	431(22)	-53(18)	-49(18)	-3(18)
C(16)	393(21)	378(21)	372(20)	-6(17)	-1(17)	24(16)
C(17)	507(24)	439(23)	337(20)	-74(19)	-1(18)	-28(17)

....cont.

....cont. Table A9

C(18)	477(24)	510(3)	432(23)	-27(19)	37(19)	-24(19)
C(19)	620(3)	600(3)	520(3)	-99(23)	166(23)	-9(22)
C(20)	890(4)	530(3)	402(24)	-100(3)	146(24)	45(20)
C(21)	820(3)	660(3)	386(24)	-100(3)	-132(23)	52(21)
C(22)	356(21)	332(21)	610(3)	4(17)	-4(19)	-43(18)
C(23)	413(22)	361(21)	495(23)	39(17)	77(18)	89(18)
C(24)	365(20)	359(20)	269(20)	59(16)	1(16)	69(16)
C(25)	327(19)	391(21)	385(20)	65(16)	47(16)	43(16)
C(26)	462(23)	394(22)	373(21)	101(18)	-32(17)	-44(17)
C(27)	490(3)	520(3)	1120(4)	-122(22)	-70(3)	-19(3)
C(28)	690(3)	690(3)	680(3)	33(25)	271(24)	278(25)
C(29)	520(3)	590(3)	486(24)	108(21)	-102(19)	98(20)
C(30)	455(25)	720(3)	520(3)	121(21)	162(20)	165(22)
C(31)	790(3)	750(3)	414(24)	190(3)	-113(22)	-113(22)
B	760(4)	600(4)	670(4)	100(3)	130(3)	290(3)
F(1)	152(3)	812(24)	1750(4)	341(22)	310(3)	565(24)
F(2)	197(4)	1090(3)	1770(4)	590(3)	1190(3)	550(3)
F(3)	198(5)	3360(7)	850(3)	1330(5)	60(3)	590(4)
F(4)	152(4)	1250(4)	3490(8)	-600(3)	-70(5)	220(4)

The anisotropic displacement factor exponent =  $-2\pi^2(U_{11}h^2a^{*2} + U_{22}K^2b^{*2} + U_{33}l^2c^{*2} + 2U_{12}hka^*b^*\cos\gamma + 2U_{13}hla^*c^*\cos\beta + 2U_{23}klb^*c^*\cos\alpha)$

**Table A10.** Hydrogen atom coordinates for [Cp\*RhL<sup>19</sup>Cl]BF<sub>4</sub>  
( $\times 10^3$ ) and isotropic thermal parameters ( $\text{\AA}^2 \times 10$ )

Atom	x	y	z	B <sub>eq</sub>
H(1)	1063	315	377	51
H(2)	1094	205	496	58
H(3)	883	71	580	57
H(4)	650	42	416	49
H(7)	426	56	330	41
H(10)	236	-69	320	52
H(11)	-29	-155	336	61
H(12)	-249	-131	235	65
H(13)	-205	-25	114	60
H(14)	56	66	100	53
H(15)	311	93	66	43
H(18)	837	202	47	46
H(19)	908	251	-101	56
H(20)	691	280	-203	56
H(21)	416	262	-159	56
H(27A)	1051	570	351	64
H(27B)	1103	529	251	64
H(27C)	1028	643	273	64
H(28A)	952	561	101	63
H(28B)	837	470	45	63
H(28C)	777	589	67	63
H(29A)	505	458	62	49

....cont.

....cont. Table A10

H(29B)	424	367	114	49
H(29C)	374	488	137	49
H(30A)	339	386	284	53
H(30B)	443	347	363	53
H(30C)	381	465	372	53
H(31A)	665	464	464	61
H(31B)	854	448	448	61
H(30C)	787	565	462	61

---

Hydrogen atoms are labelled according to the carbon atom to which they are attached.

**Table A11.** Bond distances (Å) in [Cp\*RhL<sup>19</sup>Cl]BF<sub>4</sub>

Rh-Cl	2.3984(10)	C(10)-C(11)	1.382(6)
Rh-N(1)	2.086(3)	C(11)-C(12)	1.371(8)
Rh-N(2)	2.197(3)	C(12)-C(13)	1.370(8)
Rh-C(22)	2.132(4)	C(13)-C(14)	1.382(6)
Rh-C(23)	2.163(4)	C(15)-C(16)	1.385(5)
Rh-C(24)	2.194(3)	C(16)-C(17)	1.495(5)
Rh-C(25)	2.153(3)	C(17)-C(18)	1.379(5)
Rh-C(26)	2.151(3)	C(18)-C(19)	1.390(6)
N(1)-C(1)	1.343(5)	C(19)-C(20)	1.358(7)
N(1)-C(5)	1.344(5)	C(20)-C(21)	1.369(7)
N(2)-C(6)	1.367(4)	C(22)-C(23)	1.456(5)
N(2)-C(16)	1.350(4)	C(22)-C(26)	1.417(7)
N(3)-C(17)	1.346(5)	C(22)-C(27)	1.493(5)
N(3)-C(21)	1.346(5)	C(23)-C(24)	1.407(5)
C(1)-C(2)	1.371(6)	C(23)-C(28)	1.496(5)
C(2)-C(3)	1.377(7)	C(24)-C(25)	1.442(5)
C(3)-C(4)	1.378(6)	C(24)-C(29)	1.488(5)
C(4)-C(5)	1.388(5)	C(25)-C(26)	1.424(5)
C(5)-C(6)	1.476(5)	C(25)-C(30)	1.491(5)
C(6)-C(7)	1.377(5)	C(26)-C(31)	1.497(5)
C(7)-C(8)	1.391(5)	B-F(1)	1.310(6)
C(8)-C(9)	1.480(5)	B-F(2)	1.330(7)
C(8)-C(15)	1.387(5)	B-F(3)	1.287(7)
C(9)-C(10)	1.388(6)	B-F(4)	1.316(8)
C(9)-C(14)	1.393(6)		

**Table A12.** Bond angles (°) in [Cp\*RhL<sup>19</sup>Cl]BF<sub>4</sub>

Cl-Rh-N(1)	87.61(8)	C(9)-C(10)-C(11)	120.5(4)
Cl-Rh-N(2)	101.39(8)	C(10)-C(11)-C(12)	120.3(4)
Cl-Rh-C(22)	94.34(10)	C(11)-C(12)-C(13)	120.5(4)
Cl-Rh-C(23)	95.04(10)	C(12)-C(13)-C(14)	119.4(4)
Cl-Rh-C(24)	127.32(9)	C(9)-C(14)-C(13)	121.3(4)
Cl-Rh-C(25)	158.37(10)	C(8)-C(15)-C(16)	121.3(3)
Cl-Rh-C(26)	127.0(10)	N(2)-C(16)-C(15)	121.9(3)
N(1)-Rh-N(2)	75.94(11)	N(2)-C(16)-C(17)	118.7(3)
N(1)-Rh-C(22)	116.22(13)	C(15)-C(16)-C(17)	119.3(3)
N(1)-Rh-C(23)	155.78(13)	N(3)-C(17)-C(16)	115.5(3)
N(1)-Rh-C(24)	144.96(12)	N(3)-C(17)-C(18)	123.4(3)
N(1)-Rh-C(25)	107.34(12)	C(16)-C(17)-C(18)	120.9(3)
N(1)-Rh-C(26)	94.32(13)	C(17)-C(18)-C(19)	118.3(4)
N(2)-Rh-C(22)	160.68(12)	C(18)-C(19)-C(20)	119.4(4)
N(2)-Rh-C(23)	126.65(12)	C(19)-C(20)-C(21)	118.6(4)
N(2)-Rh-C(24)	96.76(12)	N(3)-C(21)-C(20)	124.4(4)
N(2)-Rh-C(25)	97.45(12)	Rh-C(22)-C(23)	71.34(20)
N(2)-Rh-C(26)	130.46(12)	Rh-C(22)-C(26)	71.42(20)
C(22)-Rh-C(23)	39.61(15)	Rh-C(22)-C(27)	126.9(3)
C(22)-Rh-C(24)	64.51'(13)	C(23)-C(22)-C(26)	107.5(3)
C(22)-Rh-C(25)	65.26(14)	C(23)-C(22)-C(27)	125.4(4)
C(22)-Rh-C(26)	38.63(15)	C(26)-C(22)-C(27)	126.9(4)
C(23)-Rh-C(24)	37.67(13)	Rh-C(23)-C(22)	69.04(20)
C(23)-Rh-C(25)	64.90(13)	Rh-C(23)-C(24)	72.36(20)

....cont.

....cont. Table A12

C(23)-Rh-C(26)	64.97(14)	Rh-C(23)-C(28)	126.1(3)
C(24)-Rh-C(25)	38.72(13)	C(22)-C(23)-C(24)	107.5(3)
C(24)-Rh-C(26)	64.10(13)	C(22)-C(23)-C(28)	125.5(3)
C(25)-Rh-C(26)	38.64(13)	C(24)-C(23)-C(28)	126.9(4)
Rh-N(1)-C(1)	125.4(3)	Rh-C(24)-C(23)	69.97(20)
Rh-N(1)-C(5)	114.75(22)	Rh-C(24)-C(25)	69.11(18)
C(1)-N(1)-C(5)	119.7(3)	Rh-C(24)-C(29)	129.2(3)
Rh-N(2)-C(6)	107.91(21)	C(23)-C(24)-C(25)	108.8(3)
Rh-N(2)-C(16)	129.76(23)	C(23)-C(24)-C(29)	126.4(3)
C(6)-N(2)-C(16)	116.9(3)	C(25)-C(24)-C(29)	124.7(3)
C(17)-N(3)-C(21)	115.9(3)	Rh-C(25)-C(24)	72.17(19)
N(1)-C(1)-C(2)	121.7(4)	Rh-C(25)-C(26)	70.60(19)
C(1)-C(2)-C(3)	118.8(4)	Rh-C(25)-C(30)	127.6(3)
C(2)-C(3)-C(4)	119.9(4)	C(24)-C(25)-C(69)	107.2(3)
C(3)-C(4)-C(5)	118.6(4)	C(24)-C(25)-C(30)	126.0(3)
N(1)-C(5)-C(4)	121.1(3)	C(26)-C(25)-C(30)	126.5(3)
N(1)-C(5)-C(6)	115.3(3)	Rh-C(26)-C(22)	69.95(20)
C(4)-C(5)-C(6)	123.5(3)	Rh-C(26)-C(25)	70.76(19)
N(2)-C(6)-C(5)	114.4(3)	Rh-C(26)-C(31)	126.1(3)
N(2)-C(6)-C(7)	122.5(3)	C(22)-C(26)-C(25)	108.8(3)
C(5)-C(6)-C(7)	123.0(3)	C(22)-C(26)-C(31)	126.7(4)
C(6)-C(7)-C(8)	120.7(3)	C(25)-C(26)-C(31)	124.5(3)
C(7)-C(8)-C(9)	121.9(3)	F(1)-B-F(2)	112.4(4)
C(7)-C(8)-C(15)	116.0(3)	F(1)-B-F(3)	113.5(6)
C(9)-C(8)-C(15)	122.1(3)	F(1)-B-F(4)	107.3(5)
C(8)-C(9)-C(10)	121.1(4)	F(2)-B-F(3)	109.5(5)
C(8)-C(9)-C(14)	120.9(4)	F(2)-B-F(4)	111.0(6)
C(10)-C(9)-C(14)	118.0(4)	F(3)-B-F(4)	102.8(5)

---